GEOCHRONOLOGY AND GEOCHEMISTRY OF BASALTS IN THE WESTERN FOOTHILLS, TAIWAN

WEN-SHING JUANG

National Museum of Natural Science, Taichung, Taiwan 404, R. O. C.

ABSTRACT — Contemporaneous volcanism took place sporadically in Taiwan during the deposition of the Miocene sediments in the western basin, but the volcanic rocks are distributed in different areas within strata of different geologic ages. In northern Taiwan, nearly all the Miocene units contain contemporaneous volcanic effusions locally, each varying widely in size and in areal distribution. The Miocene volcanism events in western Taiwan were previously divided into three volcanic stages: the Kungkuan, the Chienshih and the Chiaopanshan volcanic stages. The volcanic rocks of the Kungkuan and the Chiaopanshan stages occur mostly as small, disseminated tuff lenses, patches or lava flows in the clastic sediments. Furthermore, the Chienshih stage of volcanism seems inactive, and the outcrops are scarce. Based on K-Ar age dating, Miocene volcanism in the Western Foothills of Taiwan can be divided into two episodes: Early Miocene (21.2 $\pm$ 0.4 to 16.3 $\pm$ 0.4 Ma) and Middle to Late Miocene (14.1 $\pm$ 0.4 to 7.1 $\pm$ 0.5 Ma), equivalent to the Kungkuan and Chiaopanshan stages, respectively. The studied areas of Kungkuan volcanism include the Nankang-Shenkeng, Shantzechia (Sulin-Shanjia), and Chingshuikeng (Jungho-Tucheng) areas; the areas of Chiaopanshan volcanism include Chiaopanshan (Tachi-Fuhsing), Kuanhsi-Chutung and other small scattered volcanic bodies (Chienshan, Hengchi, Taliaodi and Mucha).

The Miocene basaltic rocks of the Western Foothills are composed mainly of alkali basalts and tholeiites. The alkali basalt is characterized by its higher K, Ti, P, Ba, Li, Nb, Rb, Sr, V, Y, Zr, and LREE contents as compared with the tholeiite. However, the very highly incompatible element ratios of both alkali basalt and tholeiite are similar to E-type MORB, strongly reflecting their derivation from a common fertile mantle source.

Based on Ti-Zr-Y, Hf-Th-Ta and Nb-Zr-Y tectonomagmatic discrimination diagrams and incompatible element spidergrams, all the basaltic rocks from the Miocene Western Foothills are similar to those of typical intraplate continental rifting basalts.

The systematic compatible trace element variations suggest that the possibility of fractional crystallization can not be excluded in the evolutionary history of the magmas. The fractionations of olivine, pyroxene and plagioclase are predominant in Kungkuan basalts. The diversity of systematic incompatible trace element variation in Kungkuan and Chiaopanshan basalts suggests that amphibole fractionation can not be excluded for the derivation of Chiaopanshan volcanics.

REE data and other evidence suggest that the alkali basalt may have been derived from relatively deeper mantle which had been metasomatized by LILE-enriched fluid through partial melting. But the tholeiite may have originated from unmetasomatized mantle lherzolite at relatively shallow levels by 5-10% equilibrium batch partial melting.

The volcanic rocks of the Western Foothills of Taiwan and those of the Penghu Islands are similar in geochemistry and geochronology. They are closely related to Cenozoic rifting tectonism along the Asiatic continental margin caused by the 3rd heating and rifting episodic evolution of the South China Sea.

Bulletin of National Museum of Natural Science, No. 7, pp. 45-98, 1996

Sr, Nd and Pb isotopic compositions of Miocene basalts in western Taiwan and the Penghu Islands show that there regional variations with the Chiaopanshan stage volcanics characterized by a Dupal anomaly. The variation trends of highly incompatible-element ratios demonstrate that the enrichment processes that produced the Dupal anomaly in the basalts from Miocene strata are gradational. Addition of upper continental crustal materials into the asthenosphere is difficult to explain the trace element variations of these basalts. It is suggested that the Dupal mantle component was formed by mantle metasomatism.

KEY WORDS: Basalt, Western Taiwan, Geochemistry, K-Ar dating, Petrogenesis

INTRODUCTION

Taiwan is located on the eastern continental slope of the Asiatic plate. Formation of this island was a consequence of an uprising continental slope due to the motion of the Philippine Sea plate beginning in the early Pliocene.

Since the Cenozoic Era, intraplate volcanism related to continental rifting has prevailed in the passive continental margin of China. As a portion of this region, Taiwan and the neighboring islets of the Penghu Islands (Penghu) were inevitably affected by such tectonism. Therefore, products of Miocene volcanism such as alkali basalts and tholeiites in western Taiwan and Penghu, seem to follow prevailing physiographic trends.

In eastern Taiwan, the convergence of the Manila Trench is marked by eastward subduction of the South China Sea plate underneath the Luzon volcanic arc system on the Philippine Sea plate along the Eastern Longitudinal Valley. In eastern Taiwan, andesitic volcanism occurred chiefly during the Miocene and Pliocene to the Pleistocene. Additionally, Taiwan is also situated in the western end of the Ryukyu arc-trench system. The subduction of the Philippine Sea Plate beneath the Eurasia plate is marked by the volcano groups in northern Taiwan.

Thus, based on the tectonic framework, volcanism can be divided into three volcanic provinces: the western province, of a continental-rifting type; the eastern province, of an island-arc type; and the northern province, of a continental-margin type (text-fig. 1).

Based on preliminary study, among the 3 volcanic provinces of Taiwan, Quaternary volcanic rocks in northern Taiwan belong to island-arc calc-alkaline andesite suites in a broad sense, ranging from basaltic rocks to andesites and dacites. They occur in the Tatun volcano group, Chilung volcano group, Kuanyinshan, Tsaolingshan, and some other offshore islets such as Pengchiahsu and Mienhuahsu in the north. These rocks may be related to the Ryukyu volcanic arc (Chen, 1978, 1983, 1989; Chen and Kato, 1989; Juang and Chen, 1989; Yen *et al.*, 1981).

The volcanic arcs of eastern Taiwan consist of the Coastal Range and two offshore islets, Lutao (Green Island) and Lanhsu (Orchid Island), which have generally been considered as the northern extension of the Luzon arc. The K-Ar data indicate that volcanic activity occurred from the Early Miocene to Early Pliocene in the Coastal Range and Lanhsu, and from the Pliocene to Pleistocene in Lutao and Hsiaolanhsu. A significant increase in incompatible elements is found in the Pliocene to Recent andesite samples. The chemical variations in the volcanic rocks may be related to crustal thickening linked with the transition from subduction to collision regimes (Juang and Chen, 1990). As a member of the western volcanic province of Taiwan, the Penghu Islands are composed mainly of alkali basalts and tholeiites of Miocene age (Juang and Chen, 1992). The presence of many half-graben-type basins in the Tertiary sequence in western

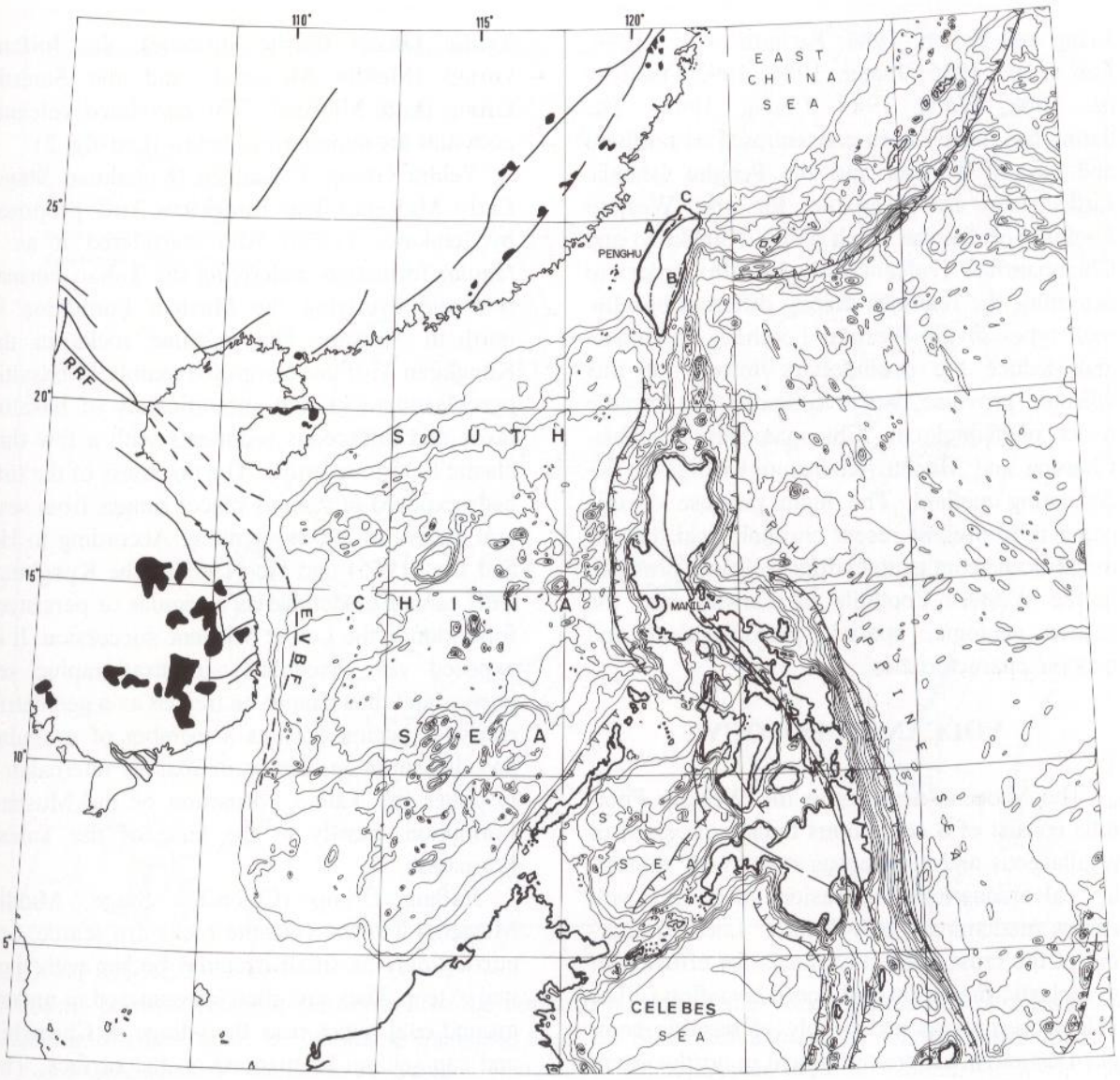

TEXT-FIGURE 1
Map showing the principal tectonic features in the Ryukyu-Taiwan and Luzon areas and 3 igneous provinces in Taiwan: A. western, B. eastern and C. northern districts. Black areas show the distribution of basalts; RRF, Red River Fault; EVBF, East Vietnam Boundary Fault.

Taiwan indicates a continental rifting environment in which intraplate volcanism has occurred.

Neogene basaltic rocks of western Taiwan and Penghu have been deduced to have occurred mainly in 3 episodes, namely the Early Miocene Kungkuan, the Late Miocene Kuanhsi-Chiaopanshan and the Middle to Late Miocene Penghu volcanic stages.

Radiometric dating (K-Ar, Ar-Ar, Sr-Rb and fission track) in volcanic studies of Taiwan has been carried out by many authors (Ho, 1969a;

Juang and Bellon, 1984; Richard *et al.*, 1986; Lan *et al.*, 1986; Juang, 1988, 1993; Yang *et al.*, 1988; Wang, 1989; Chung, 1992). The dating has mostly been concentrated on northern and eastern Taiwan and the Penghu Islands. Little data are available for the Western Foothills of Taiwan, such as the Kungkuan and Chiaopanshan volcanic stages. In order to determine the relations among different basaltic rock types in the Western Foothills of Taiwan and deduce the evolutionary history of this volcanic province, we investigated the basaltic rocks of Kungkuan, Chiaopanshan, Kuanhsi-Chutung and Mucha (Kaohsiung) using the K-Ar dating method. The main purpose of this paper is to present recent chronological data of the Miocene continental rifting volcanic province in the Western Foothills of Taiwan, and the related geologic, spatial, petrochemical and tectonic characteristics.

VOLCANIC GEOLOGY

The Miocene deposits in the Western Foothills consist of a continuous thick succession of argillaceous and arenaceous rocks with subsidiary calcareous lenses. Effusions of basaltic volcanics predominate only locally. Local fracturing of the crust opened channels for effusion of pyroclastic materials and some lava flows. The volcanic eruptions are largely of basaltic composition and are more prominent in northwestern Taiwan. The most extensive and important volcanic phase occurred in the early sedimentary cycle and is defined as the Kungkuan volcanic stage of Lower Miocene age (Ho, 1969b). In the middle sedimentary cycle, volcanic activity was quite infrequent and of very limited distribution. There was a resumption in volcanism during the late sedimentary cycle when the coal-bearing Nanchung Formation was being deposited. These volcanic eruptions were distributed widely in north-central Taiwan, also extending sporadically to southern Taiwan. According to Ho (1969b), the Miocene stratigraphic unit in northern Taiwan is divided into three groups: the Yehliu Group (Early Miocene), the Juifang Group (Middle Miocene), and the Sanhsia Group (Late Miocene). The correlated volcanic activities are summarized below (text-fig. 2).

Yehliu Group Volcanism (Kungkuan Stage, Early Miocene) The Kungkuan Tuff proposed by Ichikawa (1930) who considered it as a regular formation underlying the Taliao Formation and overlying the Mushan Formation in northern Taiwan. The volcanic rocks in the Kungkuan Tuff are composed mainly of basaltic pyroclastic rocks and subordinately of basaltic lavas and tuffaceous sediments with a few thin clastic limestone lentils. The thickness of the tuff beds exposed in various places ranges from several meters to 200 m or more. According to Ho and Lin (1965) and Ho (1969b), the Kungkuan Tuff cannot be defined as a regular or persistent formation in the Lower Miocene succession. It is exposed very irregularly in stratigraphic sequence and thus cannot be treated as a geometric entity. It occurs only as a member of irregular and discontinuous lenses or masses intercalated in either the Taliao Formation or the Mushan Formation, mostly at the base of the Taliao Formation.

Juifang Group (Chienshih Stage, Middle Miocene) Tuff or volcanic rocks are scarce, occurring only as small irregular bodies with limited extent. They are often encountered in underground coal mines near the village of Chienshih and can seldom be mapped on the surface. The main volcanic rocks are basaltic tuff or tuff breccia. Lava flows are uncommon and are represented by olivine basalt or teschenite.

Sanhsia Group (Chiaopanshan Stage, Late Miocene) This group represents the youngest Miocene sedimentary cycle in western Taiwan, and is divided into a lower coal-bearing Nanchuang Formation and an upper marine Kueichulin Formation in northern Taiwan. The Nanchuang Formation in Taoyuan and Hsinchu Counties is characterized by the occurrence of many volcanic beds in its middle and lower succession. The volcanic rocks are mainly basaltic tuff or tuff breccia and subordinately basaltic

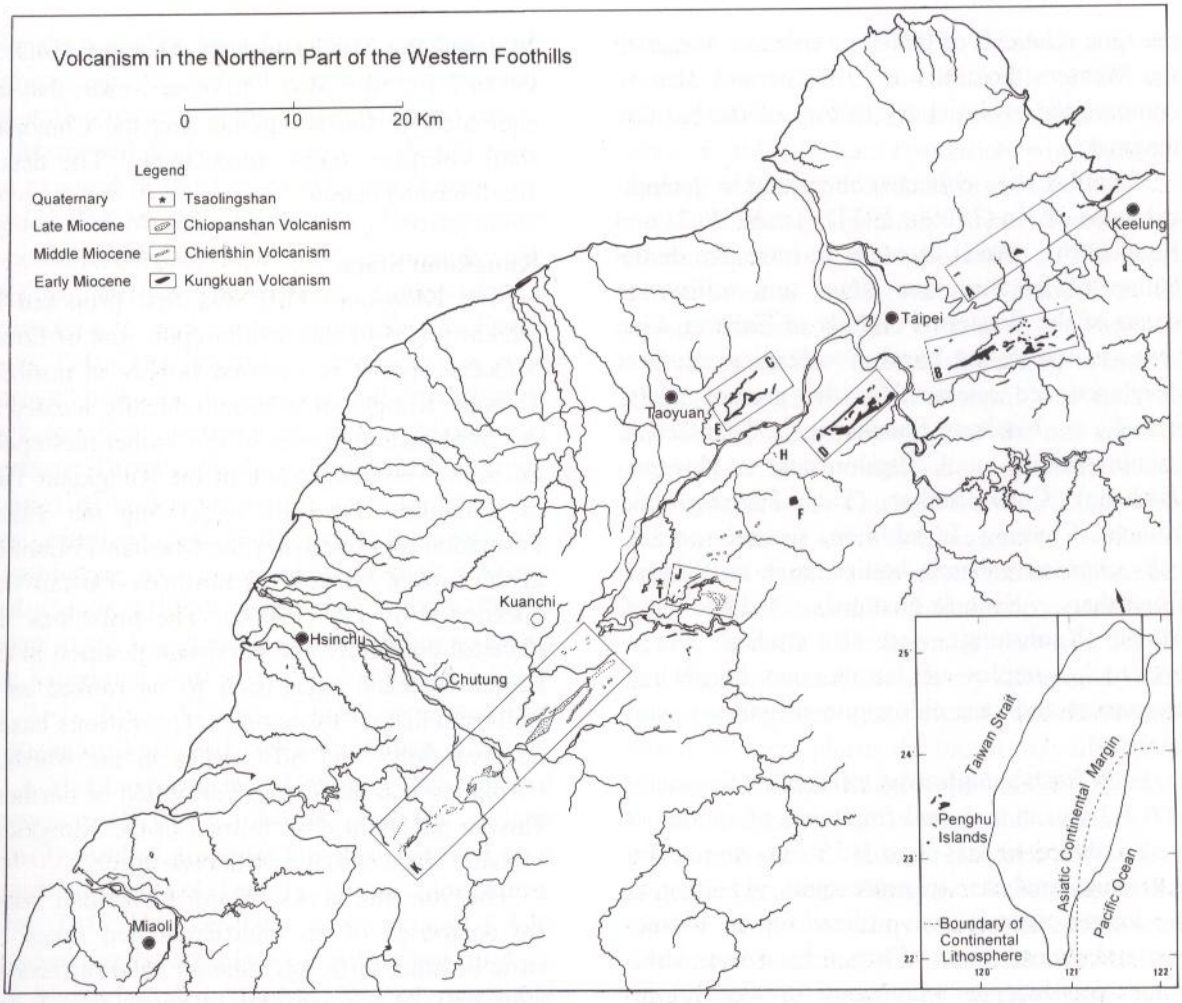

TEXT-FIGURE 2
Miocene basaltic volcanic distribution in the northern portion of the Western Foothills of Taiwan. A. Keelung-Mushan area; B. Nankang-Shenkeng area; C. Shantzechia area; D. Chingshuiken area; E. Yingko Chienshan; F. Taliaodi; H. Sanhsia Hengchi; J. Chiaopanshan area; K. Kuanhsi-Chutung area and T. Tsaolingshan (Quaternary). The distribution areas of basalts from Ho (1988).

lava flows. This volcanic activity has been ascribed to the Chiaopanshan volcanic stage due to its extensive distribution and development in the vicinity of the village of Chiaopanshan, Fushing, Taoyuan County (Yen, 1958; Tsan, 1962). Evidence of volcanic activity is scarce in the Kueichulin Formation, with only small volcanic lenses appearing in petroleum prospecting drilling holes in the lower Kueichulin Formation of the Taoyuan and Hsinchu areas. In the southern part of Taiwan, the equivalent of the Kueichulin Formation is also characterized by the occurrence of many basaltic lava flows in the village of Mucha, Kaohsiung (Keng, 1967).

K-Ar GEOCHRONOLOGY

The basaltic rocks and the megacrysts therein of the Western Foothills of Taiwan were dated here by the K-Ar method in order to determine

the time relations of different volcanic stages in the Western Foothills of Taiwan and also to compare the evolutionary history of the basaltic magmas.

Samples were collected according to geological maps of Ho (1969b, 1971), Tsan (1962) and Keng (1961, 1962) in order to trace the distribution of basaltic lava flows and tuffaceous strata of the Western Foothills of Taiwan. Five areas in which the basaltic volcanics are best developed are selected for the present study, namely, Nankang-Shenkeng, Shantzechia (Shulin-Sanjia), Chingshuikeng (Jungho-Tucheng), Chiaopanshan (Tachi-Fushing) and Kuanhsi-Chutung. In addition, several sporadically exposed volcanic bodies, such as Yingko-Chienshan, Sanhsia-Henghsi, Taliadi and Mucha (Kaohsiung), were also studied. Forty-one rock samples of basalt, one hornblende megacryst and one phlogopite megacryst were analyzed.

Each fresh sample was crushed to fragments of 0.5-1 mm in size, and fragments of an aliquot were reduced to less than 0.15 mm in size for potassium analysis. In most cases, 15-25 g of the coarser material was utilized for the extraction and measurement of argon by isotope dilution, according to techniques previously described by McDougall *et al.* (1969). Prior to argon extraction, the sample was baked in a vacuum line at a temperature not exceeding 100 ℃ to minimize the possibility of isotopic fractionation of the air-argon component associated with the samples. Isotopic analysis of the extracted argon was performed in a substantially modified AEI MS10 mass spectrometer being operated in the static mode. Potassium was determined by atomic absorption with the nitric-boric acid technique (Juang, 1981). Delay constants and conversion factors are those recommended by Steiger and Jäger (1977). The analytical results are shown in table 1.

The volcanic history of the Western Foothills of Taiwan can be divided into two stages on the basis of geochronological and field relationship: the Early Miocene (21.2 ± 0.4 to 16.3 ± 0.4 Ma) and the Middle to Late Miocene (14.1 ± 0.4 to 7.1 ± 0.5 Ma). In other words, they are equivalent to the Kungkuan and the Chiaopanshan volcanic stages, respectively. The details are described below.

Kungkuan Stage

The Kungkuan Tuff was first proposed by Ichikawa (1930) as a stratigraphic unit of Lower Miocene age. It is exposed largely in northern Taiwan. Kungkuan is geographically located at the southeastern corner of the Taipei metropolitan area. The designation of the Kungkuan Tuff as a regular rock unit underlying the Taliao Formation and overlying the Mushan Formation in the Lower Miocene of northern Taiwan was questioned by Ho (1969b). The tuffs lack the physical continuity and persistent position in the Lower Miocene succession to be ranked as a well-established "formation". The various basaltic lava flows and tuff bodies in the Mushan Formation and the Taliao Formation of northern Taiwan are defined as formed in the Kungkuan volcanic stage of Lower Miocene age.

The volcanic rocks of the Kungkuan stage are composed of an undifferentiated series of vitric or lithic tuffs, agglomerate, and tuffaceous sediments. Minor amounts of basaltic lavas are associated with these pyroclastic rocks. The geographic distribution of the volcanic rocks of the Kungkuan stage is limited to northern Taiwan (text-fig. 2). The best development of the Kungkuan Tuff is known from 4 areas of northern Taiwan. According to Ho (1969b), these 4 areas are Keelung-Neihu, Nankang-Shenkeng, Shantzechiao, and Chingshuikeng (text-fig. 2). Selecting suitable samples for dating was very difficult among these areas, except for the Keelung-Neihu area where mixed vitric and lithic tuff predominate and only little-altered basalt and limestone are exposed. The K-Ar dating results and field relationship for the volcanic rocks in different geographic districts are briefly described.

(1) Chingshuikeng (Jungho-Tucheng Area): The Chingshuikeng area, covering Jungho

(Nanshichiao)-Tucheng-Hsintien, contains the highest percentage of volcanic rocks in comparison with sediments in the Lower Miocene strata.

Many tuff bodies and lentils or basalt lavas are exposed in the Lower Miocene Taliao Formation and Mushan Formation. The maximum exposed thickness is nearly 280 m in Nanshichiao (Ho, 1969b). The lenticular limestone is a characteristic rock associated with the Kungkuan Tuff. The limestone has become a good horizon indicator because no other carbonate rock has been found in the Lower Miocene of northern Taiwan. Fossil evidence in the Kungkuan Tuff is derived mainly from the sedimentary interbeds in the tuff series, especially the fossiliferous limestone and some shale. Wang and Huang (1953) recognized 3 main faunal zones in the Kungkuan Tuff. According to them, the Kungkuan Tuff is of Burdigalian age (21.8 to 16.6 Ma). Chang (1962) correlated the Kungkuan Tuff with the Aquitanian (23.7 to 21.8 Ma) based on the planktonic foraminiferal sequence of the Caribbean Tertiary. Huang (1979) reached a similar conclusion based on a biometric study of *Lepidocyclina* in the Kungkuan Tuff. The respective K-Ar ages of 8 Chingshuikeng basaltic lavas fall between 20.7 $\pm$ 0.3 Ma and 17.8 $\pm$ 0.4 Ma. This is compatible with the fission-track ages of 23.0 $\pm$ 4.6 to 20.0 $\pm$ 2.0 Ma (Chung, 1992). The slight discrepancy may be caused by sediment contamination. Based on the statistic age of the fission-track of zircon, invincible mixing with an old basement material in the basaltic lavas or in tuffaceous breccias was indicated (Chung, 1992).

(2) Shantzechiao (Shulin-Sanjia Area): According to Ho (1969b), limestone or tuffaceous limestone is best developed in the Shantzechiao area. One calcareous bed extends more or less ubiquitously throughout the entire anticlinal fold in Shantzechiao. This limestone bed lies on top of the main tuff unit. The volcanic rock fragments in the limestone are mostly glassy and chloritized or filled with secondary calcite and therefore unsuitable for K-Ar dating. Fortunately, there are some fresh lava flows in the Mushan Formation (Sample S313A). The observed age of 21.2 $\pm$ 0.4 Ma (table 1) falls into the period deduced from calcareous nannofossils NN1 of the Mushan Formation which ranged from 23.0 Ma to 21.0 Ma (Chi, 1981).

(3) Nankang-Shenkeng Area: Many pyroclastics, ash tuffs to lapilli tuffs, agglomerate, and tuffaceous sediments are exposed in the Lower Miocene Taliao Formation and Mushan Formation in the Nankang-Shenkeng area. The tuffaceous rock is easily susceptible to weathering. Well-exposed outcrops of the tuff are rare and can be found mostly along streams or new road excavations. The weathered tuff looks like maroon-colored soil which may serve as a useful field guide to trace the distribution of the tuff bodies. The basaltic lava flows occur randomly among the tuffs. The boundary between the tuff and the lava cannot be clearly delineated where the exposure is poor or covered with dense vegetation. In some places the basalt may also occur as isolated bodies in the sediments. Fresh basalt in the Kungkuan Tuff is black and compact. The weathered basalt, however, is dark gray, greenish gray, or brownish gray. According to Yen (1950), a nice outcrop occurs in Shihtzushui, south of Nankang. It possesses well-defined stratigraphic relations to its overlying and underlying rock units. Stratigraphically, the lapilii tuffs or agglomerates can be recognized either in the Taliao Formation or even can be traced continuously from the Taliao Formation to the Mushan Formation. The respective K-Ar ages of the basalts are 20.0 $\pm$ 0.5 to 19.1 $\pm$ 0.4 Ma (table 1), which are rather compatible with the field occurrences. In the Nankang-Shenkeng area, bulging lenticular basaltic bodies have been exposed by excavation of the tunnel of the North Secondary Turnpike near the backside of National Chengchi University, Mucha, Taipei. The volcanic bodies are truncated by a fault trough (Ho, 1969b). In this place, the tuff is comparatively more continuous and occurs largely at the middle to lower part of the Taliao Formation. The K-Ar dating yields 16.3 $\pm$ 0.4 Ma (table 1) which is the upper-most strata of

TABLE 1
Analytical results of K-Ar ages of Late Cenozoic basaltic rocks from the Western Foothills of Taiwan

Sample no.	Rock type	Ages (Ma) ±uncertainty	$^{40}Ar^*$ ($\times 10^{-11}$ mole/g)	K(%)	$^{40}Ar^*/^{40}Ar_T$	weight analysed(g)
			Kungkuan Stage			
Nankang-Shenkeng Area						
N201	alk	19.1±0.4	4.7264	1.42	0.803	3.36447
N202	alk	20.0±0.5	4.9411	1.42	0.618	3.34555
N202A	alk	19.9±0.5	4.8325	1.39	0.703	2.9854
N206	alk	16.3±0.4	5.5446	1.95	0.784	1.9419
Shantzechiao Area (Shulin-Shanjia Area)						
S314A	alk	21.2±0.4	4.8583	1.31	0.934	2.0091
Chingshuikeng Area (Jungho-Tucheng Area)						
J405	alk	17.8±0.4	5.3451	1.72	0.721	3.6640
J406	alk	17.7±0.4	3.6037	1.18	0.666	2.3240
J407A	alk	20.3±0.3	8.2822	2.34	0.938	2.9496
J408C	alk	20.7±0.3	6.8345	1.89	0.929	2.9551
J409B	alk	18.7±0.3	8.2305	2.52	0.878	2.2526
J410	alk	18.7±0.4	3.4802	1.07	0.708	2.2942
J411	alk	19.5±0.4	5.2040	1.53	0.828	1.7281
J412	alk	20.0±0.5	5.6754	1.63	0.757	2.11623
J412A	alk	19.9±0.5	5.0958	1.47	0.754	2.58352
			Chiaopanshan Stage			
Chiaopanshan Area (Tachi-Fushing Area)						
C701	alk	12.3±0.3	2.7152	1.27	0.653	1.9811
C702	alk	14.0±0.4	2.9058	1.19	0.585	2.26632
C704	th	10.9±0.3	0.9745 } 0.9826	0.52	0.540	2.5690
			0.9907		0.533	1.7841
C714A	th	11.1±0.3	1.2160 } 1.2156	0.63	0.346	2.2620
			1.2152		0.281	2.1252
C716B	th	11.9±0.5	1.0975	0.53	0.0338	2.52364
C719	th	13.1±0.4	1.7771	0.78	0.505	1.5811
C730	th	14.1±0.4	1.0783	0.44	0.241	2.5459
C730A	th	12.5±0.6	1.0428	0.48	0.227	2.34572
C734C	th	10.6±0.5	0.8297	0.45	0.282	2.23675
C736	th	10.7±0.3	1.0786	0.58	0.339	1.5312
C742A	alk	13.0±0.5	2.5343 } 2.5308	1.12	0.283	2.1224
			2.5274		0.284	2.4756

To be continued

Continued

Sample no.	Rock type	Ages (Ma) ±uncertainty	$^{40}Ar^*$ ($\times 10^{-11}$ mole/g)	K(%)	$^{40}Ar^*/^{40}Ar_T$	weight analysed(g)
Kuanhsi-Chutung Area						
K801A	th	13.0±0.4	1.5424	0.68	0.538	2.7624
K808D	th	12.3±0.4	1.1539	0.54	0.553	2.5242
K810B	alk	12.0±0.4	2.7533	1.32	0.531	3.1049
K812	Hb	12.1±0.3	3.8387	1.82	0.874	1.0282
K812C	alk	11.5±0.3	3.1572	1.58	0.740	3.7136
K812D	Phl	11.6±0.3	15.7548	7.83	0.755	0.6305
K815A	alk	10.3±0.5	3.3022	1.85	0.497	2.9927
K821	alk	12.9±0.6	0.9421	0.42	0.233	1.6749
K822	alk	12.8±0.4	2.6379	1.18	0.515	1.8233
K832	alk	14.1±0.4	2.2090	0.90	0.539	1.7579
Chienshan, Yingko						
E622	th	7.8±0.3	1.1999	0.88	0.442	1.7094
Hengchi, Sanhsia						
H502	th	7.1±0.5	0.6578	0.53	0.133	2.03591
H503	th	7.6±0.4	0.8482	0.64	0.276	2.06087
H504	th	9.2±0.4	0.8437	0.53	0.386	1.6155
H504A	th	9.1±0.5	0.8059	0.51	0.342	2.2334
Taliaodi						
T901	th	7.6±0.5	0.9140	0.83	0.332	2.50160
Mucha, Kaohsiung						
M001	alk	7.8±0.3	2.0162	1.78	0.392	0.95208

Sample localities are shown in text-fig 2.
alk : alkali basalt; th : tholeiite, whole rock.
Hb : Hornblende megacryst; Phl : Phlogopite.

Burdigalian age of the Lower Miocene.

Chiaopanshan Stage (Chiaopanshan and Kuanhsi-Chutung Area)

Chiaopanshan stage volcanism was active during the lower Nanchuang deposition, producing several basaltic belts in northern Taiwan. The Nanchung Formation has been used by many authors to replace the old term "Upper coal-bearing formation" which does not carry a geographic name. Ho *et al.* (1954) first used this name, calling it the Nanchung coal-bearing formation. The Nanchung Formation in Taoyuan and Hsinchu Counties is characterized by the

occurrence of many volcanic beds in its middle and lower parts. The basaltic volcanics of the Chiaopanshan stage are found in Chiaopanshan (Fuhsing, Taoyuan) and the Kuanhsi-Chutung district.

(1) Chiaopanshan Area: This volcanic activity has been described as the Chiaopanshan volcanic stage due to its extensive distribution and development in the vicinity of Chiaopanshan, Taoyuan County (Yen, 1958; Tsan, 1962). The volcanic rocks are mainly basaltic tuff breccia and subordinately basaltic lava flows. There are 3 to 5 tuff beds intercalated randomly in the sedimentary rocks without any definite stratigraphic sequence. These tuff beds extend discontinuously along the strike of the strata or slightly cut across it. They are several meters thick and vary from scores of meters to 2 or 3 km long. Some thick tuffaceous lens may reach nearly 100 m thick. Ages of 14.1 $\pm$ 0.4 Ma to 10.9 $\pm$ 0.3 Ma (table 1) were notably observed from K-Ar radiometry. These are equivalent to the Serravallian of the Middle Miocene to Lower Tortonian of the Upper Miocene, and seem to correlate with the field relationship.

(2) Kuanhsi-Chutung District: The basaltic rocks from the Kuanhsi-Chutung district are chiefly associated with Tertiary sedimentary rocks. They occur as lava flows, dikes, sills, agglomerates, tuffs or pyroclastics. Samples were collected according to geologic maps of Ho and Hsu (1961), Ho *et al.* (1954), Ho (1971), Keng (1961, 1962) and Tu and Chen (1990, 1991). The studied area included Lumanku Nanchung, Miaoli (Sample K801A), Netaping (Samples K808D, K810B), Mafu (K812), the Maohoshan quarry of the Asian Cement Co. (Sample K815A), Luhchuh Mawudu (Samples K821, K822) and Suliao Kuanhsi (Sample K832). These basaltic volcanics occur in the Nanchung Formation of Miocene age as shown on previous geologic maps. The analytical results of 14.1 $\pm$ 0.4 to 10.3 $\pm$ 0.5 Ma are rather compatible with the interpretation of the stratigraphic succession.

(3) Others: Volcanic bodies are described here which occur in many places as irregular and discontinuous lenses or masses, change shapes and dimensions, and intercalate in the Nanchung Formation or equivalent successions.

A. Chienshan, Yingko: An isolated monticule with an elevation of 128 m is located about 4 km southwest of Yingko, a small railroad station in Taipei County. The exposed basement rocks are characterized by a succession of grayish sandstone and shale. In a previous geologic map and report, Ichimura (1931) inferred from the invasion of Chienshan volcanics into the Plio-Pleistocene Toukoushan Formation which is widely developed in western Taiwan that this monticule belongs to the Quaternary volcanism. The respective K-Ar age is 7.8 $\pm$ 0.3 Ma (table 1, Sample E622) which is very inconsistent with Ichimura's (1932) suggestion.

B. Hengchi, Sanhsia: Several thin beds of volcanic lava and tuff were interbeded with sedimentary rocks of the upper Nanchuang Formation in Hengchi, Sanhsia. The pyroclastic rocks include an undifferentiated series of tuffs, agglomerates and tuffaceous sediments. Some clastic rocks may represent ejected volcanic deposits and show ambiguous bedding. Two layers of basalts crop out sporadically among the massive tuffs. The upper cropped-out basaltic lava flow seems to be concentrated in an irregular land form and forms intriguing columnar joints like the Devil's Postiple, California (Juang, 1992). The K-Ar age of the lower lava is 9.2 $\pm$ 0.6 Ma which is rather compatible with the results 9.5 $\pm$ 0.6 to 10.2 $\pm$ 0.5 Ma obtained by Tsao *et al.* (1992). The ages of the upper part at 7.1 $\pm$ 0.5 to 7.6 $\pm$ 0.4 Ma (table 1) are rather compatible with K-Ar the ages of 7.91 $\pm$ 0.45 Ma obtained by Miki (1991). However, the fission-track age of 1.27 $\pm$ 0.17 Ma (Chen, 1991) raises some questions. This date is not comparable with the field relationship of the prevailing stage of lava flows (Hong, 1988). This discrepancy may be caused by inappropriate treatment or perhaps by some, still unclear, geologic meaning.

C. Mucha, Kaohsiung: The equivalent of the Nanchuang Formation in the southern part of Taiwan (Kaohsiung) has been named the Shihnei Formation by Keng (1967). The Shihnei Formation is predominately dark gray shale with a few sandstone interbeds. The massive variety may grade into mud or siltstone. The sediments contain a rich fauna of foraminifers and molluscs. Small and thin basaltic tuff lenses or lavas have also been found in the Shihnei Formation. The radiometric result gives an age of 7.8 $\pm$ 0.3 Ma (table 1).

From the above discussion it is suggested that the Miocene volcanism in the Western Foothills of Taiwan can be divided into two stages: the Former (Early Miocene; 21.2 $\pm$ 0.4 to 16.3 $\pm$ 0.4 Ma) and the Later (Middle to Upper Miocene; 14.1 $\pm$ 0.4 to 7.1 $\pm$ 0.5 Ma), which are equivalent to the Kungkuan and Chiaopanshan stages respectively. These basalts displaying temporal variations may also display spatial, chemical or isotopic variations which reflect the interaction between the asthenosphere and the continental lithosphere.

GEOCHEMISTRY

Analytical Procedures

52 basaltic rock samples collected from the Western Foothills of Taiwan were analyzed in the present study. The samples used in the chemical analyses were prepared as follows. The rocks were crushed into pieces using a hammer. Rock pieces were then ground into powder in an Al_2O_3 spex mill. Al_2O_3 contamination was considered to be negligible since no residue was found following dissolution.

For chemical analyses, 1.0 g of rock powder was dissolved in a mixture of ultrapure HNO_3 and HF. All chemical analyses, except Si, Al, Ti, P, Nb, Y, Zr, REE, Hf, Sc, Ta, Th and U, were conducted with a Perkin-Elmer Model 5100 PC atomic absorption spectrophotometer using solutions of various dilutions. U.S. Geological Survey rock standards BCR-1, AGV-1, GSP-1, G-2, W-1 and NBS rock standards (Basaltic Rock, Obsidian Rock) were employed for construction of the working curves. For SiO_2, Al_2O_3, TiO_2, and P_2O_5 determinations the techniques suggested by Shapiro and Brannock (1962) were used with slight modification.

The concentrations of Nb, Y, U and Zr were determined by the inductively coupled plasma (ICP) emission spectrochemical method at National Tsing-Hua University. Analytical uncertainties ranged from 1 to 4% for major elements and from 2 to 5% for trace elements.

The concentration of REEs (rare earth elements), Hf, Sc, Ta and Th in the volcanic rocks were analyzed by the radiochemical neutron activation method using the open pool reactor at National Tsing-Hua University. Around 25 mg of powder samples packed with an aluminum foil were irradiated for 38 hours with a thermal neutron flux of 10^{12} n/cm^2 sec. Carrier solutions were prepared according to the procedure described by Smet *et al.* (1978). U.S.G.S. standard rocks AGV-1, BCR-1 and W-1 were utilized as standards. After 5 days cooling, the rare earth elements in the irradiated samples were separated into a group and counted by an ORTEC-high-purity-Ge coaxial detector and a Series 85 Canbera 4096-multichannel analyzer. Samples were counted 4 times between 5 days and 3 months following irradiation. Durations of counting times varied from 5000 to 25000 seconds, depending upon the length of cooling and the rare earth element contents of interest. This method precludes the determination of Dy, Ho and Er which all have a half life less than 30 hours. Precision was estimated to be better than 10% for all REEs. Major and trace element data for volcanics from northern Taiwan are listed in tables 2 and 3, and average values are listed in table 4.

Major Element Geochemistry

The major element data and C.I.P.W. Norms for volcanics from the Western Foothills of Taiwan are listed in table 2. In the (Na_2O+K_2O)

TABLE 2
Chemical compositions of basaltic rocks from the Western Foothills of Taiwan

Sample No.	N201	N202	N216	N217	J405	J406	J407A	J408C	J409B	J410A	J411
Rock Type	alk	alk	alk	alk	alk	alk	alk	alk	alk	alk	alk
%											
SiO_2	48.66	48.40	48.73	49.11	45.08	48.30	48.30	48.73	50.79	49.49	48.34
Al_2O_3	15.48	16.07	16.04	14.96	15.50	16.27	17.35	16.42	17.85	15.29	16.23
ΣFeO	10.55	10.49	8.53	9.15	10.71	10.20	9.95	11.02	7.72	9.79	10.50
MgO	6.56	6.65	4.87	5.33	6.62	5.90	4.24	4.97	3.16	6.29	5.18
CaO	8.51	8.94	8.31	8.86	10.26	7.25	7.73	8.01	8.78	8.15	8.43
Na_2O	3.79	2.80	4.62	4.69	3.36	4.63	3.51	3.69	4.45	4.08	3.25
K_2O	1.66	1.81	2.29	1.98	2.07	1.41	2.79	2.28	3.08	1.18	2.01
TiO_2	2.76	2.74	2.76	2.77	4.10	3.12	2.64	3.40	2.80	3.24	2.55
MnO	0.158	0.158	0.163	0.176	0.167	0.173	0.187	0.119	0.140	0.161	0.238
P_2O_5	0.51	0.49	1.00	0.89	1.32	1.01	1.31	0.86	0.72	1.22	0.63
L.O.I	1.41	1.70	2.27	2.36	1.16	1.61	1.23	0.85	1.19	1.48	2.89
Total	100.048	100.248	99.583	100.276	100.347	99.873	99.237	100.349	100.680	100.371	100.248
ppm											
Ba	653	394	643	801	823	899	2127	719	868	715	522
Co	45	42	32	33	51	43	32	45	29	48	42
Cr	188	170	109	160	139	78	54	33	28	165	117
Cu	36	38	54	59	53	43	27	36	66	47	54
Li	14	27	15	20	19	17	15	8	6	13	43
Nb	39	40	70	78	90	98	100	79	97	82	49
Nd	33	31	44	48	54	49	62	44	38	59	34
Ni	109	98	88	90	106	86	57	66	55	112	77
Rb	27	28	63	57	38	15	44	49	81	15	39
Sc	22	22	19	28	33	21	15	19	18	25	21
Sr	742	625	1550	1210	1209	1157	1461	998	1317	1142	673
V	211	209	222	219	306	222	156	249	241	248	183
Y	24	30	27	27	33	27	31	27	30	29	33
Zn	96	96	96	96	113	88	103	110	81	86	108
Zr	192	232	263	245	311	342	407	324	432	314	235
C. I. P. W. Norms											
Q	-	-	-	-	-	-	-	-	-	-	-
or	9.82	10.71	13.55	11.71	12.24	8.34	16.50	13.49	18.22	6.98	11.89
ab	28.38	23.66	27.52	27.65	16.88	34.42	28.74	29.55	25.90	34.48	27.47
an	20.29	25.89	16.23	13.89	21.06	19.41	23.30	21.46	19.59	19.89	23.72
ne	1.98	-	6.25	6.50	6.24	2.55	0.50	0.88	6.35	-	-
di	15.40	12.67	15.54	20.19	17.84	8.64	6.07	10.83	16.17	10.83	11.82
hy	-	9.28	-	-	-	-	-	-	-	8.90	5.69
ol	13.36	9.54	8.33	8.12	11.15	13.80	12.14	11.75	4.15	8.20	10.50
mt	3.06	3.04	2.48	2.65	3.10	2.96	2.89	3.19	2.23	2.84	3.04
il	5.24	5.21	5.24	5.26	7.79	5.93	5.02	6.46	5.32	6.16	4.85
ap	1.11	1.07	2.18	1.94	2.88	2.20	2.86	1.88	1.57	2.66	1.38

To be continued

Continued

Sample No.	J412	J413	S313A	S314A	H502	H503	H504	E615B	E622	C701	C702
Rock Type	alk	alk	alk	alk	th	th	th	th	th	alk	alk
%											
SiO_2	48.34	45.11	50.21	50.50	52.06	52.03	51.34	52.22	51.25	48.20	49.30
Al_2O_3	15.52	14.41	16.49	15.08	14.17	13.87	14.24	14.19	13.81	13.86	12.89
ΣFeO	10.72	10.44	9.20	9.81	10.27	10.19	10.07	9.24	8.89	10.32	9.95
MgO	6.51	8.78	5.35	5.77	7.09	7.15	7.39	4.87	5.66	8.31	6.03
CaO	7.22	11.10	7.78	10.26	9.55	10.46	9.67	10.87	9.40	9.77	10.02
Na_2O	4.13	3.34	3.47	3.08	2.87	2.71	2.83	3.29	2.96	2.66	2.98
K_2O	1.94	0.86	1.56	1.55	0.74	0.81	0.94	1.29	1.20	1.52	1.43
TiO_2	2.77	4.20	2.51	2.86	2.24	2.16	2.08	3.48	2.23	2.36	2.42
MnO	0.155	0.158	0.091	0.192	0.149	0.147	0.149	0.147	0.118	0.166	0.180
P_2O_5	0.59	0.84	0.44	0.53	0.36	0.35	0.36	0.39	0.44	0.59	0.45
L.O.I	1.94	1.09	2.10	1.28	0.73	0.93	1.06	0.76	3.31	1.31	3.42
Total	99.835	100.328	99.201	100.912	100.229	100.807	100.129	100.747	99.268	99.066	99.070
ppm											
Ba	616	759	762	419	159	163	149	281	201	479	415
Co	41	58	47	43	44	45	46	46	43	46	49
Cr	119	273	229	266	217	230	248	163	225	267	258
Cu	43	59	55	57	57	57	56	62	55	51	62
Li	29	25	39	24	6	6	7	6	8	13	12
Nb	45	72	43	46	31	30	30	50	33	43	52
Nd	45	54	25	29	25	25	16	23	19	22	25
Ni	82	155	120	119	149	163	162	107	219	176	146
Rb	37	28	34	29	5	4	9	22	18	34	36
Sc	20	30	23	28	32	26	26	35	26	28	21
Sr	582	1056	661	705	390	395	386	513	441	613	698
V	174	302	209	267	176	172	178	255	168	191	182
Y	30	27	16	22	29	28	27	22	33	28	24
Zn	102	83	107	97	101	99	104	95	104	102	100
Zr	251	273	186	220	166	160	139	222	235	192	176
					C. I. P. W. Norms						
Q	-	-	-	-	2.54	2.15	0.75	2.40	3.29	-	-
or	11.47	5.09	9.23	9.17	4.38	4.79	5.56	7.63	7.10	8.99	8.46
ab	29.27	18.77	29.33	26.03	24.26	22.90	23.92	27.81	25.02	22.48	25.19
an	18.04	21.75	24.77	22.71	23.56	23.26	23.34	20.11	20.82	21.35	17.54
ne	3.06	5.12	-	-	-	-	-	-	-	-	-
di	11.65	22.71	9.16	20.40	17.63	21.59	18.27	25.58	18.88	19.12	24.05
hy	-	-	14.86	9.91	19.12	17.36	19.57	6.32	13.08	8.51	10.59
ol	14.75	12.95	1.87	2.71	-	-	-	-	-	11.35	1.87
mt	3.10	3.03	2.67	2.84	2.97	2.96	2.91	2.68	2.58	2.99	2.89
il	5.26	7.98	4.77	5.43	4.26	4.10	3.95	6.61	4.24	4.48	4.60
ap	1.29	1.83	0.96	1.16	0.79	0.76	0.79	0.85	0.96	1.29	0.98

To be continued

Continued

Sample No.	C703	C714	C734B	C742A	C742B	C704	C713A	C714A	C715	C716A
Rock Type	alk	alk	alk	alk	alk	th	th	th	th	th
%										
SiO_2	48.83	50.60	50.17	52.04	52.02	52.59	52.98	50.98	51.75	51.22
Al_2O_3	12.33	14.45	14.96	14.91	14.42	14.55	12.80	13.76	14.40	15.46
ΣFeO	10.49	8.30	8.66	8.99	8.93	9.26	10.29	10.11	7.95	8.25
MgO	8.53	7.28	6.39	6.19	6.07	6.92	7.43	6.28	6.69	6.24
CaO	10.27	9.68	10.39	9.43	9.61	10.12	9.06	10.50	11.43	10.64
Na_2O	2.73	3.27	3.31	3.51	3.47	3.05	2.82	3.19	3.14	3.17
K_2O	1.69	2.10	1.03	1.35	1.29	0.62	0.86	0.75	1.05	0.58
TiO_2	2.75	2.21	1.80	1.99	1.92	1.63	1.96	2.28	1.34	1.89
MnO	0.179	0.126	0.119	0.124	0.129	0.155	0.179	0.139	0.120	0.138
P_2O_5	0.53	0.38	0.40	0.50	0.56	0.33	0.28	0.50	0.55	0.54
L.O.I	2.28	2.06	2.45	1.25	1.15	0.68	0.93	0.80	1.71	2.46
Total	100.609	100.456	99.679	100.284	99.569	99.905	99.589	99.289	100.130	100.588
ppm										
Ba	522	702	263	337	304	249	250	306	248	322
Co	53	49	47	55	51	48	50	48	36	43
Cr	270	343	260	300	289	347	391	315	347	274
Cu	63	61	57	65	74	41	50	87	28	44
Li	14	13	8	5	5	6	5	5	6	8
Nb	55	53	37	49	41	24	23	26	38	31
Nd	24	24	24	24	28	15	14	20	31	25
Ni	159	201	159	209	204	147	176	182	101	107
Rb	42	52	17	30	28	11	17	10	25	16
Sc	23	25	25	26	24	21	26	26	27	22
Sr	818	820	453	569	552	389	304	402	594	467
V	176	215	164	174	185	158	196	232	157	183
Y	23	16	20	22	24	18	14	24	23	18
Zn	110	102	87	101	101	94	112	100	78	89
Zr	185	208	169	218	217	107	125	136	201	139
					C. I. P. W. Norms					
Q	-	-	-	-	-	2.10	3.80	0.63	-	1.28
or	10.00	12.42	6.09	7.99	7.63	3.67	5.09	4.44	6.21	3.43
ab	23.07	26.76	27.97	29.67	29.33	25.78	23.83	26.96	26.54	26.79
an	16.37	18.51	22.89	20.91	19.93	24.15	19.70	20.98	22.06	26.21
ne	-	0.48	-	-	-	-	-	-	-	-
di	25.39	21.96	21.34	18.63	19.88	19.59	19.18	22.95	25.43	18.96
hy	5.30	-	8.18	12.98	14.17	17.44	19.75	14.18	10.85	14.30
ol	11.57	10.83	5.33	1.87	0.02	-	-	-	1.71	-
mt	3.04	2.41	2.51	2.61	2.60	2.68	2.99	2.93	2.31	2.39
il	5.23	4.20	3.42	3.78	3.65	3.10	3.72	4.33	2.55	3.59
ap	1.16	0.83	0.87	1.09	1.22	0.72	0.61	1.09	1.20	1.18

To be continued

Continued

Sample No.	C716B	C719	C723B	C723C	C725	C730	C734C	C736	C737	K810B
Rock Type	th	th	th	th	th	th	th	th	th	alk
%										
SiO_2	50.85	52.75	52.13	52.80	52.97	50.73	51.27	52.41	52.57	47.88
Al_2O_3	14.80	14.50	15.07	14.05	14.82	15.12	13.21	14.12	14.15	14.40
ΣFeO	8.20	7.87	8.48	9.05	7.73	9.24	9.46	8.63	9.82	9.59
MgO	5.93	5.92	6.85	7.87	6.45	6.37	7.97	5.96	5.24	8.31
CaO	10.64	9.11	9.76	9.30	8.09	10.19	9.54	9.13	9.98	10.62
Na_2O	3.26	3.05	3.32	3.05	2.60	3.18	3.15	3.03	2.02	3.41
K_2O	0.64	0.90	0.94	0.51	0.36	0.42	0.54	0.62	0.15	1.59
TiO_2	1.90	1.61	1.90	1.72	1.22	1.73	1.73	1.57	1.84	2.70
MnO	0.143	0.109	0.152	0.157	0.108	0.156	0.161	0.130	0.108	0.178
P_2O_5	0.48	0.40	0.54	0.56	0.26	0.63	0.54	0.27	0.12	0.94
L.O.I	2.25	3.73	0.88	1.24	4.50	1.80	2.15	4.16	3.05	1.18
Total	99.093	99.949	100.022	100.307	99.108	99.566	99.721	100.030	99.048	100.798
ppm										
Ba	350	213	290	308	198	260	298	153	213	642
Co	47	42	42	48	31	47	52	37	26	53
Cr	298	271	288	328	275	296	306	280	254	377
Cu	44	40	55	47	29	44	49	44	35	48
Li	10	11	6	6	6	7	8	9	5	13
Nb	37	35	37	29	22	26	27	29	15	64
Nd	22	20	29	25	11	26	24	12	8	50
Ni	118	150	149	182	157	134	193	168	139	175
Rb	18	20	21	17	2	14	17	2	2	42
Sc	26	20	21	24	19	22	23	18	17	28
Sr	464	443	507	312	259	379	353	412	149	779
V	176	138	184	163	95	165	156	131	79	287
Y	17	24	23	19	12	13	18	21	12	33
Zn	88	97	85	113	74	101	98	96	67	98
Zr	128	166	182	131	102	102	128	162	88	276
					C. I. P. W. Norms					
Q	1.09	4.91	0.44	2.89	8.76	1.14	0.60	5.05	11.07	-
or	3.79	5.32	5.56	3.02	2.13	2.48	3.19	3.67	0.89	9.40
ab	27.55	25.78	28.06	25.78	21.97	26.88	26.62	25.61	17.07	21.18
an	23.83	23.18	23.41	24.11	27.67	25.71	20.28	23.06	29.06	19.25
ne	-	-	-	-	-	-	-	-	-	4.14
di	21.20	15.95	17.66	15.96	8.87	17.21	19.32	16.80	16.20	22.46
hy	12.36	14.87	16.76	21.20	20.07	17.01	20.34	15.60	15.11	-
ol	-	-	-	-	-	-	-	-	-	13.21
mt	2.38	2.28	2.47	2.62	2.25	2.68	2.74	2.51	2.84	2.78
il	3.61	3.06	3.61	3.27	2.32	3.29	3.29	2.98	3.50	5.13
ap	1.05	0.87	1.18	1.22	0.57	1.38	1.18	0.59	0.26	2.05

To be continued

Continued

Sample No.	K812C	K815A	K821	K822	K823	K832	K801A	K808D	T901	M001
Rock Type	alk	alk	alk	alk	alk	alk	th	th	th	alk
%										
SiO_2	47.91	46.33	45.81	48.92	47.58	47.00	52.20	52.37	51.17	48.83
Al_2O_3	13.67	15.83	12.34	13.23	13.86	14.22	14.60	13.02	14.00	14.29
ΣFeO	9.83	8.43	11.28	10.05	9.98	9.82	8.51	9.24	9.25	9.75
MgO	9.48	8.47	11.31	8.92	7.83	8.52	6.47	8.31	6.04	8.10
CaO	9.98	11.92	9.34	9.95	9.77	11.22	11.16	10.43	9.99	8.71
Na_2O	3.15	2.86	3.91	3.22	2.95	2.96	3.24	2.79	2.69	2.61
K_2O	1.89	2.22	0.56	1.42	1.02	1.09	0.82	0.64	0.86	1.76
TiO_2	2.58	2.38	3.22	2.85	2.58	2.75	1.61	1.38	2.06	2.40
MnO	0.175	0.158	0.175	0.163	0.166	0.183	0.165	0.180	0.127	0.143
P_2O_5	1.03	0.98	0.90	0.83	0.78	0.65	0.49	0.48	0.35	0.59
L.O.I	0.50	1.14	1.04	1.22	3.25	1.87	1.03	1.46	3.84	2.47
Total	100.195	100.718	99.885	100.773	99.766	100.283	100.295	100.300	100.377	99.653
ppm										
Ba	587	934	868	737	667	934	227	174	143	360
Co	55	50	62	57	58	53	41	46	40	44
Cr	412	373	400	385	350	294	298	344	211	292
Cu	57	64	69	62	54	64	41	52	56	54
Li	6	30	14	15	12	20	7	6	10	11
Nb	62	70	60	65	62	57	27	26	27	42
Nd	50	54	57	47	37	39	20	24	30	44
Ni	256	204	364	293	285	168	110	169	102	153
Rb	44	44	25	30	28	15	17	13	4	25
Sc	23	23	25	23	25	18	26	28	30	24
Sr	788	1083	665	980	785	698	417	332	374	580
V	240	258	226	164	230	255	203	208	189	199
Y	27	29	33	34	27	24	20	20	28	26
Zn	108	80	101	100	102	93	104	99	95	96
Zr	235	259	179	280	200	218	134	125	160	215
					C. I. P. W. Norms					
Q	-	-	-	-	-	-	0.31	1.56	3.82	-
or	11.18	13.13	3.31	8.40	6.03	6.45	4.85	3.79	5.09	10.41
ab	20.70	9.64	23.05	26.84	24.93	20.86	27.38	23.58	22.73	22.06
an	17.54	23.76	14.44	17.42	21.53	22.26	22.84	21.08	23.55	22.04
ne	3.21	7.87	5.42	0.20	-	2.25	-	-	-	-
di	20.82	23.76	21.33	21.77	18.06	23.81	24.06	22.52	19.49	14.29
hy	-	-	-	-	9.69	-	13.24	19.97	14.50	14.49
ol	16.24	12.31	19.94	14.78	8.96	13.30	-	-	-	6.88
mt	2.86	2.45	3.28	2.91	2.90	2.84	2.47	2.68	2.68	2.83
il	4.90	4.52	6.12	5.42	4.90	5.23	3.06	2.62	3.91	4.56
ap	2.25	2.14	1.96	1.81	1.70	1.42	1.07	1.05	0.76	1.29

TABLE 3
Neutron activation analysis data of basaltic rocks from the Western Foothills of Taiwan

Sample no.	Rock type	La	Ce	Nd	Sm	Eu	Tb	Yb	Lu	Hf	Ta	Th	U
						(ppm)							
Kungkuan Stage													
Nankang-Shenkeng Area													
N201	alk	34.5	85.0	33	6.9	2.08	0.94	2.6	0.40	6.8	4.3	3.7	0.8
N202	alk	32.2	76.6	31	7.4	2.05	0.91	2.3	0.30	5.9	4.0	3.8	0.8
N216	alk	37.8	95.9	44	7.7	2.38	1.03	2.6	0.34	6.5	5.6	6.9	1.5
Shantzechiao Area (Shulin-Shanjia Area)													
S314A	alk	36.2	81.0	29	6.9	2.17	1.11	2.4	0.33	6.3	5.5	5.2	n.d.
Chingshuikeng Area (Jungho-Tucheng Area)													
J405	alk	43.2	103.5	54	9.5	3.15	1.13	3.2	0.34	8.8	4.1	5.9	1.3
J406	alk	47.7	114.4	49	10.0	2.96	1.33	2.6	0.29	10.1	5.2	6.4	1.5
J407A	alk	51.6	129.3	62	9.9	2.74	1.42	3.3	0.37	11.0	6.4	7.3	1.7
J408C	alk	34.2	85.5	44	7.3	2.71	1.05	2.5	0.27	5.4	3.1	3.7	0.9
J409B	alk	27.6	52.3	38	7.0	2.08	1.13	2.8	0.32	6.2	4.3	3.9	1.0
J410A	alk	42.5	106.2	59	10.2	2.57	1.20	3.2	0.35	7.2	7.3	8.4	2.0
J411	alk	28.7	53.1	34	6.3	2.06	1.13	2.5	0.28	6.9	4.7	3.7	0.8
J412	alk	34.9	81.1	45	9.0	2.48	1.05	2.8	0.34	6.0	3.7	5.1	1.1
Chiaopanshan Stage													
Chiaopanshan Area (Tachi-Fushing Area)													
C701	alk	29.2	44.8	22	5.8	2.01	0.86	1.9	0.25	6.4	4.8	3.4	0.9
C702	alk	32.2	43.8	25	6.2	2.25	0.90	1.8	0.28	6.2	4.2	2.8	0.8
C714	alk	33.9	45.6	24	5.5	1.87	1.04	1.7	0.25	6.2	4.4	3.4	0.9
C742A	alk	30.6	50.3	24	4.8	1.81	0.95	1.9	0.28	4.5	2.4	2.0	0.5
C742B	alk	32.2	51.2	28	5.2	1.92	0.75	1.5	0.26	4.8	2.0	2.6	0.7
Kuanhsi-Chutung Area													
K810B	alk	35.9	87.7	50	7.7	2.59	1.15	2.8	0.35	6.9	4.7	5.6	1.2
K812C	alk	39.9	100.3	50	7.8	2.49	1.03	2.6	0.30	6.2	4.7	4.9	1.1
K815A	alk	40.1	94.3	54	8.0	2.50	1.10	2.8	0.30	6.3	5.1	6.4	1.4
K821	alk	46.8	96.9	57	9.4	2.66	1.28	3.1	0.30	6.6	4.6	5.8	1.4
K822	alk	44.2	82.8	47	8.2	2.48	0.92	3.0	0.32	6.2	4.4	5.5	1.2
K832	alk	31.2	72.5	39	6.8	1.81	1.13	2.8	0.27	6.8	3.1	4.9	1.0
Mucha, Kaohsiung													
M001	alk	41.5	72.0	44	10.1	2.31	1.13	3.2	0.27	5.4	3.6	4.8	n.d.

To be continued

Continued

Sample no.	Rock type	La	Ce	Nd	Sm	Eu	Tb	Yb	Lu	Hf	Ta	Th	U
						(ppm)							
Chiaopanshan Area													
C704	th	12.6	26.4	15	3.8	1.38	0.69	1.5	0.20	3.6	1.8	2.0	0.6
C714A	th	15.8	35.2	20	4.1	1.75	0.90	1.6	0.29	4.5	1.4	1.9	0.6
C716B	th	13.6	29.0	22	4.2	1.17	0.67	1.58	0.20	3.1	1.7	2.4	0.7
C719	th	14.9	34.5	20	4.5	1.53	0.72	1.56	0.21	5.8	2.1	4.1	1.2
C725	th	8.2	17.2	11	3.2	1.20	0.51	1.46	0.20	3.2	1.4	1.7	0.6
C730	th	15.6	36.4	26	6.2	1.70	0.87	1.50	0.21	3.2	1.5	2.2	0.6
C736	th	9.4	20.8	12	3.7	1.36	0.53	1.50	0.21	4.3	1.9	2.8	0.8
C737	th	6.2	12.0	8	2.2	0.85	0.52	1.49	0.20	2.7	0.8	1.2	0.4
Kuanhsi-Chutung Area													
K801A	th	14.6	36.4	20	5.9	1.75	0.75	1.70	0.22	3.7	1.8	2.8	n.d.
K808D	th	16.0	38.8	24	5.2	1.72	0.72	1.84	0.23	3.5	1.9	3.0	n.d.
Chienshan, Yingko													
E622	th	13.7	33.0	19	5.2	1.84	0.75	1.89	0.25	5.9	1.6	2.9	n.d.
Hengchi, Sanhsia													
H502	th	18.2	41.1	25	5.7	2.06	0.92	2.28	0.25	4.3	1.7	2.4	n.d.
H503	th	16.6	44.0	25	6.2	1.67	0.68	2.15	0.20	4.6	1.7	2.3	n.d.
H504	th	12.5	22.7	16	4.5	1.45	0.61	1.72	0.22	3.8	1.7	1.9	n.d.
Taliaodi													
T901	th	25.3	46.0	30	7.9	2.08	0.75	2.24	0.28	5.1	1.2	2.3	n.d.

vs. Al_2O_3 plot (Kuno, 1959), basalts of the Kungkuan stage fall into the domain of alkali rock. While the volcanics of the Chiaopanshan stage are mainly alkalic and tholeiitic (text-fig. 3). In the (Na_2O+K_2O) vs. SiO_2 plot, the alkali rocks are subdivided into nephelinite, basanite and alkali basalt (text-fig. 4). The alkali rocks from the Western Foothills of Taiwan fall into the basanite and alkali basalt fields. Chen (1990) proposed that the basaltic volcanics from western Taiwan can be divided into basanitoid-alkali olivine basalt series, teschenite-alkali synite series and tholeiites. Accordingly, the volcanics of the Kungkuan stage may be correlated with the basanitoid-alkali olivine basalt series or provisionally be recognized as alkali basalts. The basaltic rocks of the Chiaopanshan stage, on the other hand, are comprised of variable types including alkali basalt and tholeiite.

The AFM plots of figure 5 show a comparison of the variation trends of pigeonitic and hypersthenic rock series of the Hakone area, Japan (Kuno, 1950) and alkali basalts of Penghu. The Kungkuan stage volcanics are notably more alkali rich and more iron rich than the alkali basalts of the Chiaopanshan stage or the Penghu Islands. The AFM plots (text-fig. 5) reveal that the Chiaopanshan stage volcanics fall substantially in the domain of alkali basalts of the Penghu Islands. The average chemical

TABLE 4
Average chemical compositions of the basaltic rocks from the Western Foothills of Taiwan and the Penghu Islands

Rock type	Alkali basalt				Tholeiite		
Locality	Kungkuan	Chiaopan-shan	Kuanhsi-Chutung	Penghu	Chiopan-shan	Kuanchi-Chutung	Penghu
Sample no.	15	7	7	60	14	2	46
%							
SiO_2	48.54	50.17	47.35	45.72	52.00	52.29	50.79
Al_2O_3	15.93	13.97	13.94	14.33	14.34	13.81	14.53
ΣFeO	9.92	9.38	9.85	11.17	8.88	8.88	10.33
MgO	5.75	6.97	8.98	8.94	6.58	7.39	7.17
CaO	8.64	9.88	10.40	9.62	9.82	10.80	9.22
Na_2O	3.79	3.13	3.21	2.81	3.00	3.02	2.88
K_2O	1.90	1.49	1.40	1.29	0.64	0.73	0.40
TiO	3.01	2.21	2.72	2.71	1.74	1.50	2.06
MnO	0.162	0.146	0.171	0.179	0.140	0.173	0.154
P_2O_5	0.82	0.49	0.87	0.63	0.43	0.49	0.25
ppm							
Ba	781	432	767	421	261	201	133
Co	42	50	55	51	43	44	45
Cr	142	284	370	243	305	321	231
Cu	48	62	60	62	46	47	65
Li	21	10	16	9	7	7	5
Nb	43	47	63	67	29	27	29
Nd	41	24	48	46	20	22	15
Ni	95	179	249	195	150	140	167
Rb	39	34	33	32	14	10	7
Sc	23	25	24	25	22	27	25
Sr	1006	646	825	639	388	375	288
V	228	184	237	229	158	206	192
Y	28	22	30	24	18	20	20
Zn	97	100	97	107	92	102	104
Zr	282	195	235	271	136	130	135

composition of alkali basalts of the Chiaopan-shan stage and the Penghu Islands are very similar (table 4).

The Ne-Ol-Di-Hy-Qz tetrahedron (Yoder and Tilley, 1962) gives a good separation of basaltic rocks into alkali basalt, olivine tholeiite and tholeiite rock series (text-figs. 6a and 6b). In the tetrahedron diagram, the alkali basalts of the Kungkuan and Chiaopanshan stages fall into the nepheline-olivine-diopside and olivine-diopside-hypersthene fields, whereas tholeiites of the Chiaopanshan stage are predominately in the quartz-hypersthene-diopside domain. Grossly speaking, the alkali basalts of the Kungkuan stage, Kuanhsi-Chutung, and Chiaopanshan and the tholeiites of Kuanhsi-Chutung to Chiaopanshan

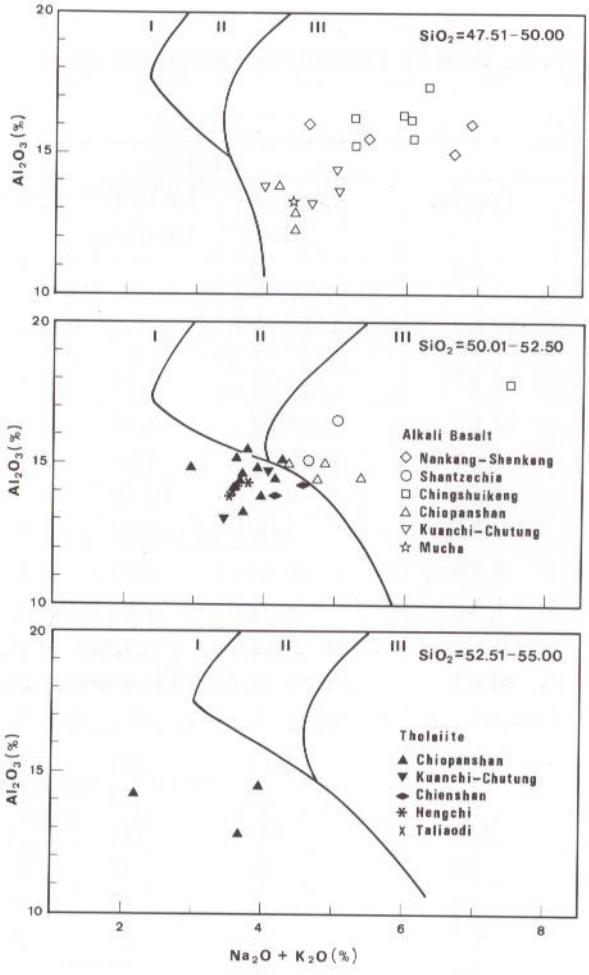

TEXT-FIGURE 3
Plot of basaltic rocks from the western Taiwan volcanic province in the Al_2O_3-Na_2O+K_2O-SiO_2 variation diagram (Kuno, 1959, 1966). I. Tholeiite, II. High-alumina basalt, III. Alkali-olivine basalt.

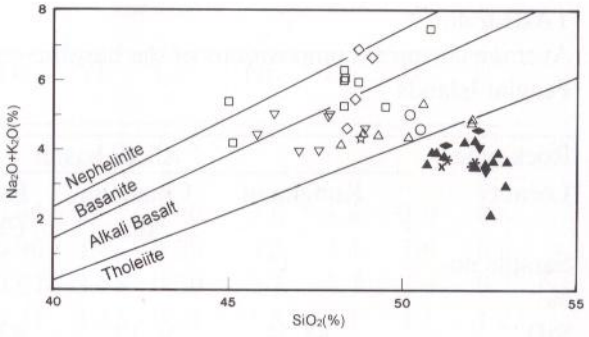

TEXT-FIGURE 4
Variation diagram of Na_2O+K_2O vs. SiO_2 for basaltic rocks from the western Taiwan volcanic province. Nephelinite-Basanite-Alkali basalt-Tholeiite field boundary from McDonald and Katsura, 1964; Strong, 1972; Saggerson and Williams, 1964. Symbols as text-figure 3.

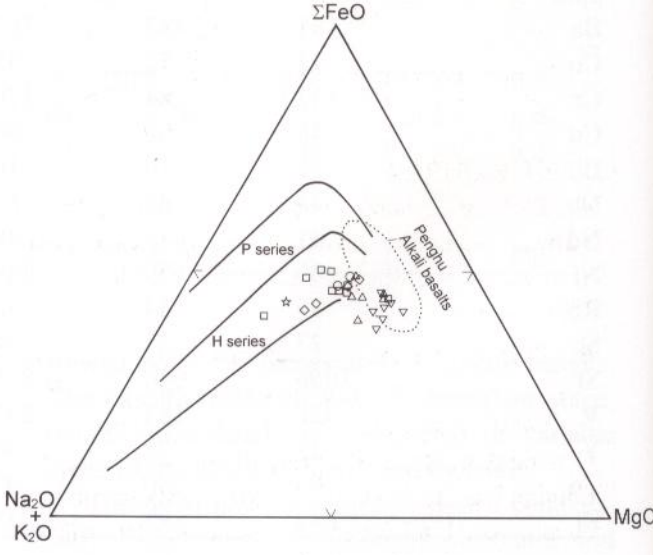

TEXT-FIGURE 5
AFM, (Na_2O+K_2O)-MgO- Σ FeO, diagram illustrating the variation of basaltic rocks from the western Taiwan volcanic province. The Penghu basalt distribution area is after Chen (1973). P and H represent the regions for pigeonitic and hypersthenic rock series in Hakone, Japan (Kuno, 1950). Symbols as text-figure 3.

show a variation trend from nepheline, hypersthene toward quartz (text-fig. 6a). Based on the ages of volcanism (table 1), the basaltic volcanic activity took place in two distinct periods: the early Miocene (21.2 - 16.3 Ma), predominantly with the eruption of alkali basalt, and the Middle to Late Miocene (14.1 - 7.6 Ma), marked by the eruption of various basalt types. Those 2 periods of basalts may display a spatial

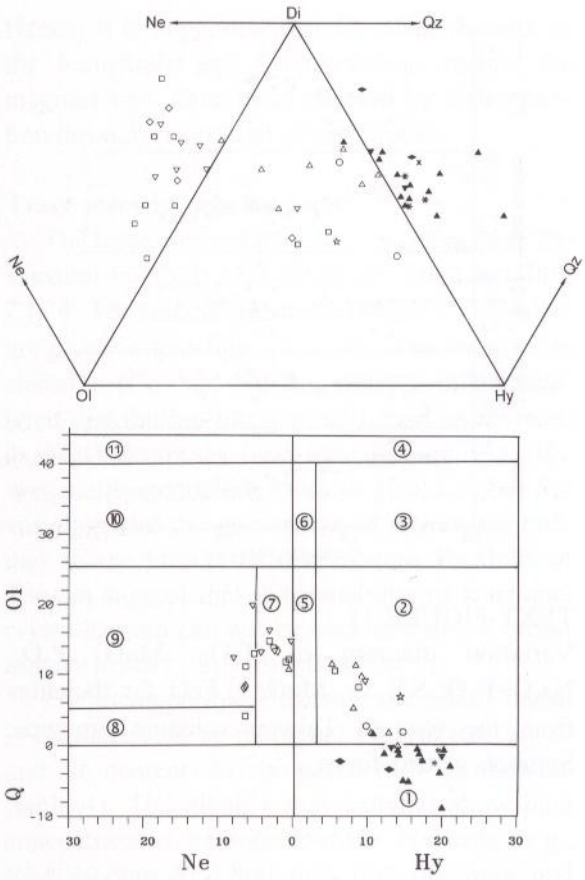

TEXT-FIGURE 6

A. Plot of basaltic rocks from the western Taiwan volcanic province in the expanded normative basaltic tetrahodron (Yoder and Tilley, 1962).

B. Plot of basaltic rocks from the western Taiwan volcanic province in Ol-Qz-Ne-Hy (OQNH) diagrams. 1. Quartz tholeiite, 2. Olivine tholeiite, 3. Picrite-tholeiite, 4. Picrite, 5. Olivine basalt, 6. Picrite-basalt, 7. Alkali olivine basalt, 8. Alkali basalt, 9. Basanite, 10. Alkali picrite-basalt, 11. Alkali picrite. Symbols as text-figure 3.

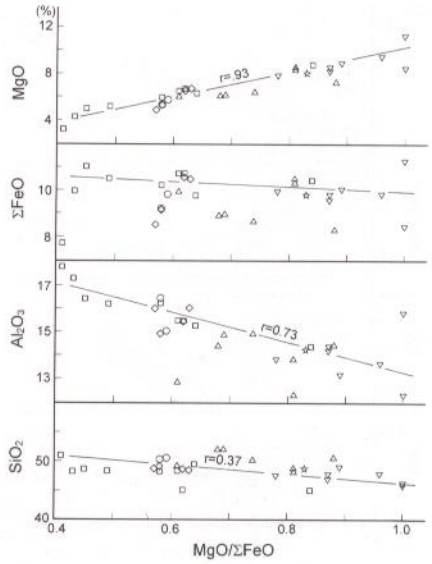

TEXT-FIGURE 7

Variation diagram of SiO_2, Al_2O_3, Σ FeO, MgO vs. MgO/ Σ FeO for alkali basalts from the western Taiwan volcanic province. Symbols as text-figure 3.

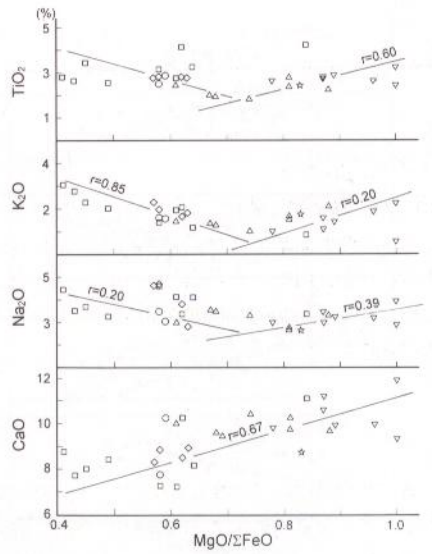

TEXT-FIGURE 8

Variation diagram of CaO, Na_2O, K_2O, TiO_2 vs. MgO/ Σ FeO for alkali basalts from the western Taiwan volcanic province. Symbols as text-figure 3.

chemical variation to reflect the variation of the C.I.P.W. norms (text-figs. 6a and 6b). For major elements and solidification index (S.I.) vs. MgO/ Σ FeO plots (text-figs. 7 to 11), it should be

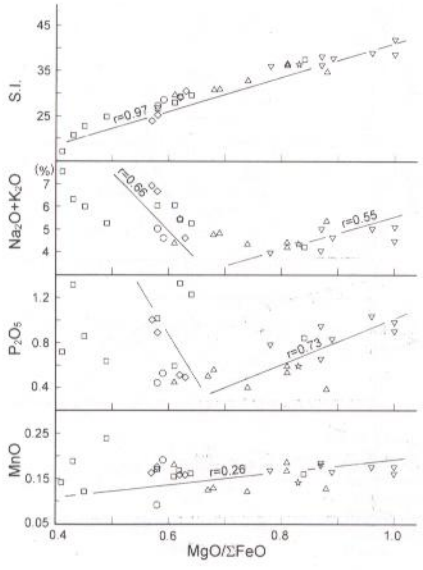

TEXT-FIGURE 9
Variation diagram of MnO, P_2O_5, Na_2O+K_2O, S.I. vs. MgO/ Σ FeO for alkali basalts from the western Taiwan volcanic province. Symbols as text-figure 3.

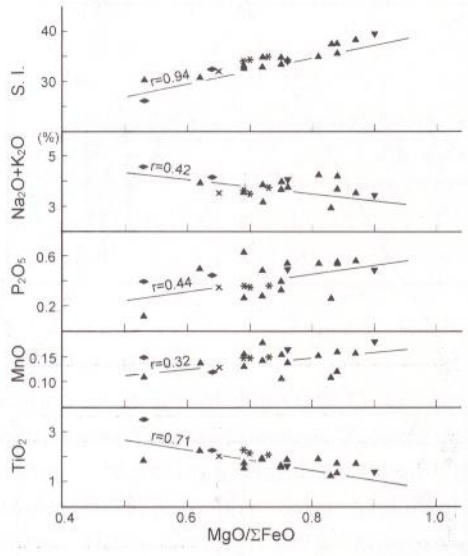

TEXT-FIGURE 11
Variation diagram of TiO_2, MnO, P_2O_5, Na_2O+K_2O, S.I. vs. MgO/ Σ FeO for tholeiites from the western Taiwan volcanic province. Symbols as text-figure 3.

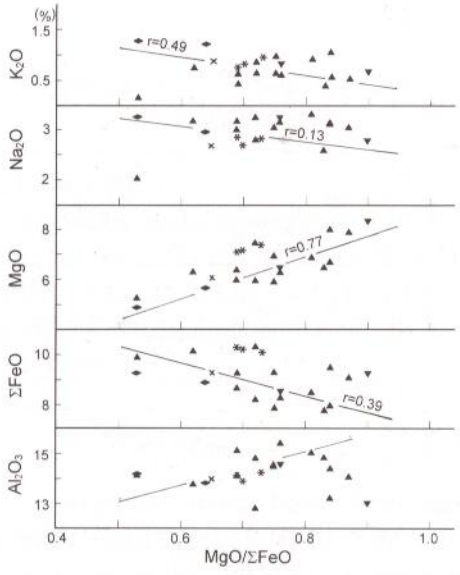

TEXT-FIGURE 10
Variation diagram of Al_2O_3, Σ FeO, MgO, Na_2O, K_2O vs. MgO/ Σ FeO for tholeiites from the western Taiwan volcanic province. Symbols as text-figure 3.

noted that most oxides have scattered distributions. Relatively good correlations have been found in the plots of S.I., MgO, CaO and MnO vs. MgO/ Σ FeO, while SiO_2 and Al_2O_3 decrease as MgO/ Σ FeO increases. These compositional changes may be controlled by differentiation of mafic minerals. A marked decrease of TiO_2, Na_2O, K_2O and Na_2O+K_2O contents with increasing MgO/ Σ FeO has been found in Kungkuan volcanics and tholeiites of the Chiaopanshan volcanic stage, while the alkali basalts of the Chiaopanshan stage have very distinct variation trends. The concentrations of Ti and K could hardly have been affected by fractionation through removal of major mantle minerals such as olivine, pyroxenes and garnet (Shaw, 1972; Philpotts and Schnetzler, 1970; Coleman *et al.*, 1965; Hart and Brooks, 1974), however, the abundance of these elements could have been affected by low silica amphibole fractionation (Gast, 1968; Aoki, 1963, 1970).

Hence, it is suggested that for alkali basalts of the Kungkuan and Chiaopanshan stages, the magmas may have been affected by differentiation through separation of amphibole.

Trace element geochemistry

The trace element data for volcanics from the Western Foothills of Taiwan are listed in tables 2 to 4. The trace elements vs. MgO/ Σ FeO plots are given in text-figs. 12 to 15. The compatible elements (Co, Cr, Ni, Sc) show a rather scattered distribution but generally tend to decrease as MgO decreases (text-figs. 12 and 13). The systematic compatible element (Co, Cr, Ni, Sc) variation and the occurrence of ultramafic nodules in the basalts of the Western Foothills of Taiwan suggest that the possibility of fractional crystallization can not be excluded in the evolutionary history of the magmas.

For incompatible elements, the alkali basalt is characterized by its higher Ba, Li, Rb, Sr, Zr and Nb contents as compared with the tholeiite (table 4). The alkali basalt samples show high concentrations of incompatible elements, e.g., Rb ≅ 40 ppm, Sr ≅ 800 ppm, Ba ≅ 600 ppm, and Nb ≅ 60 ppm. This feature is typical for alkali basalts as previously pointed out by Gast (1968) among others. Generally speaking, volcanics containing higher Ni (250-300 ppm) and Cr (500-600 ppm) contents and higher MG values ($Mg/Mg + Fe^{2+} \sim 0.68$-$0.75$) can be considered to be primary magmas (Bultitude and Green, 1971; Ringwood, 1975; Frey et al., 1978; Perfit et al., 1980). Kungkuan alkali basalts have MG values of 45-62, Co 29-58 ppm, Cr 28-266 ppm and Ni 55-155 ppm. These values are lower than those of the Chiaopanshan stage alkali basalts in which MG values range 0.55-0.67, Co 46-62 ppm, Cr 258-400 ppm, and Ni 146-364 ppm (table 2). This indicates without ambiguity that these rocks from the Kungkuan stage are derivatives and have experienced more differentiation than the alkali basalts of the Chiaopanshan stage.

The concentrations of incompatible elements such as Ti, K, Rb, Sr, Ba, Zr and Th could

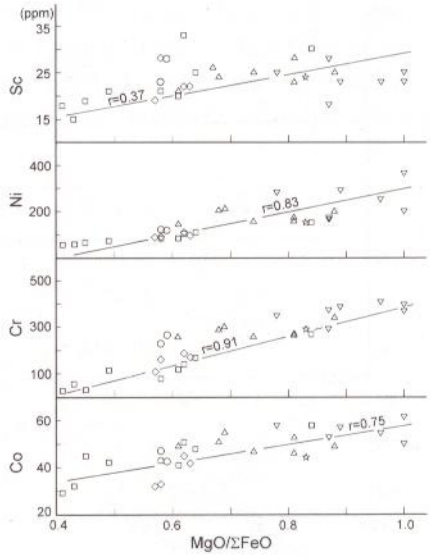

TEXT-FIGURE 12
Variation diagram of trace elements Co, Cr, Ni, Sc vs. MgO/ Σ FeO for alkali basalts from the western Taiwan volcanic province. Symbols as text-figure 3.

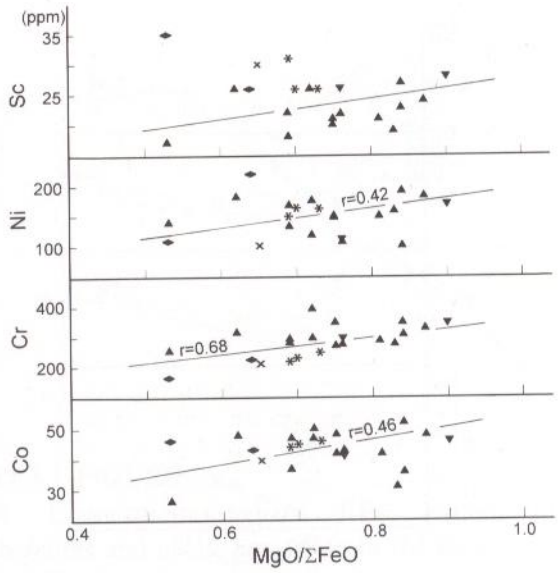

TEXT-FIGURE 13
Variation diagram of trace elements Co, Cr, Ni, Sc vs. MgO/ Σ FeO for tholeiites from the western Taiwan volcanic province. Symbols as text-figure 3.

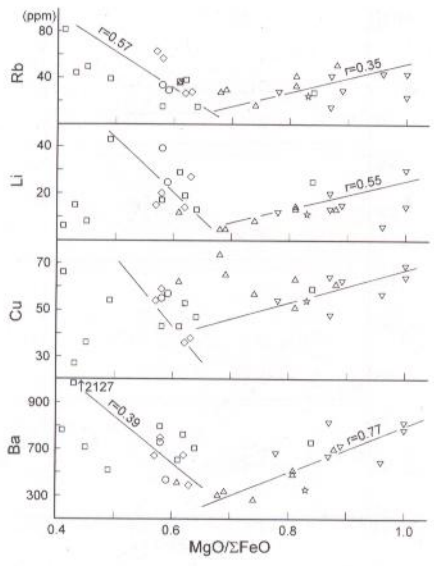

TEXT-FIGURE 14
Variation diagram of trace elements Ba, Cu, Li, Rb vs. MgO/ Σ FeO for alkali basalts from the western Taiwan volcanic province. Symbols as text-figure 3.

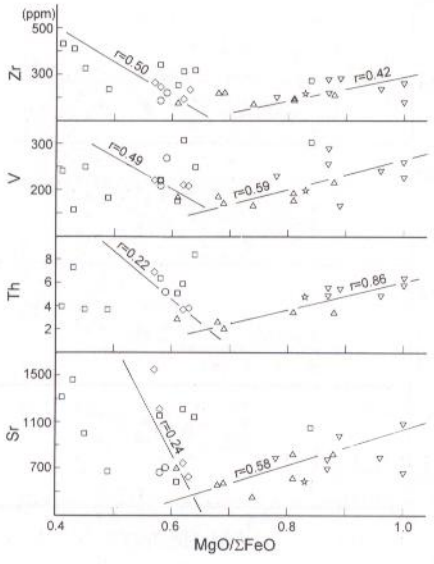

TEXT-FIGURE 15
Variation diagram of trace elements Sr, Th, V, Zr vs. MgO/ Σ FeO for alkali basalts from the western Taiwan volcanic province. Symbols as text-figure 3.

hardly have been affected by fractionation through removal of major mantle minerals such as olivine, pyroxenes and garnet (Shaw, 1970; Philpotts and Schnetzler, 1970; Coleman *et al.*, 1965; Hart and Brooks, 1974). The higher contents of the incompatible elements (Rb, Sr, Ba, Zr, Th and REE) in volcanics of the Kungkuan stage than in the Chiaopanshan stage alkali basalt (tables 3 and 4) and the systematic incompatible element variation found in alkali basalts of the Chiaopanshan stage (text-figs. 14 and 15) cannot be explained by ferromagnesian minerals fractional crystallization. However, the abundances of these elements can be affected by differentiation through separation of amphibole (Gast, 1968; Aoki, 1963, 1970). In alkali basalts of western Taiwan (Mafu) and the Penghu Islands (Tungchihsu), Ti-rich hornblende (kaersutite), Al-augite and phlogopite were found as megacrysts. Irving (1978) has suggested that megacrysts are formed by flow crystallization in which crystals are continuously plated onto walls of narrow channels of mantle peridotite from slowly moving basaltic magmas. This mechanism could produce both fractional crystallization of the alkali magma at various depths and formation of megacrysts. The energetic burst of a later magma through the same conduit could break off these minerals on the walls and capture them as various forms of megacrysts. Chen *et al.* (1987) and Chung and Chen (1990), based on the observed REE contents of both megacrysts and the host magmas and appropriate distribution coefficients, suggested that the megacrysts of Al-augite and kaersutite represent the direct crystallization products of deep-seated magmas which were then captured by the alkali basalt. The decrease in the contents of the incompatible elements, Ti, K, Ba, Rb, Sr, Th, V, and Zr, with increasing differentiation indicates that a low-silica amphibole fractionation may have been the important mechanism for the derivation of alkali basaltic magmas in the Chiaopanshan stage. The kaersutite found in ultramafic xenoliths and as megacrysts in alkali basalts provides good

evidence for amphibole fractionation at high pressure.

The chondritic-normalized REE patterns of Kungkuan alkali basalts, Chiaopanshan stage alkali basalts and tholeiites are shown in text-figs. 16 and 17. The REE spectra of these rocks are marked by typical LREE (light rare earth element) enrichment; the $(La/Yb)_N$ ranges from 9.4 to 7.3 in Kungkuan stage alkali basalts, and 10.4 to 9.1 for Chiaopanshan stage alkali basalts and 4.8 to 2.5 in tholeiites. Juang and Chen (1992) have shown that the $(La/Yb)_N$ in Penghu basalts ranges from 6.4 to 28.9 in alkali basalts and 2.7 to 6.4 in tholeiites. These values for basaltic rocks from the Western Foothills and the Penghu Islands are comparable with basalts from continental environments (Ratcliffe, 1987; Auchapt *et al.*, 1987; Dupuy and Dostal, 1984).

DISCUSSIONS AND CONCLUSIONS

Petrotectonically, the late Tertiary-Quaternary volcanics of Taiwan can be divided into northern, eastern and western provinces. The geographical distribution of island-arc volcanic rocks of the northern province (Juang, 1988, 1993; Chen, 1990) and the rifting-continental-margin basalts of the western province exhibit some overlap. The two major criteria for discriminating among tectonic settings are the chronology and geochemistry.

Based on preliminary studies, the intraplate continental-rifting volcanism took place sporadically during the Miocene in the western deposition basin of Taiwan, especially, in the Western Foothills and the Penghu Islands. The continental-margin-rifting volcanism in northern Taiwan apparently ceased in the late Miocene. No preeminent volcanism of a later age has been found in the vicinity of Taiwan. Such a phenomenon may be explained by the effect of an intense arc-continent collision hampering continental rifting. It is interesting to note that the onset of arc magmatism in northern Taiwan has been postulated to have its origin in the west-northwesterly encroachment of the subducting Philippine Sea plate beneath the collision orogen since 5 Ma (Teng *et al.*, 1992) and that arc volcanism was very active in the Quaternary in northern Taiwan (Juang and

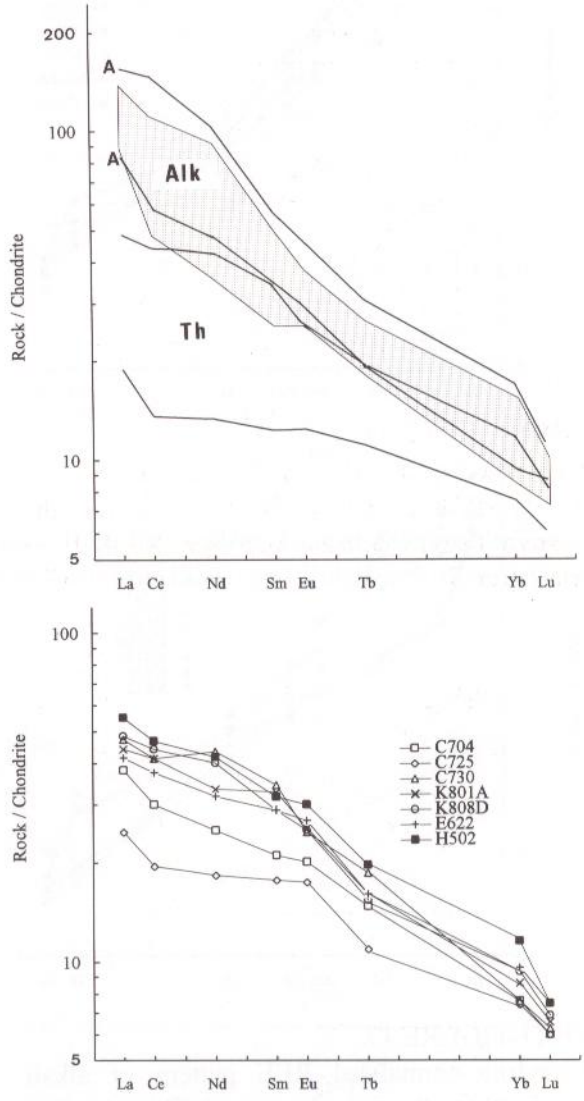

TEXT-FIGURE 16

A. Chondritic-normalized REE pattern of tholeiites and alkali basalts from the Kungkuan and Chiaopanshan stages. Condritic values from Frey *et al.*, 1968. A-A, Kungkuan stage; Alk, Chiaopanshan stage alkali basalts and Th, Chiaopanshan stage tholeiites.

B. Chondritic-normalized REE pattern of tholeiites from the Chiaopanshan stage.

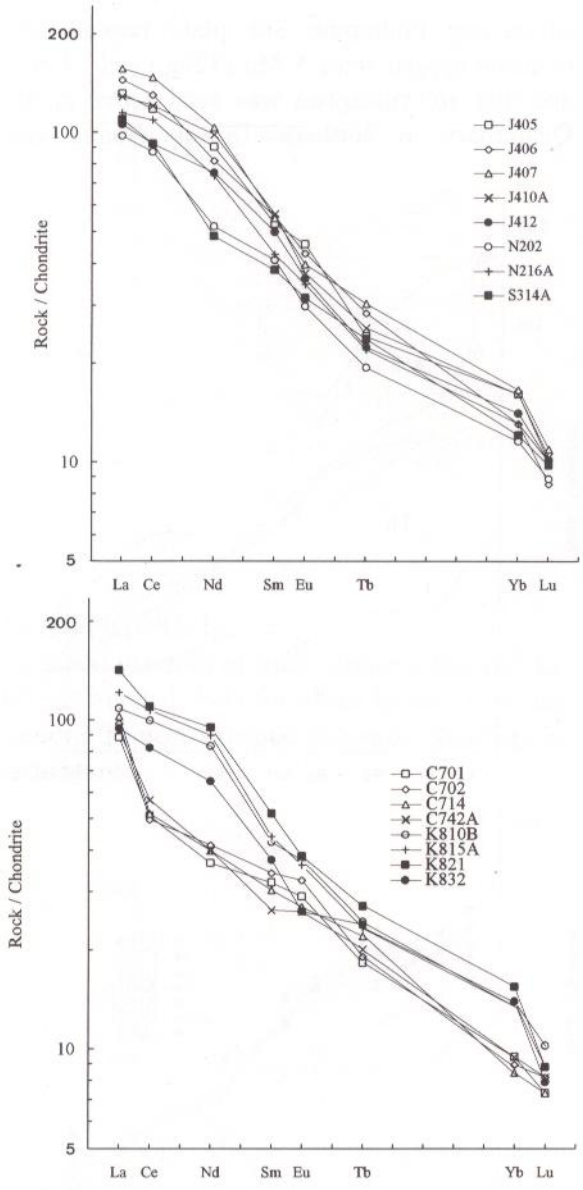

TEXT-FIGURE 17
Chondritic-normalized REE pattern of alkali basalts from the Kungkuan and Chiaopanshan stages.

Chen, 1989; Juang, 1993). From the spatial distribution, both the intraplate-continental-rifting and subduction-related island-arc volcanic rocks have been found in northwestern Taiwan. To envisage the geochemical character in association with its controlling tectonic environment, the key trace-element parameters useful in evaluating petrographic indicators are briefly discussed.

Magma and Source Mantle Geochemical Diagnosis

Ratios of highly incompatible trace elements, such as isotopic ratios, are indicative of source compositions because they do not change appreciably during either melting or fractionation. Based on La-Ba, La-Th, La-Nb and La-Ta plots (text-fig. 18), the Ba/La, Th/La, La/Nb and La/Ta ratios are more similar to those of E-MORB than to those of depleted MORB. The continental rifting basalts of the Western Foothills of Taiwan are geochemically "enriched" relative to the "depleted" MORB. The Ti-group elements, such as Zr, Hf, Nb and Ta, have high field strengths (charge/ionic radius) and consequently are not incorporated appreciably into common minerals, except for Ti in magnetite and ilmenite. As a result, all of these elements correlate positively with each other and with indices of differentiation in silica-saturated magmas, especially those not precipitating Fe-Ti oxides or amphiboles. Ratios of these elements to one another remain quite constant in basalts of all tectonic environments: Ti/Zr=80 to 100; Zr/Hf=39; Nb/Ta=17 $\pm$ 4 (text-fig. 19).

Tectonomagmatic discrimination elements

On the basis of tectonic setting, Wilson (1989) considered that 4 distinct environments exist in which magmas may be generated: constructive plate margins, destructive plate margins, oceanic intra-plate settings and continental intra-plate settings. During the past 20 years, a number of papers have appeared in which the major, minor and trace element compositions of young basaltic rocks have been related to the tectonic environment in which the basalts were generated. These have led to the development of "tectonomagmatic discrimination diagrams" which may be used to elucidate the tectonic setting of volcanic suites (Pearce and Cann, 1973;

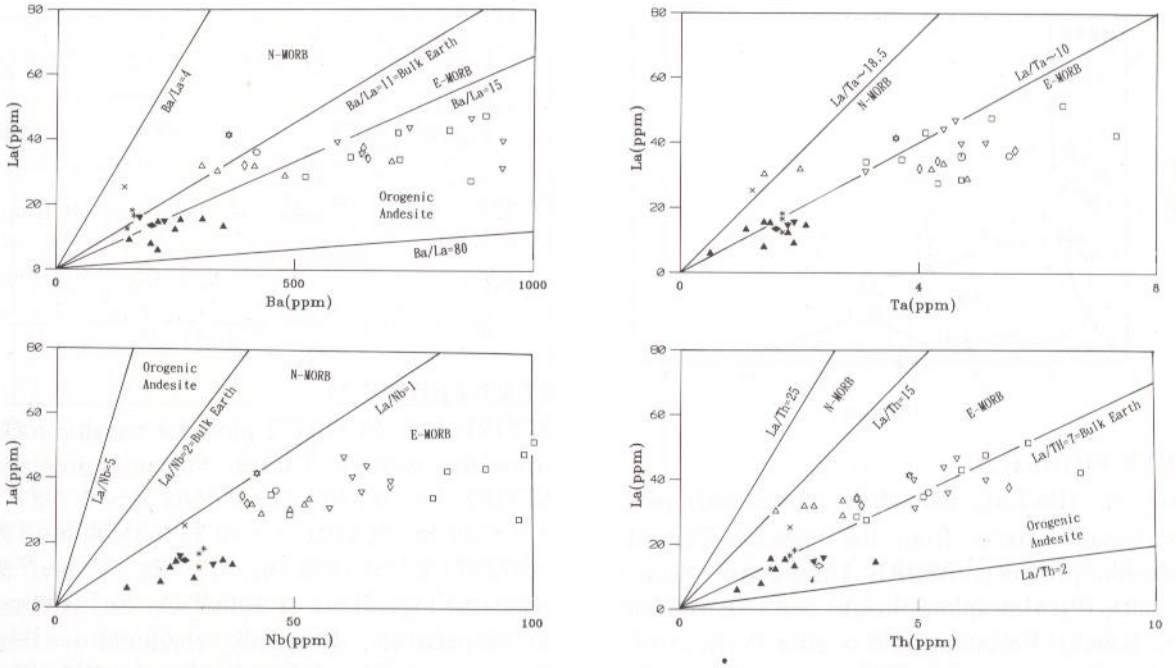

TEXT-FIGURE 18

La-Ba, La-Th, La-Nb and La-Ta plots for basaltic rocks from the western Taiwan volcanic province. The elements ratios of E-MORB and N-MORB are from Saunder (1984), and Bulk Earth from Anders (1977). Symbols as text-figure 3.

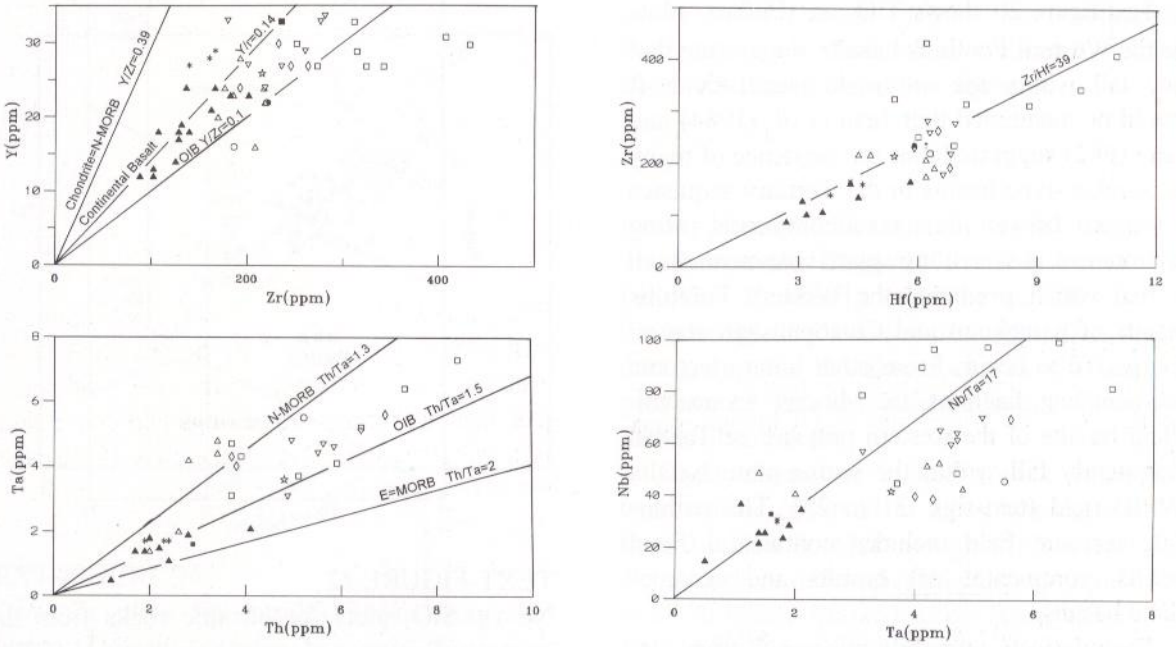

TEXT-FIGURE 19

Y-Zr, Th-Ta, Hf-Zr and Ta-Nb plots for basaltic rocks from the western Taiwan volcanic province. The elements ratio of chondrite are from Sun and Nesbitt (1977). Symbols as text-figure 3.

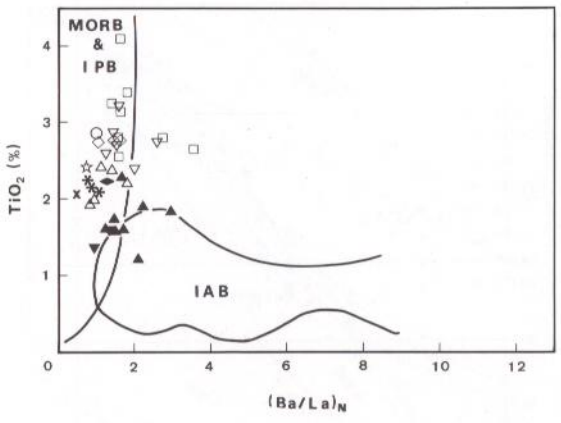

TEXT-FIGURE 20
TiO_2 vs. $(Ba/La)_N$ (chondrite normalized) plot for basaltic rocks from the western Taiwan volcanic province. MORB (Mid-ocean Ridge Basalt), IPB (Intraplate Basalt) and IAB (Island Arc Basalt). Variation field is after Perfit *et al.* (1980). Symbols as text-figure 3.

Pearce and Norry, 1979; Pearce, 1983; Davidson, 1987; Wilson, 1989).

Text-figure 20 shows TiO_2 vs. $(Ba/La)_N$ plots for the Western Foothills basalts, suggesting that they fall within the intraplate basalt field. It should be mentioned that Juan *et al.* (1984) and Sun (1982) suggested that the existence of many half-graben-type basins in the Tertiary sequence in western Taiwan indicates a continental rifting environment in which intraplate volcanism, such as that which produced the Western Foothills basalts of Kungkuan and Chiaopanshan stages, is expected to occur. From other binary tectonic discriminating diagrams, the Miocene continental-rifting basalts of the western province of Taiwan consistently fall within the within-plate basalts (WPB) field (text-figs. 21 to 25). The within-plate tectonic field includes continental flood basalts, continental rift basalts and oceanic-island basalts.

The relatively immobile minor and trace elements are used to identify the tectonic setting of volcanic suites; the most commonly used are the

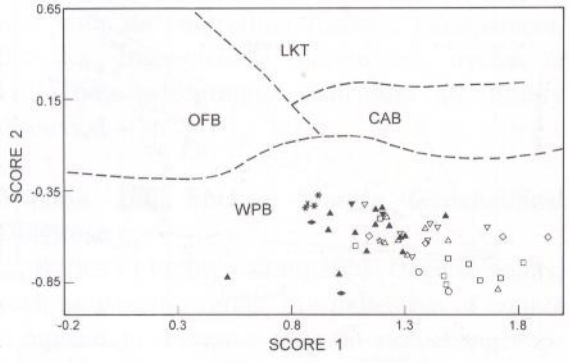

TEXT-FIGURE 21
SCORE 1 vs. SCORE 2 plots for basaltic rocks from the western Taiwan volcanic province. SCORE 1 = -0.3707 Ti - 0.0668 Zr - 0.3987 Y + 0.8362 Sr; SCORE 2 = -0.3376Ti -0.5602 Zr +0.7397 Y +0.1582 Sr; Ti, Zr, Y and Sr represent logarithms of $100xTiO_2$, Zr, 3xY and Sr respectively. Boundary condition is from Bulter and Woronow (1986). LKT: low Potassium tholeiite, OFB: ocean floor basalt, CAB: calc-alkaline basalt, WPB: within-plate basalt. Symbols as text-figure 3.

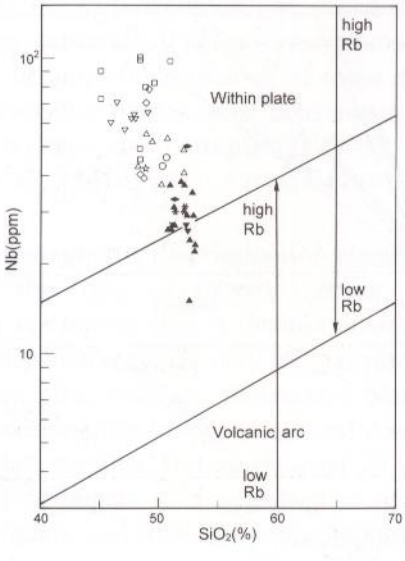

TEXT-FIGURE 22
Nb vs. SiO_2 plots for basaltic rocks from the western Taiwan volcanic province. Variation field is after Pearce and Gale (1977). Symbols as text-figure 3.

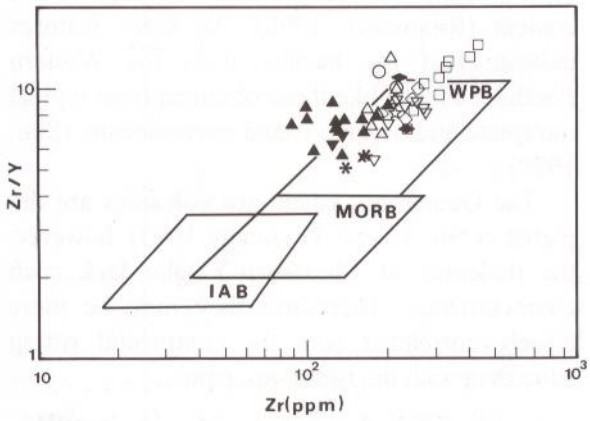

TEXT-FIGURE 23
Zr/Y vs. Zr plots for basaltic rocks from the western Taiwan volcanic province. Variation field is after Pearce and Norry (1979). WPB: within-plate basalt, MORB: mid-ocean ridge basalt, IAB: island arc basalt. Symbols as text-figure 3.

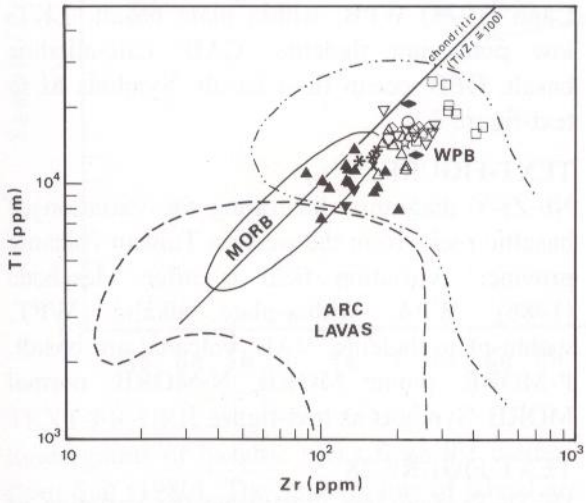

TEXT-FIGURE 24
Ti vs. Zr plots for basaltic rocks from the western Taiwan volcanic province. Variation field is after Pearce (1980). Symbols as text-figure 3.

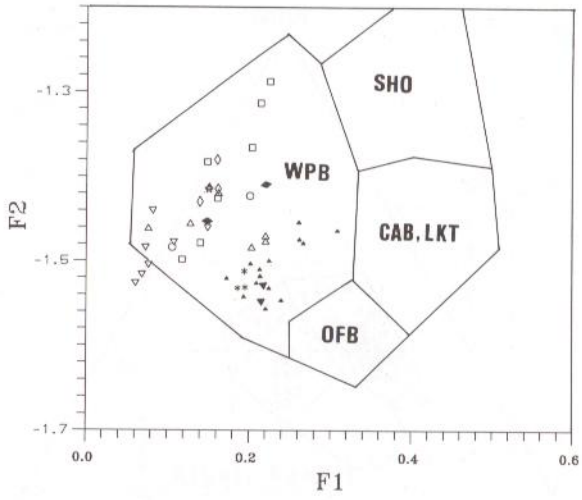

TEXT-FIGURE 25
F1 vs. F2 plots for basaltic rocks from the western Taiwan volcanic province. Variation field is after Pearce (1976). F1 = $+0.0088(SiO_2)$- $0.0774(TiO_2)$ + $0.0102(Al_2O_3)$ + $0.0066(FeO)$ - $0.017(MgO)$ - $0.0143(CaO)$ - $0.0155(Na_2O)$-$0.0007(K_2O)$, F2=- $0.0130(SiO_2)$- $0.0185(TiO_2)$ - $0.0129\ (Al_2O_3)$ - $0.0134(FeO)$- $0.0300(MgO)$-$0.0204(CaO)$-$0.0481(Na_2O)$ $+0.715(K_2O)$. WPB: within plate basalt, OFB: ocean floor basalt, LKT: low potassium tholeiite, CAB: calc-alkaline basalt, SHO: shoshonite. Symbols as text-figure 3.

ternary diagrams Ti/100 - Zr - Y $\times$3 (text-fig. 26; Pearce and Cann, 1973), 2Nb - Zr/4 - Y (text-fig. 27; Meschede, 1986) and Th - Hf/3 - Ta (text-fig. 28; Wood *et al.*, 1979). The major data points for basaltic rocks in the western province of Taiwan consistently fall within the within-plate basalts.

Highly distinctive "spiked" trace element patterns can be observed in the spiderdiagram defined by Sun & McDonough (1989) (text-fig. 29) regardless of whether they belong to tholeiite or alkali basalt. Marked spikes occur at Ba, Nb, Ta and Ti. Pronounced troughs occur at Rb, Th and K, which is particularly interesting when considering that the basaltic rocks of a non-arc

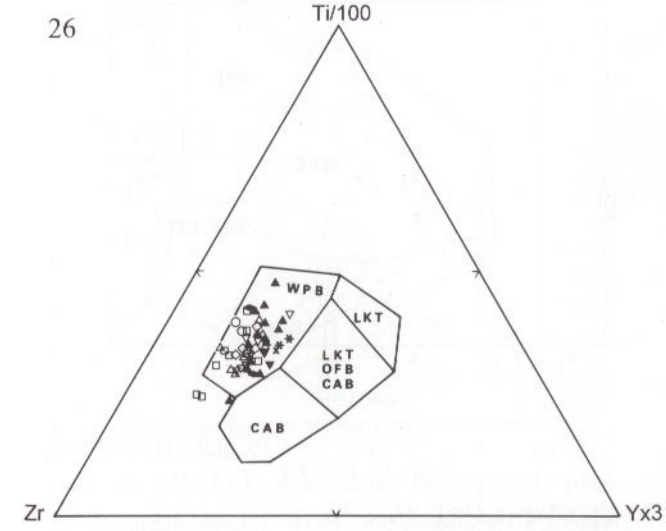

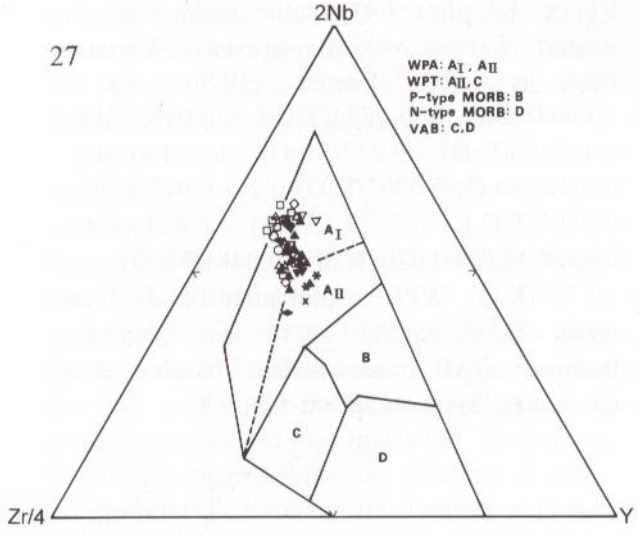

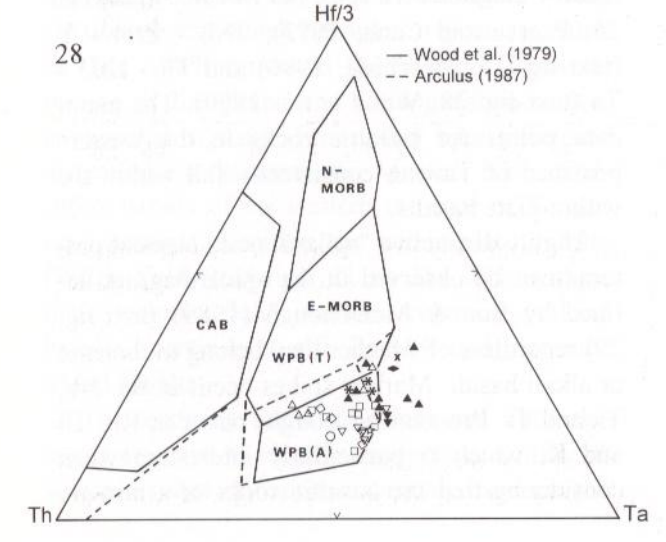

setting characteristically have a very high HFSE content (Ringwood, 1990). All these features indicate that the basalts from the Western Foothills behave like those obtained from typical intraplate and oceanic island environments (Sun, 1980).

The Quaternary island-arc volcanics are depleted in Nb, Ta and Ti (Juang, 1993), however, the tholeiites of Chienshan-Yingko lack such characteristics. Therefore, they may be more closely correlated with the continental rifting suite than with the island-arc suite.

Differentiation and Partial Melting

Based on MgO - ΣFeO/MgO + ΣFeO plots (text-fig. 30), the alkali basalts of the Chiaopanshan stage seem to have experienced olivine and pyroxene fractional crystallization, while the

TEXT-FIGURE 26
Ti-Zr-Y diagrams illustrating the variation of basaltic rocks from the western Taiwan volcanic province. Variation field is after Pearce and Cann (1973) WPB: within plate basalt, LKT: low potassium tholeiite, CAB: calc-alkaline basalt, OFB: ocean floor basalt. Symbols as in text-figure 3.

TEXT-FIGURE 27
Nb-Zr-Y diagrams illustrating the variation of basaltic rocks from the western Taiwan volcanic province. Variation field is after Meschede (1986). WPA: within-plate alkalic, WPT: within-plate tholeiite, VAB: volcanic arc basalt, P-MORB: plume MORB, N-MORB: normal MORB. Symbols as text-figure 3.

TEXT-FIGURE 28
Hf-Th-Ta diagrams illustrating the variation of basaltic rocks from the western Taiwan volcanic province. Variation field is after Wood *et al.* (1979). N-MORB: normal MORB, E-MORB: plume MORB, WPB: within-plate basalt, T: Tholeiite, A: alkali basalt, CAB: calc-alkali basalt. Symbols as text-figure 3.

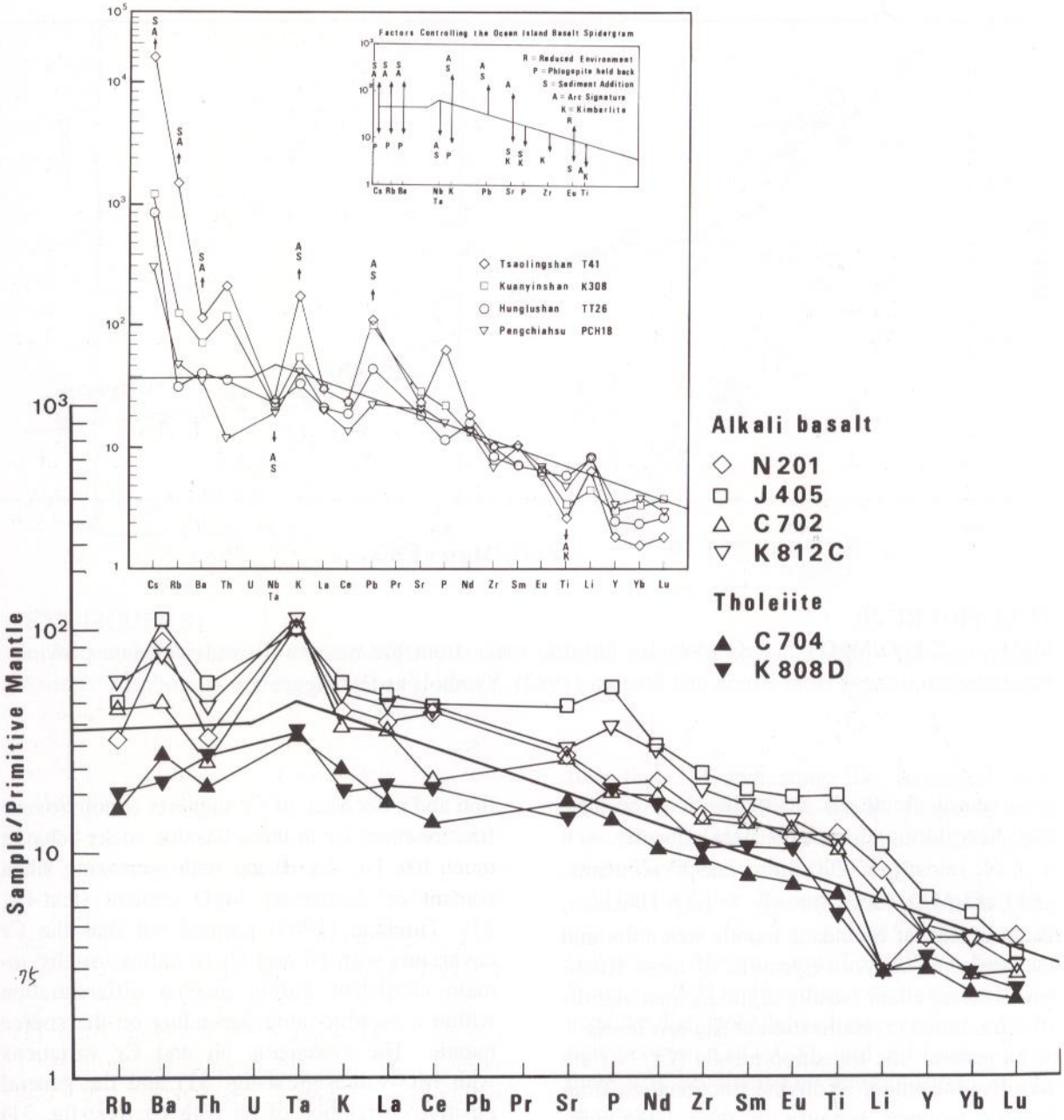

TEXT-FIGURE 29
Spidergrams of basaltic rocks from the western Taiwan volcanic province. Primitive mantle value is from Sun (1980). The spidergrams of island arc type basaltic rocks from northern Taiwan are shown for comparison.

tholeiites and alkali basalts of the Kungkuan stage show the fractionation of olivine, clinopyroxene and plagioclase.

Most of the Western Foothills basalts have

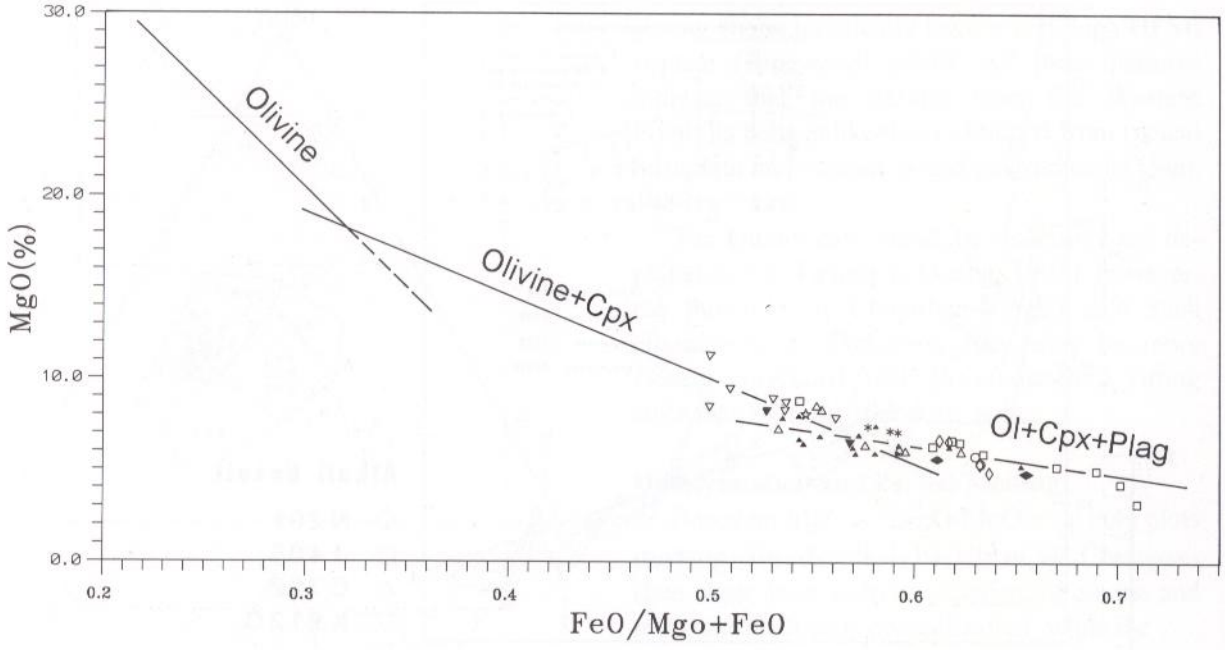

TEXT-FIGURE 30
MgO vs. Σ FeO/MgO+ Σ FeO plots for basaltic rocks from the western Taiwan volcanic province. Fractionation trend is from Brook and Nielsen (1982). Symbols as text-figure 3.

experienced fractional crystallization, because they have low and variable MgO (mostly < 8 %), Ni (mostly < 200 ppm) and Cr contents, and CaO/Al_2O_3 ratios (mostly > 1.2). However, the presence of abundant mantle xenoliths and the nepheline-normative feature of most Kuanhsi-Chutung alkali basalts argue against significant fractional crystallization at shallow levels.

In general, the transition metals (Cr, Ni) are sensitive indicators of olivine fractionation from basaltic magmas because of their large mineral/melt partition coefficients. The partition coefficients D of nickel for olivine, clinopyroxene, and plagioclase are 10, 2, and 0.01, respectively (Cox *et al.*, 1979). Similarly, the partition coefficients D of Cr for olivine, clinopyroxene, and plagioclase are 0.2, 10, and 0.01, respectively (Cox *et al.*, 1979). As a consequence, a decrease of Ni in the basaltic series of the Western Foothills suggests olivine fractionation and a decrease of Cr suggests clinopyroxene fractionation. Cr in these basaltic rocks behaves much like Ni, decreasing with increasing silica content or decreasing MgO content (text-fig. 31). Turekian (1963) pointed out that the Cr covariants with Ni and Cr/Ni ratios usually remain consistent during magma differentiation within a basaltic suite depending on the source mantle. The systematic Ni and Cr variations with MG-values (text-fig. 31) and the general positive correlation of Ni with Cr (text-fig. 31) suggest fractional crystallization of both olivine and pyroxene. The compatible element Sc is also concentrated more in clinopyroxene than in coexisting melt (Frey and Green, 1974; Irving, 1974) and consequently correlates positively with MgO (text-fig. 31). The systematic decrease of CaO/Al_2O_3 ratios with S.I. (text-fig. 32) could be interpreted to be due to the segregation of clinopyroxene. V shows a general positive correlation with Ti in the samples studied

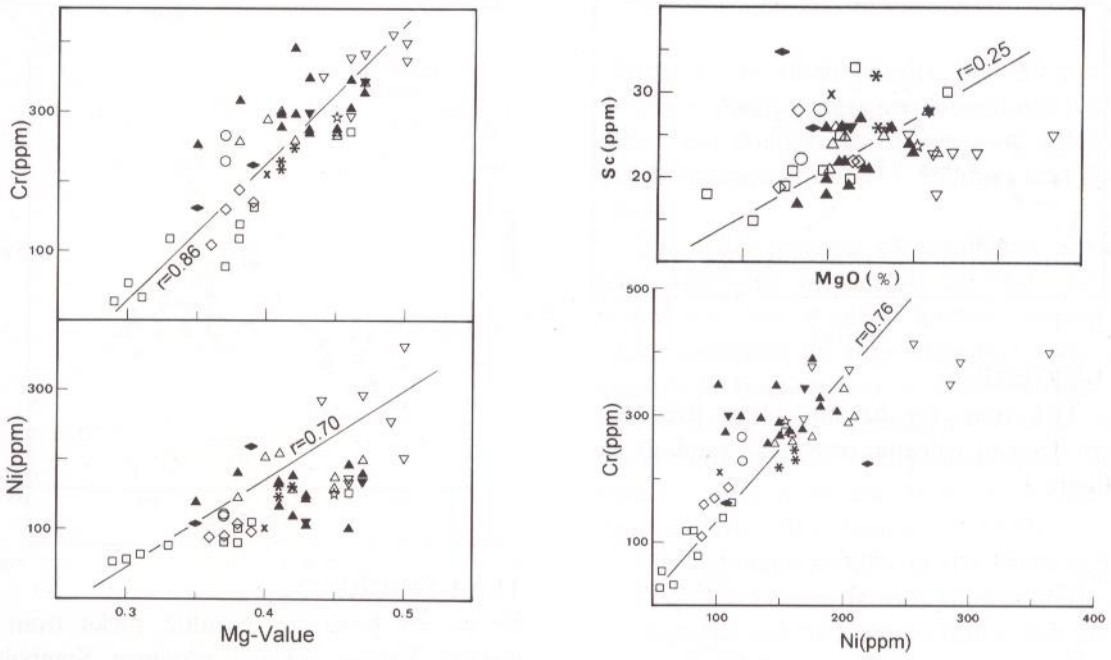

TEXT-FIGURE 31
Cr, Ni vs. MG-value, Cr-Ni, Sc-MgO plots for basaltic rocks from the western Taiwan volcanic province. Symbols as text-figure 3.

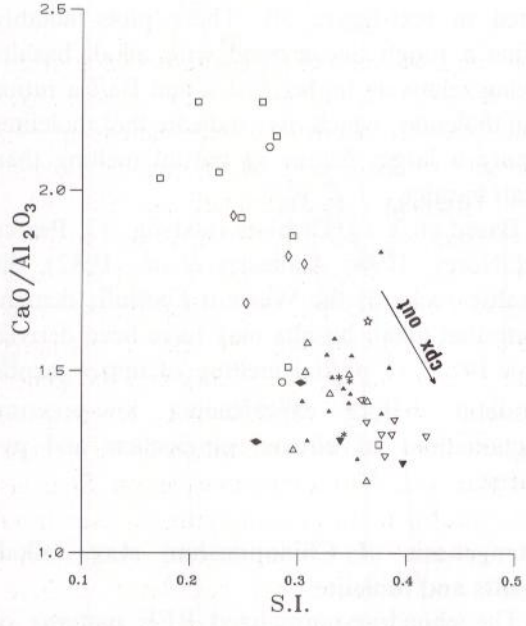

TEXT-FIGURE 32
CaO/Al_2O_3 vs. S.I. plots for basaltic rocks from the western Taiwan volcanic province. Symbols as text-figure 3.

(text-fig. 33) indicating the fractional crystallization of the Fe-Ti oxides (ilmenite or titanomagnetite) in the evolution of basaltic rocks of the Western Foothills of Taiwan.

The La/Zr vs. La and Zr vs. Sr plots (text-figs. 34 and 35) may reflect plagioclase involvement (Hwang and Lo, 1986; Fan and Hooper, 1991). However, the absence of a negative Eu anomaly and the negative correlation between CaO/Al_2O_3 and S.I. suggest that there was no significant crystallization of plagioclase.

Perhaps olivine and clinopyroxene fractionation played the most important role in the magmatic differentiation process, yet the segregation of plagioclase and Fe-Ti oxides should also be considered during magmatic evolution.

A low degree of partial melting of mantle rocks at different depths produces a substantial enrichment of Sr and Ba in the melt, owing to the fact that the accessory minerals, i.e., phlogopite and apatite, are among the first to enter

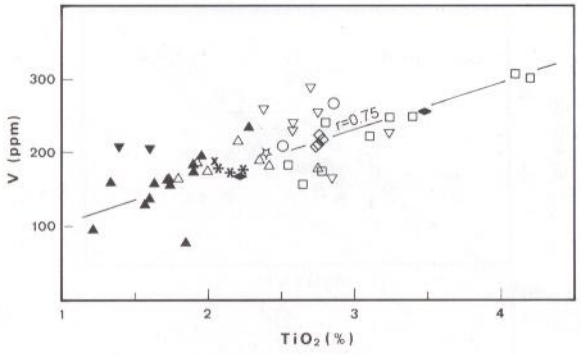

TEXT-FIGURE 33
V vs. TiO_2 plots for basaltic rocks from the western Taiwan volcanic province. Symbols as text-figure 3.

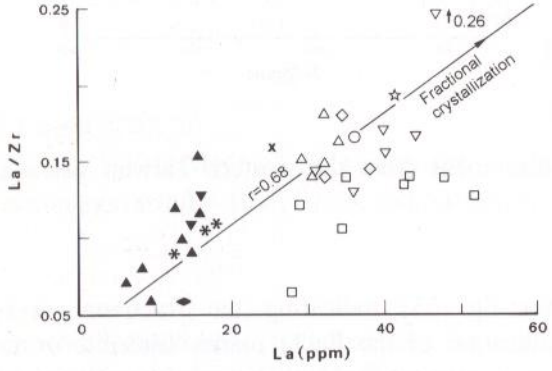

TEXT-FIGURE 34
La/Zr vs. La plots for basaltic rocks from the western Taiwan volcanic province. Fractional crystallization trend is from Hwang and Lo (1986). Symbols as text-figure 3.

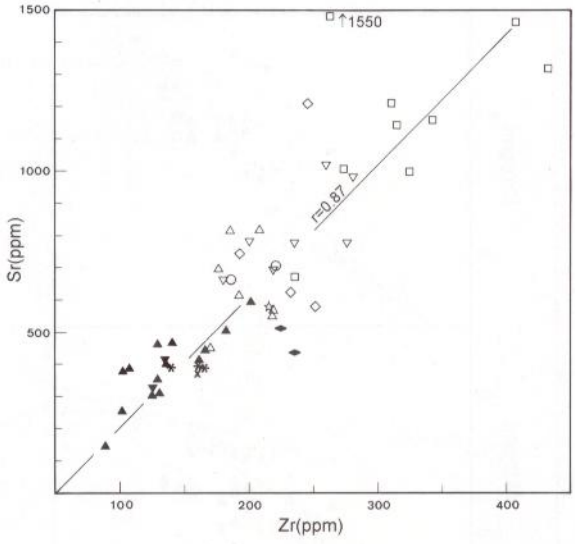

TEXT-FIGURE 35
Sr vs. Zr plots for basaltic rocks from the western Taiwan volcanic province. Symbols as text-figure 3.

the melt. The initial Sr/Ca and Ba/Ca ratios of the melt are the largest (Onuma *et al.*, 1983). An increasing degree of partial melting dilutes Sr and Ba contents in the melt with an addition of Ba- and Sr-poor major phases. The Ca content of the melt increases with the addition of Ca from garnet and clinopyroxene when these minerals begin to melt, so that Sr/Ca and Ba/Ca ratios of the melt consequently decrease with a constant Sr/Ba ratio.

The variations of Sr/Ca and Ba/Ca ratios in basaltic rocks of the Western Foothills are illustrated in text-figure 36. These plots notably define a rough linear trend with alkali basalts having relatively higher Sr/Ca and Ba/Ca ratios than tholeiites, which may indicate that tholeiites require a larger degree of partial melting than alkali basalts.

Based on Y vs. Cr plots (text-fig. 37; Pearce and Norry, 1979; Alabaster *et al.*, 1982), the basaltic rocks of the Western Foothills demonstrate that alkali basalts may have been derived by a 10~12% partial melting of upper mantle peridotite before experiencing low-pressure fractionations of olivine, plagioclase and pyroxene.

Petrogenesis of Chiaopanshan stage alkali basalts and tholeiite

The chondrite-normalized REE patterns of the Western Foothills alkali basalts and tholeiites are shown in text-figs. 16 and 17. The REE spectra of these rocks are marked by a typical LREE enrichment; $(La)_N$ ranges from

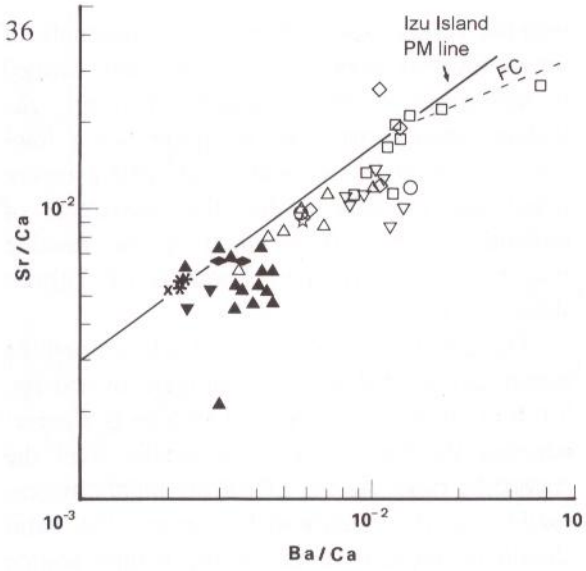

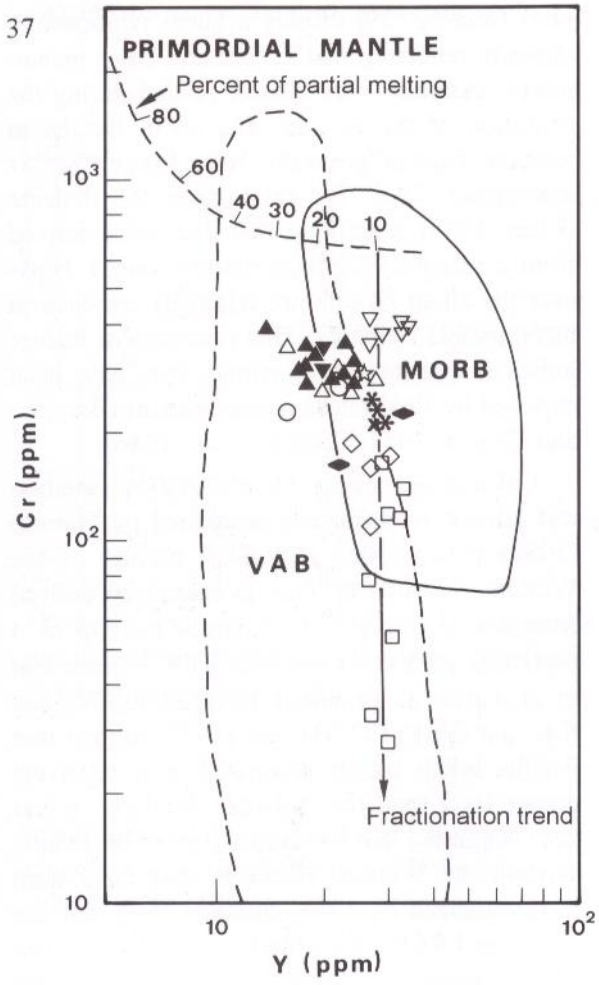

156 to 83 in alkali basalts, and 55 to 19 in tholeiites. These values are comparable with basalts from continental environments (Ratcliffe, 1987; Auchapt *et al.*, 1987; Dupuy and Dostal, 1984).

The REE patterns of amphibole separated from kaersutite megacrysts of Mafu tuff fall within the field of alkali basalts (text-fig. 38) which constrains the suggestion that a low-silica amphibole fractionation at high pressure may have been the main mechanism for the derivation of tholeiitic magma from primary alkali olivine basaltic magma in the Western Foothills of Taiwan (Hsu, 1961; Juan *et al.*, 1979).

The dominant basalts in the Western Foothills and the Penghu Islands show a minor variation in Nd and Sr isotopic ratios, but they all plot within the main OIB (ocean-island basalt) field (Chen, 1988). In addition, Chen (1988) has also determined the radiogenic isotopic ratios of two Al-augite and one kaersutitic amphibole megacrysts from the Western Foothills. The results show that these two kinds of megacrysts have Nd and Sr isotopic ratios consistent with those of the alkali basalts from Penghu and other volcanics of the Kungkuan stage ($^{87}Sr/^{86}Sr$ from 0.70352 to 0.70386 and $^{143}Nd/^{144}Nd$ from 0.51288 to 0.51296, i.e., $\varepsilon_{Nd} = 3.4$-1.7). There is a larger distribution of Sr- and Nd- isotope

TEXT-FIGURE 36
Log (Sr/Ca) vs. log (Ba/Ca) plot for basaltic rocks from the western Taiwan volcanic province. Izu Island Partial Melting Line is from Onuma *et al.* (1983). PM: Partial melting, FC: Fractional crystallization. Symbols as text-figure 3.

TEXT-FIGURE 37
Cr vs. Y plot for basaltic rocks from the western Taiwan volcanic province. Variation field VAB: Volcanic Island Arc basalt, MORB: Mid-ocean Ridge basalt are after Pearce and Norry (1979) and Alabaster *et al.* (1982). Symbols as text-figure 3.

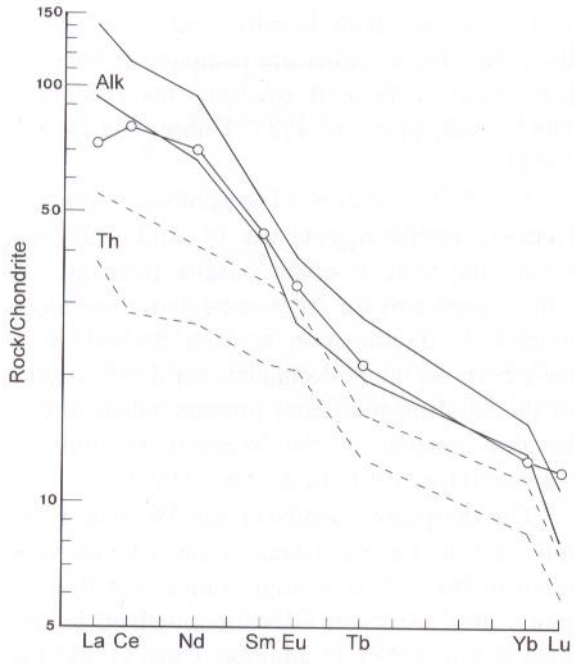

TEXT-FIGURE 38
Chondritic-normalized REE pattern of kaersutite megacryst form Mafu tuff. Alk and Th represent the distribution field of alkali basalts and tholeiites in the Kuanhsi-Chutung area.

ratios in the tholeiites than in alkali basalts of the Kuanhsi-Chutung area, which has a total range of $^{87}Sr/^{86}Sr$ = 0.70500-0.70669 and $^{144}Nd/^{143}Nd$ = 0.51255-0.51270. Consequently, derivation from a different mantle source or a mechanism of crustal contamination is plausible to account for the isotopic variation of tholeiites and alkali basalts of the Chiaopanshan stage. The isotopic ratios (Sr and Nd) of 2 Al-augite and 1 kaersutitic amphibole megacrysts from western Taiwan show that these 2 kinds of megacrysts have Sr and Nd isotopic ratios strikingly different from those of alkali basalts of the host rocks of the studied area. This suggests that these amphibole megacrysts are xenocrysts in origin with a non-equilibrium isotopic relationship between themselves and their host alkali basalts (Chen and Chung, 1985; Chung *et al.*, 1985; Chen *et al.*, 1987). These isotopic results also indicate the constraints of the megacrysts from alkali basaltic melts formed in high pressure environments. Therefore, the isotopic data restrict the possibility of a low-silica amphibole fractionation at high pressure being the mechanism for the derivation of tholeiitic magmas from alkali olivine basaltic magmas in the Western Foothills of Taiwan (Hsu, 1961; Juan *et al.*, 1979).

The LREE contents of the Western Foothills basalts are plotted against each other in text-fig. 39. It is obvious that the La-Ce slope is steeper, whereas the Sm-Ce slope is gentler than the chondritic ratio. As the LREE are highly incompatible in the mantle-melt system, the ratio should be close to those of the mantle source under a batch melting condition (Sun and Hanson, 1975). The Ce vs. K_2O and Ce vs. P_2O_5 plots (text-fig. 39) display a linear relationship, strongly reflecting that LREE and other incompatible elements were closely related during the evolution of the basalts. The alkali basalts in western Taiwan generally have lower $^{87}Sr/^{86}Sr$ and higher $^{143}Nd/^{144}Nd$ ratios than the tholeiite (Chen, 1988) suggesting that they were derived from a relatively depleted mantle source. However the alkali basalts are relatively enriched in incompatible elements. This paradoxical feature indicates that the source regions may have been enriched by fluid phase metasomatism (Barreico and Cooper, 1987; Coombs *et al.*, 1986).

Calculations using Shaw's (1970) equation and partition coefficients suggested by Hanson (1980) indicate that the alkali basalts of the Western Foothills of Taiwan cannot be derived from low-degree ($< 3\%$) partial melting of a particular mantle source with REE 3 times that of chondrite as proposed by Gast (1968) and Kay and Gast (1973). Chen (1973) argued that Penghu alkali basalt originated at a relatively deeper level than the tholeiite. Similarly, it has been suggested that the deeper part of the mantle beneath the Western Foothills may have been metasomatized by LILE-enriched fluid and enriched in LREE (Wass and Roger, 1980), then 10-20% partial melting from this metasomatized

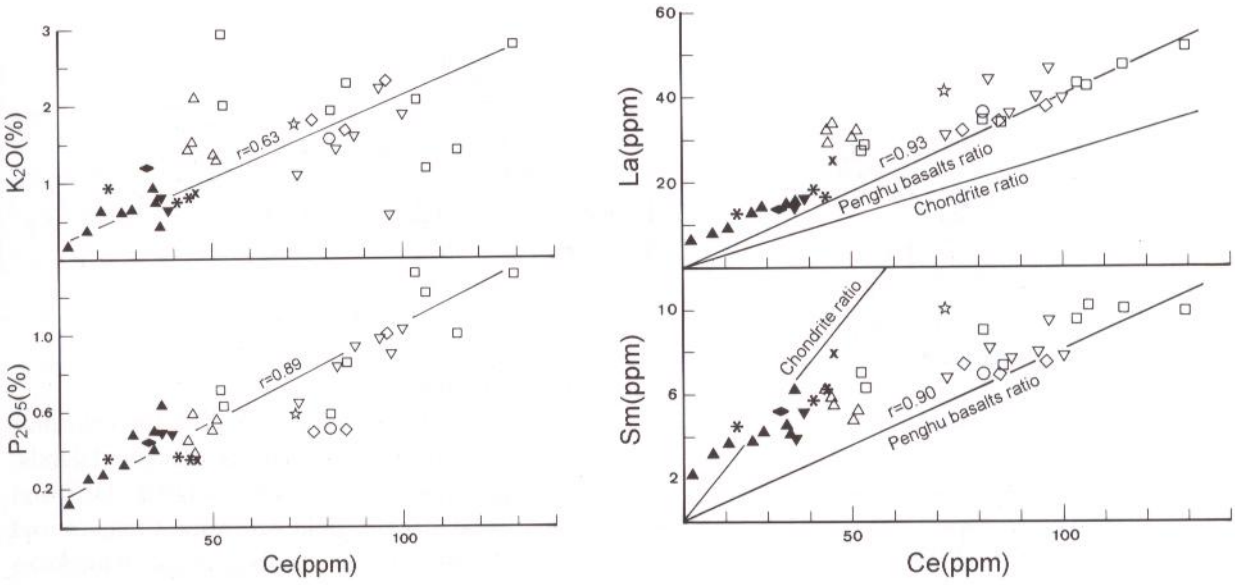

TEXT-FIGURE 39
La vs. Ce; Sm vs. Ce; Ce vs. K_2O and Ce vs. P_2O_5 plots for basaltic rocks from the western Taiwan volcanic province. Symbols as text-figure 3.

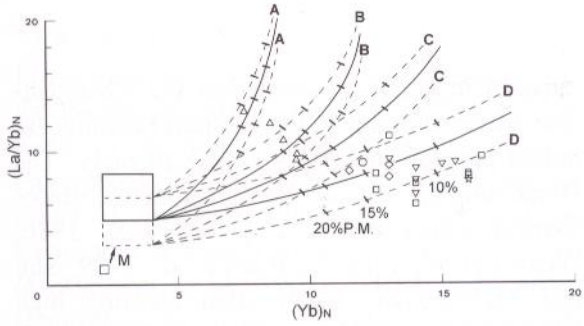

TEXT-FIGURE 40
$(La/Yb)_N$ vs. Yb_N plots for alkali basalts from the western Taiwan volcanic province. Theoretical partial melting curves are after Chauvel and Jahn (1984); M represents metasomatism, N denotes chondrite normalized. Symbols as text-figure 3.

upper mantle would yield the observed REE abundances of the Western Foothills alkali basalts (text-fig. 40).

Based on Sr- and Nd-isotopic data and present chemical data (text-figs. 12, 13 and 39) it is suggested that the tholeiite and alkali basalt of western Taiwan may represent 2 independent magmas. If the argument that the Western Foothills tholeiite originated at a relatively shallower level than that of the alkali basalt is accepted, it could be assumed that the mantle peridotite possessed 2 to 3 times more REE than chondrites. If the unmetasomatized mantle at a relatively shallow level had been composed of lherzolite with 55% olivine, 25% orthopyroxene, 15% clinopyroxene, and 5% garnet and had 2 times the chondritic REE abundances, then 5-10% equilibrium batch partial melting with a melting mode of 10:20:40:30, respectively, could have generated the Western Foothills tholeiites (text-fig. 41).

Signatures of Dupal anomaly

Late Cenozoic intraplate basalts in the Western Foothills of Taiwan and the Penghu Islands have Sr-Nd-Pb isotopic systematics similar to

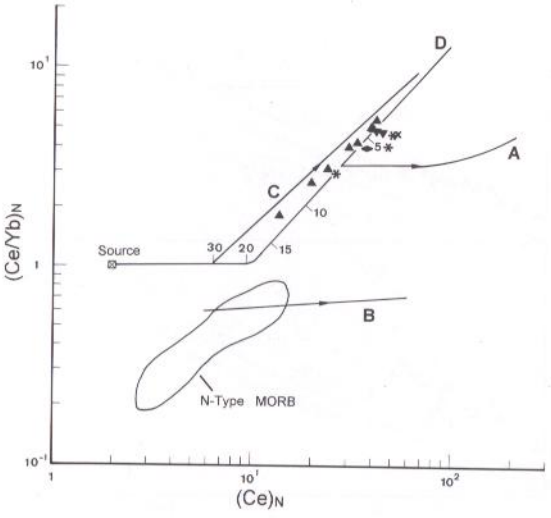

TEXT-FIGURE 41
Log-log plot of $(Ce/Yb)_N$ ratio vs. Ce_N for tholeiites. Fractionation trends are modified from Tarney *et al.* (1980). A: Closed system low fractional crystallization; B: Open system low pressure fractional crystallization (O'Hara, 1977); C: Open system high pressure eclogite fractionation; D: Equilibrium batch partial melting (garnet lherzolite source, 55% ol, 25% opx, 15% cpx, 5% gt, melting mode of 10:20:40:30, respectively, and two times chondritic REE abundances). N-type MORB is from Henderson (1984). Symbols as text-figure 3.

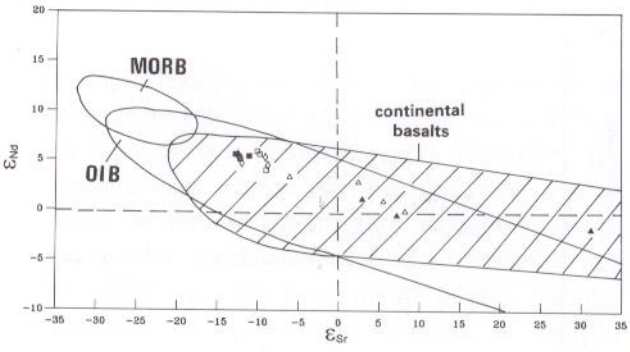

TEXT-FIGURE 42
Plots of $^{143}Nd/^{144}Nd$ versus $^{87}Sr/^{86}Sr$ for volcanics from western Taiwan and the Penghu Islands. Data are from Chen (1988). MORB, OIB and continental basalts field are after Chauvel and Jahn (1984). Open rombohedron, Kungkuan alkali basalt; Close rombohedron, Kungkuan tholeiite; Open square, Penghu alkali basalt; Close square, Penghu tholeiite; Open triangular, Kuanhsi-Chutung alkali basalt; Close triangular, Kuanhsi-Chutung tholeiite.

those of seamount basalts in the South China Sea which are characterized by a Dupal-type Pb isotopic anomaly (Chung *et al.*, 1994). This may be a result of lithospheric extension related to the opening of the South China Sea. However, the Western Foothills basalts display lower $^{143}Nd/^{144}Nd$ and $^{206}Pb/^{204}Pb$ but higher Sr isotopic ratios (text-figs. 42 and 43) than the Penghu basalts. Based on Pb isotopic diagrams (text-fig. 43), ε_{Nd} vs. $^{206}Pb/^{204}Pb$ (text-fig. 44), Zr/Nb vs. $^{87}Sr/^{86}Sr$ (text-fig. 45) and Ba/Nb vs. La/Nb plots (text-fig. 46), the Penghu basalts show signatures of normal OIB and do not have a remarkable Dupal anomaly but the Chiaopanshan stage volcanics of the Western Foothills are indeed characterized by a Dupal anomaly. The Dupal-anomaly basalts have distinctive trace-element compositions (e.g., Le Roex, 1986; Weaver *et al.*, 1986; Le Roex *et al.*, 1989; Sun and McDonough, 1989) often showing high LILE/HFSE (HFSE = high field strength element), Ba/Th and Th/U ratios compared to OIB not showing a Dupal anomaly.

The Ba/Nb vs. La/Nb plots (text-fig. 46) show that the Penghu basalts have lower Ba/Nb and La/Nb ratios. The La/Nb ratios are clearly lower, and similar to those of normal OIB, although the Ba/Nb ratios of some basalts from the Penghu Islands are comparable with those of the Samoa and Society basalts with a typical EM2 signature (Dostal *et al.*, 1982; Palacz and Saunders, 1986). In contrast to the Penghu basalts, the Chiaopanshan stage basalts of the Western Foothills are characterized by high Ba/Nb, La/Nb and Ba/U ratios (text-figs.

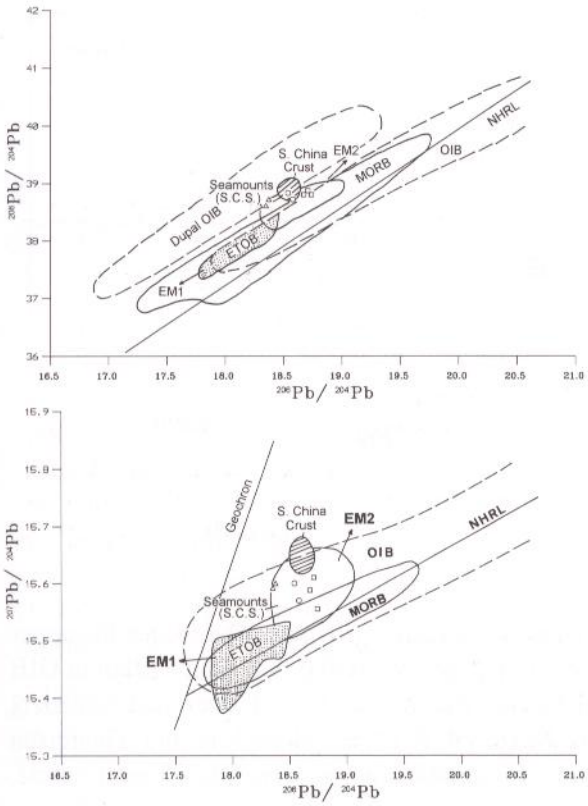

TEXT-FIGURE 43
Pb isotopic diagrams for western Taiwan and the Penghu Islands. Data are from Sun (1980). Field for the South China continental crust is represented by the Paleozoic and Mesozoic granitoids in South China (Li, 1988) and the terrigenous sediments from the South China Sea (McDermott et al., 1993). NHRL = Northern Hemisphere Reference Line (Hart, 1984), ETOB = East Taiwan Ophilite Basalt (Chung *et al.*, 1994). EM1 and EM2 represent enriched mantle type 1 and 2 (Zindler and Hart, 1986). The field of MORB, OIB and Dupal OIB are after Wilson (1989). Square, Penghu alkali basalt; Circle, Penghu tholeiite and triangular, western Taiwan basalt.

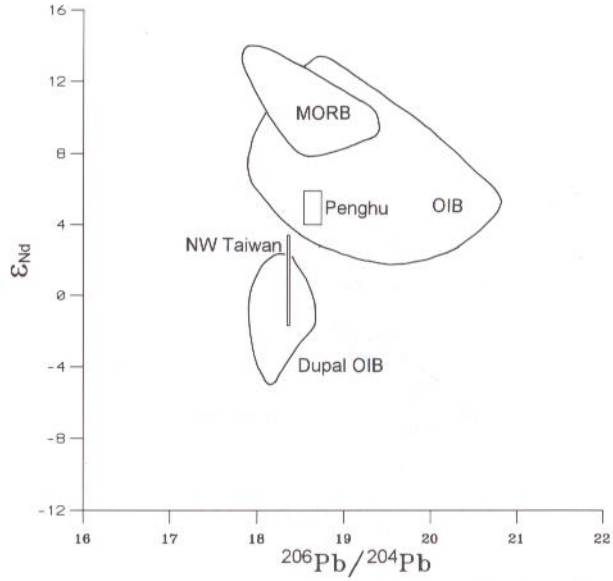

TEXT-FIGURE 44
Variation of ε_{Nd} versus $^{206}Pb/^{204}Pb$ for basaltic rocks from western Taiwan and the Penghu Islands. Field of MORB, normal OIB and Dupal OIB are from Fraser *et al.* (1985/1986) and Nelson *et al.* (1986).

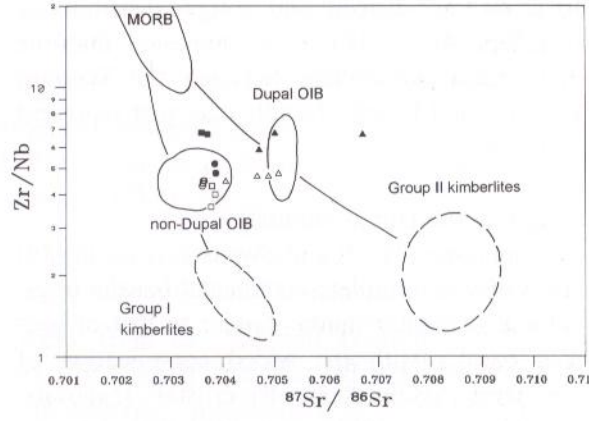

TEXT-FIGURE 45
Variation of Zr/Nb versus initial $^{87}Sr/^{86}Sr$ for basaltic rocks from western Taiwan and the Penghu Islands. Data are from Chen (1990) and the field for MORB, Dupal OIB, non-Dupal OIB are after Le Roex (1986). Symbols as text-figure 42.

46 and 47), which are the typical features of Walvis Bay Ridge, Gough and Tristan de Cunha basalts with typical Dupal anomaly (Weaver *et al.*, 1986; Sun and McDonough, 1989). However,

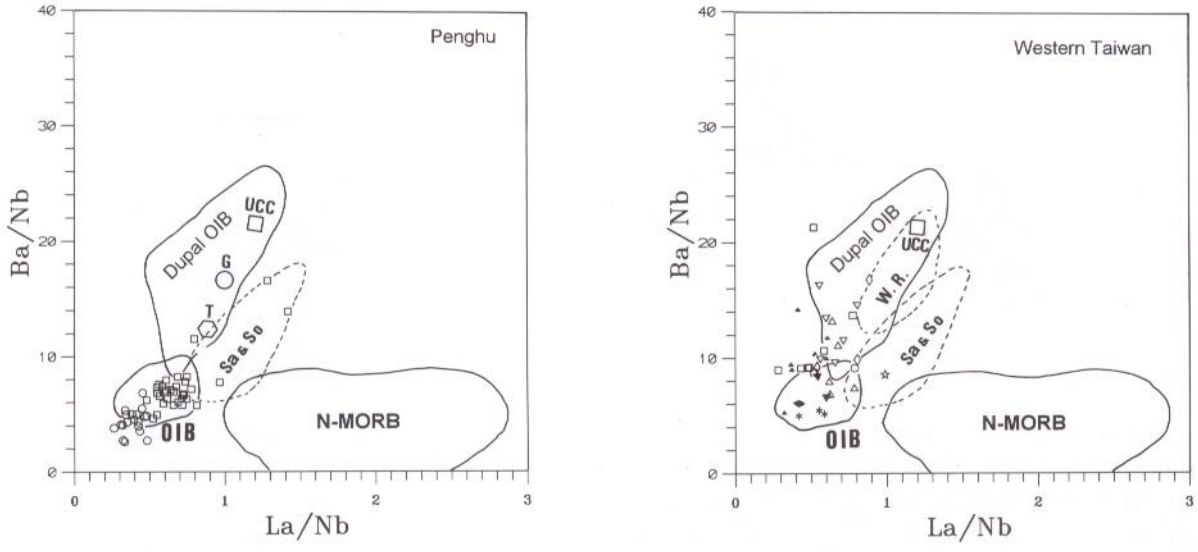

TEXT-FIGURE 46
Ba-Nb-La variations in basaltic rocks from the western Taiwan volcanic province. The values for upper continental crust (UCC) are from Taylor and McLennan (1985), for N-MORB and South Atlantic OIB after Le Roex (1986) and Samoa and Society island basalts (Sa & So) from Palacz and Saunders (1986), and Dostal *et al.* (1982), and the Walvis Bay Ridge (W.R.) from Humphris and Thompson (1983). Symbols as text-figure 3. Penghu basalt as shown for comparison, square, alkali basalt; circle, tholeiite. G, Gough and T, Tristan da Cunha basalts.

based on trace-element and isotopic distributions (text-figs. 46 to 48), it is suggested that the geochemical differences between the Western Foothills and Penghu basalts may just represent a gradation.

Origin of the Dupal anomaly

Thompson (1977) and Swanson *et al.* (1979) believed that intraplate continental basalts originated in a mantle source similar to that of oceanic basalts with the added complication of high-level assimilation of crustal materials. Weaver *et al.* (1986) contended that the geochemistry of Gough, Tristan de Cunha and Walvis Bay Ridge Dupal-anomaly OIB lavas can be explained by contamination of a normal OIB source by small amounts of ancient pelagic sediments. This model is also applicable to the La/Nb and Ba/Nb plots (text-fig. 46), but fails to account for the other trace-element variations. The lowest Rb/Ba and La/Ba, and highest Th/U and Ba/U ratios of the basalts are lower and higher, respectively, than those in the pelagic sediments reported by Ben Othman *et al.* (1989), clearly suggesting that marine sediments are unsuitable for the enriched end-member (text-figs. 47 and 48).

To evaluate the component derived from lithospheric mantle, Ti/Y ratios have been plotted against ε_{Nd} in text-fig. 49a. In this diagram, most asthenosphere-derived magmas fall in a broad array between average MORB and OIB values. In the case of OIB, the bulk of the volcanics was believed to be sublithospheric in origin. The sediment value in text-fig. 49a is taken to be representative of continental material subducted back into the upper mantle along destructive plate margins, and it may therefore be regarded as an estimate of a sediment-contaminated

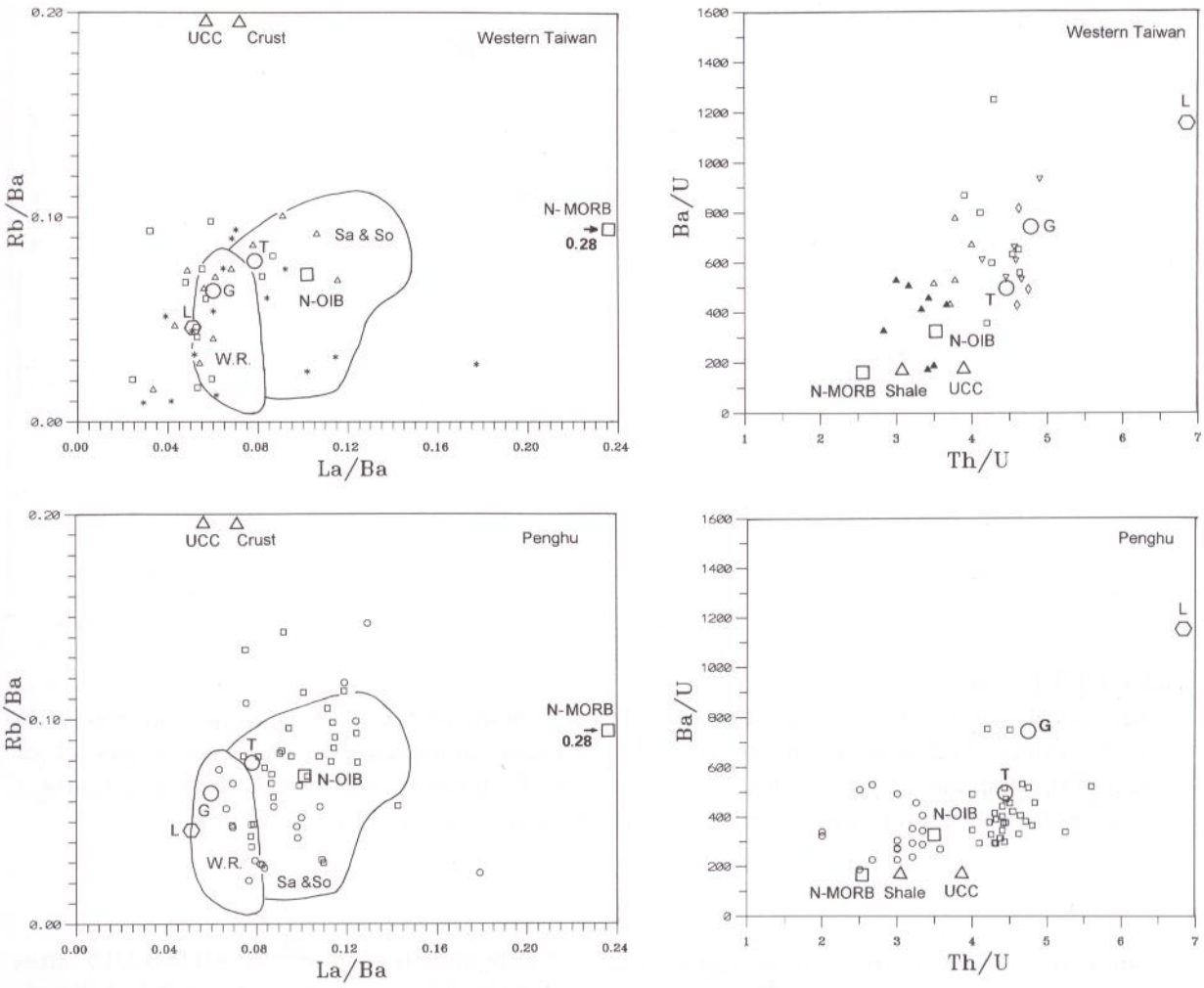

TEXT-FIGURE 47

Rb-Ba-La and Ba-Th-U variations in basaltic rocks from the western Taiwan volcanic province. Data sources are as in text-fig. 46. Symbols as text-figure 3. Penghu basalt as shown for comparison, square, alkali basalt; circle, tholeiite and L, Lamproite from Bergman (1987).

lithospheric mantle. If such lithospheric mantle was subsequently melted it would have low Ti/Y ratios and negative ε_{Nd} values. In other words, if the generation of basalts involved mixing of material from the asthenosphere and from the mantle lithosphere containing a contribution from subducted sediment, the resultant trends should be displaced from the MORB-OIB array towards the composition for subducted sediment. However, the high Ti/Y ratios in the basaltic rocks from the Western Foothills of Taiwan clearly suggest that the sediment-contaminated lithospheric mantle-derived component is unsuitable.

Furthermore, in basaltic melts, both Ti/Y and Zr/Y ratios are little affected by low-pressure fractionation processes in the absence of significant Ti-magnetite fractionation. As Ti-magnetite is not a major fractionating phase in the basaltic volcanics of the Western Foothills, these ratios

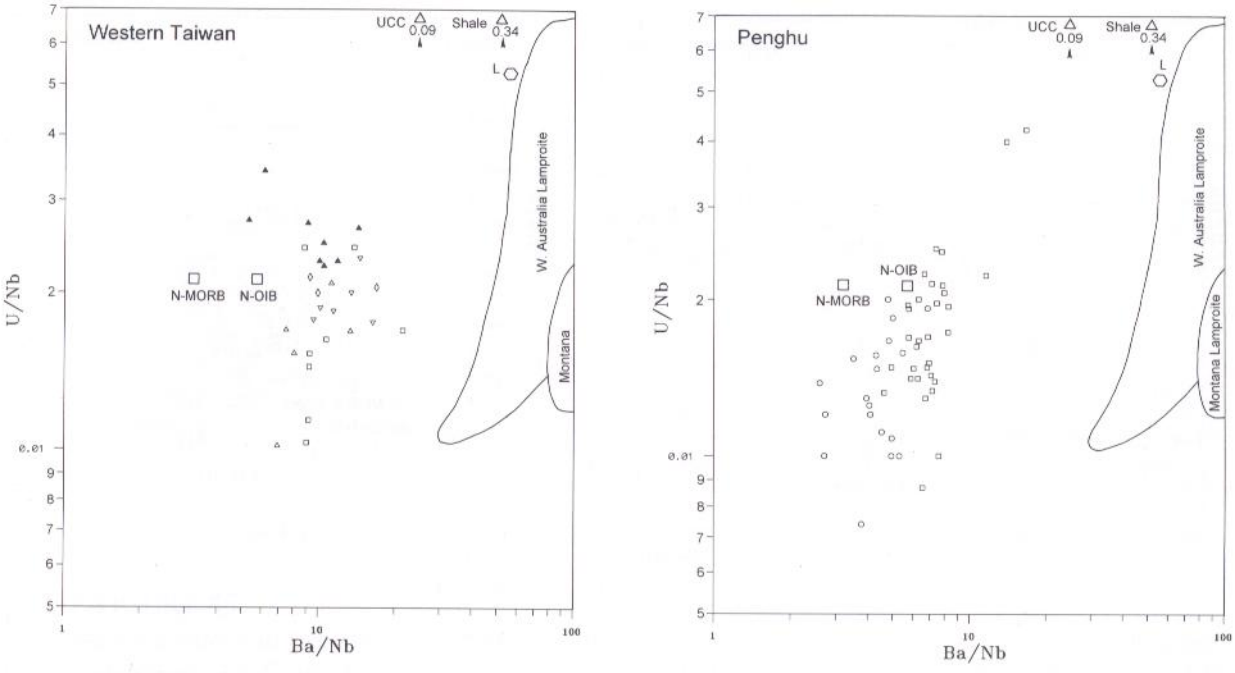

TEXT-FIGURE 48

Variations of U/Nb with Ba/Nb ratios in basaltic rocks from the western Taiwan volcanic province. The field of western Australian lamproite (A) and Montana lamproite (M) are from Fraser *et al.* (1985/1986); lamproite (L) and crust values are from Bergman (1987). Symbols as text-figure 3. Penghu basalt as shown for comparison, square, alkali basalt; circle, tholeiite.

may be used in the evaluation of the degree of crustal material involvement. On Ti/Y versus Zr/Y plots, a broad mantle array can be identified from the values of MORB and OIB (text-fig. 50). Positions along the mantle array reflect variations in the degree of partial melting and/or different Ti/Y and Zr/Y values in different source regions. It is inferred that partial melting of old segments of mantle lithosphere in which the minor and trace element ratios were controlled by the extraction or introduction of small-degree melts, would result in magma with broadly similar Ti/Zr ratios. However, if the minor and trace element inventory of segments of the mantle lithosphere was dominated by the introduction of a sedimentary component, the Ti/Y and Zr/Y ratios would be displaced toward that of crust or shale composite. The absence of distribution trend from the MORB-OIB array towards the compositions for subducted sediment should constrain the contribution of involvement of crust material in the generation of those basaltic magmas.

The observed trend for basaltic rocks from the Western Foothills of Taiwan is consistent with the mixing of a high ε_{Nd}, low Ti/Y component (similar to many OIBs), and a low ε_{Nd}, high Ti/Y component presumably derived from a metasomatized mantle component such as lamproite. The lamproite studied by Fraser *et al.* (1986) has the most suitable trace element compositions for serving as the reservoir of the Dupal components. The variation of U/Nb ratios in lamproites is great, as shown in text-fig. 47, suggesting that U is highly mobile during mantle metasomatism.

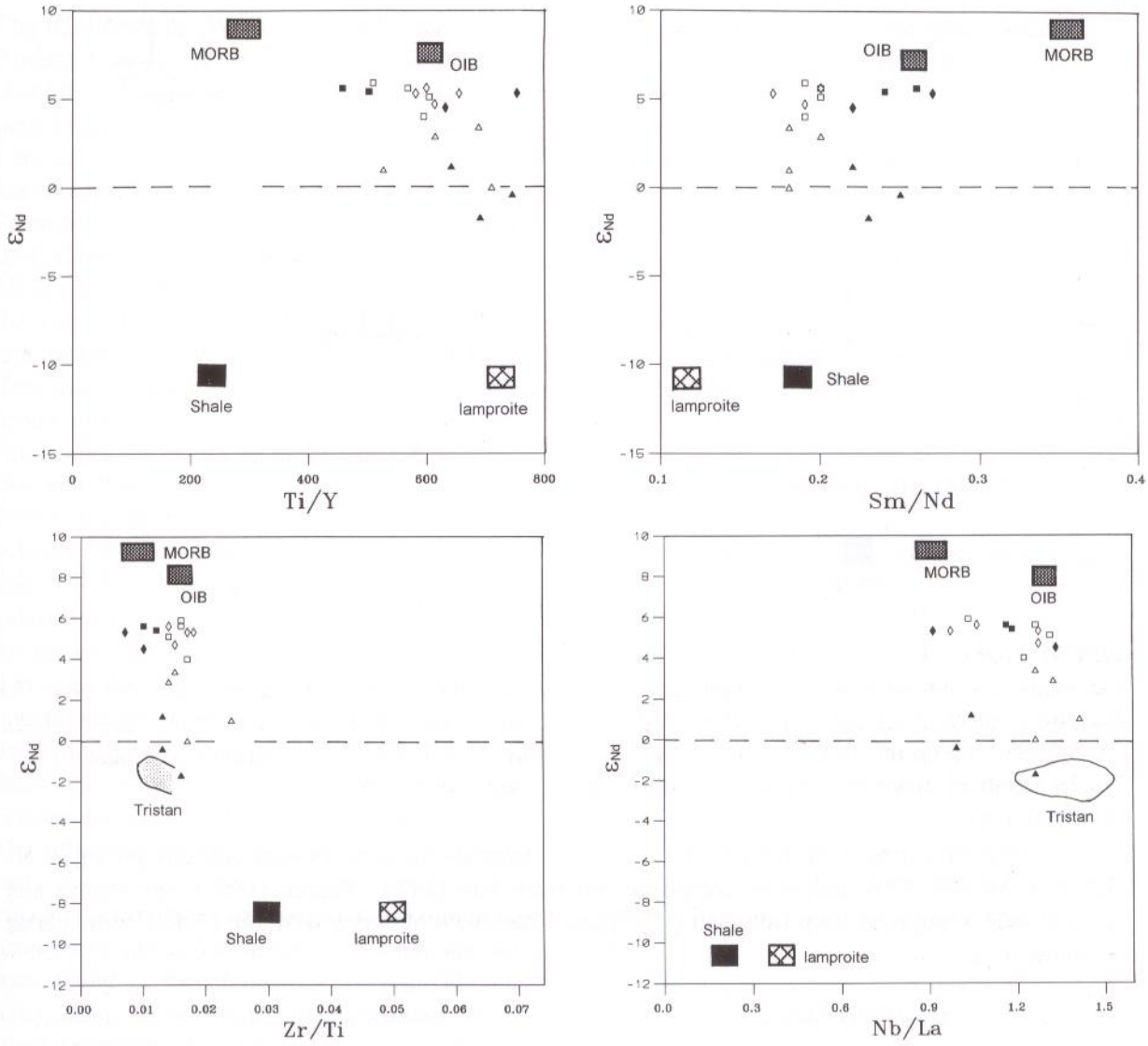

TEXT-FIGURE 49
Variations of ε_{Nd} against Ti/Y, Sm/Nd, Zr/Ti and Nb/La for basaltic rocks from the western Taiwan volcanic province. The element ratio for average MORB and OIB are from Sun and McDonough (1989), the field for the recent basalts from Tristan da Cunha are from Le Roex *et al.* (1990). The element ratio for average shale and lamproite are from Taylor and McLennan (1985) and Bergman (1987), and they are plotted with ε_{Nd}=-11, since that is the value used by Ellam and Cox (1991) in their lamproite model for the petrogenesis of the Nuanetsi picrites. Symbols as text-figure 42.

Text-figure 49 summarizes the variations in Nd isotopes and selected trace element ratios in the Western Foothills basalts. The nice correlations between ε_{Nd} and selected trace element ratios observed in text-figure 49 suggest that intraplate basalts of western Taiwan may

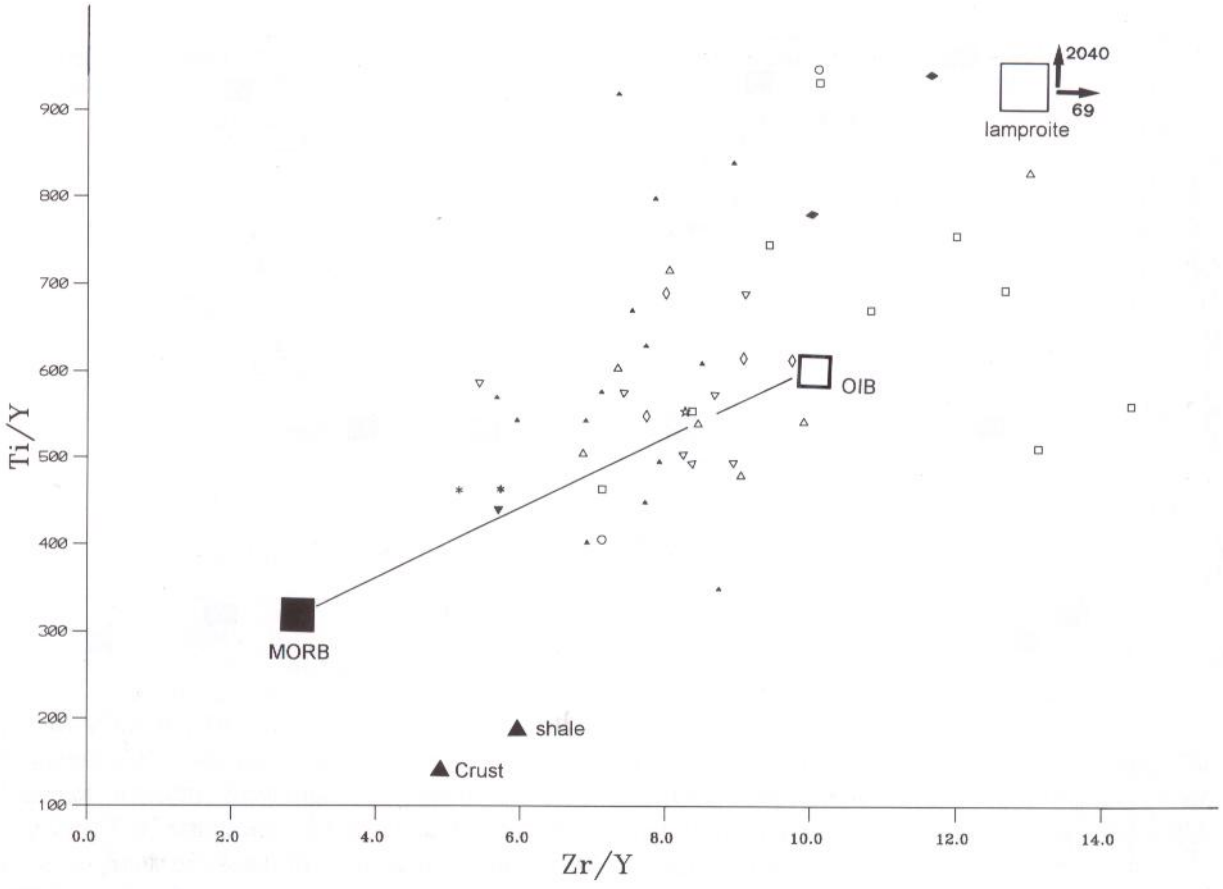

TEXT-FIGURE 50
Variation of Zr/Y versus Ti/Y ratio for basaltic rocks from the western Taiwan volcanic province. N-MORB, E-MORB, OIB and shale composite are from Sun (1980), Pearce (1982) and Mason and Moore (1982), Lamproite from Bergman (1987) and Crust from Mason and Moore (1982). Symbols as text-figure 3.

have been formed by mixing of lithosphoric and asthenospheric components. The former was regarded as small-degree melts, similar to lamproites, and the asthenospheric component was inferred with trace element characteristics similar to those in OIB. Therefore, the ascent and partial melting of asthenospheric mantle during upwelling induced melting of the overlying geochemically heterogeneous lithospheric mantle consequently generating the varieties of the continental rifting basalts in the Western Foothills of Taiwan.

Tectonic Implications of the Western Foothills and Penghu Volcanism

Contemporaneous volcanism took place sporadically during the deposition of the Miocene sediments in the Western Foothills of Taiwan. Volcanic activity was most extensive early in the sedimentary cycle. Miocene volcanic activities have also been recognized under the Western Foothills and coastal plain, and in offshore regions from subsurface well data (Yang *et al.*, 1981, Yuan, 1981).

Based on the K-Ar dates of the Western Foothills and the Penghu Islands, and Tungliang well data, I suggest that the volcanic activity in the Penghu Islands may be correlated with the Miocene volcanic activity in western Taiwan.

The basalts of the Western Foothills and of the Penghu Islands are similar in petrology, geochemistry and geochronology. It should be mentioned that the widespread basaltic flows of Late Cenozoic age found in Indochina (Vietnam-Kampuchea-Laos and Thailand), Hainan, Leijuo Peninsula, and the southeastern coast of mainland China from Guangtung, the Pearl River Mouth Basin, Fujian, Zhejiang to the mouth of the Yantze River, as well as the Penghu Islands and western Taiwan, may be related to the same Cenozoic rift tectonism along the Asiatic continental margin caused by the 3rd heating and rifting episodic evolution of the South China Sea (Ru and Pigott, 1986; Yu 1988; Baiais *et al.*, 1989). For example, Pulin-Chilin (Guangtung) volcanic activity occurred in the middle Oligocene (34.3 $\pm$ 1.0 Ma) and Kimmen and Hsiaokimmen (Liehsu) basalt, Fujian provides a K-Ar age of 13 Ma (Juang *et al.*, 1991). It seems that since the Oligocene in the eastern Asia continental margin, Cenozoic magmatism associated with lithospheric extension occurred and post dates the opening of the South China Sea (Taylor and Hayes, 1983; Ru and Pigott, 1986). The rifting-continental-margin volcanism apparently ceased in the Late Miocene owing to the effect of intensified arc-continent collision. No preeminent rifting volcanism of a later age has been found in the vicinity of Taiwan. On the other hand, in Southeast Asia including Indochina (Vietnam), Hainan and the Leijuo Peninsula, since the Plio-Pleistocene (3.7-0.1 Ma), the young prevailing stage of continental rifting basalts may be related to the Red River Fault and the Vietnam East Boundary Fault (text-fig. 1).

The Cenozoic continental basalts usually contain abundant megacrysts, granulites and mantle xenoliths (spinel lherzolite and garnet lherzolite) and display chemical and Nd-Sr-Pb isotopic characteristics similar to the seamount basalts in the South China Sea (Tu *et al.*, 1992; Chung *et al.*, 1994; Juang, 1995). The extension of the lithosphere is generally considered to have played an important role in the generation of these continental rifting basalts. The basalts of the Penghu Islands have the trace-element and isotopic signatures of normal OIB and do not have a remarkable Dupal anomaly, while the Chiaopanshan stage basalts of the Western Foothills show high LILE/Nb, Ba/Th, Ba/U, Th/U and low La/Ba ratios typical of the Dupal-anomaly oceanic island basalts. Sr, Nd and Pb isotopic compositions of the Chiaopanshan stage basalts are also characterized by a Dupal anomaly. This Dupal mantle source is inferred to have been caused by a metasomatized lithosphere rather than due to the direct incorporation of continental crustal material into the mantle.

ACKNOWLEDGMENTS

Some of the Ar isotope analyses were carried out by Prof. H. Bellon of University of Bretagne Occidental of France and by Dr. A. W. Webb of the AMDEL of Australia. The author is most grateful for their kind assistance. Thanks are also due to Mr. S. H. Chung, Central Geological Survey for helpful assistance in the field survey. The author would like to thank Professors J. C. Chen, L. C. Hsu and H. Y. Yang for their critical reading of the manuscript and valuable comments. This study was supported by the National Science Council (NSC80-0202-M-178-04).

REFERENCES

Alabaster, T., Pearce, J. A. and Malpas, J., 1982. The volcanic stratigraphy and petrogenesis of the Oman Ophiolite Complex. Contrib. Min. Petrol. 81: 168-183.

Allegre, C. J., Brevart, O., Dupre, B. and Minster, J. F., 1980. Isotopic and chemical effects produced in a continuously differentiating convecting Earth mantle. Philos. Trans. Roy. Soc. London A297.

Anders, E., 1977. Chemical composition of the moon, earth and eucrite parent body. Philos Trans Roy. Soc. London A285: 23-40.

Aoki, K., 1963. The Kaersutites and oxykaersutites from alkalic rocks of Japan and sur-

rounding areas. Jour. Petrol. 4: 198-201.

Aoki, K., 1970. Petrology of Kaersutite-bearing ultramafic and mafic inclusions in Iki Island, Japan. Contrib. Min. Petrol. 25: 270-283.

Auchapt, A., Dupuy, C., Dostal, J. and Kanika, M., 1987. Geochemistry and petrogenesis of rift-related volcanic rocks from south Kivu (Zaire). J. Volc. Geotherm. Res. 31: 33-46.

Barreico, B. A. and Cooper, A. F., 1987. Mantle metasomatism and alkaline magmatism. Geo. Soc. Am. special paper.

Ben Othman, D. B., White, M. W. and Patchett, J., 1989. The geochemistry of marine sediments, island arc magma genesis, and crust-mantle recycling. Earth Planet. Sci. Lett. 94: 1-21.

Bergman, S. C., 1987. Lamporites and other potassium-rich igneous rocks: a review of their occurrence, mineralogy and geochemistry. *In:* Fitton, J. G. & Uption, B. G. J. (eds.). Alkaline Igneous Rocks. Geological Society, London, Special Publication 30: 103-190.

Baiais, A., Tapponnier, P., Patriat, R. and Wang, K., 1989. The Tertiary opening of the South China Sea: a consequence of the collision between India and Asia. Terra Abstr. 1:210.

Brook, C. K. and Nielsen, T. F. D., 1982. The east Greenland continental margin: a transition between oceanic and continental magmatism. J. Geol. Soc. London 39: 265-275.

Bulter, J. C. and Woronow, A., 1986. Discrimination among tectonic setting using trace element abundances of basalts: Jour. Geophys. Res. 91,B10: 10289-10300.

Bultitude, R. J. and Green, D. H., 1971. Experimental study of crystal liquid relationships at high pressure in olivine nephelinite and basanite composition. J. Petrol. 12: 121-147.

Champbell, S. M. and Griffiths, R. W., 1990. Implications of mantle plumes for the evolution of flood basalts. Earth and Planetary Science Letters 99: 79-93.

Chang, L. S., 1962. Tertiary planktonic foraminiferal zones of Taiwan and overseas correlation. Mem. Geol. Soc. China 1: 107-112.

Chauvel, C. C. and Jahn, B. M., 1984. Nd-Sr isotope and REE geochemistry of alkali basalts from the Massif Central, France: Geochim. Acta 48: 93-110.

Chen, C. H., 1978. Petrochemistry and origin of Pleistocene volcanic rocks from northern Taiwan. Bull. Volcano 41: 513-528.

Chen, C. H., 1983. The geochemical evolution of Pleistocene absarokite, shoshonite and high-alumina basalt in northern Taiwan: Mem. Geol. Soc. China 5: 85-96.

Chen, C. H., 1989. Nd, Sr and O isotopic study of the Cenozoic island arc volcanic rocks of Taiwan. Ph. D. thesis. Geology, NTU.; Taipei, Taiwan (Chinese).

Chen, C. H., 1990. The Igneous Rocks of Taiwan. Cent. Geol. Surv. Pub. 1.

Chen, C. H., 1991. Plio-Pleistocene within intraplate basalts in neighbouring of Taipei. 1991 Annual Meeting Program with Abstracts, Taipei, Taiwan.

Chen, C. H. and Chung, S. L., 1985. Petrology and geochemistry of Neogene continental basalts and related rocks in Taiwan: (I) Basanitoids, alkali olivine basalts and tholeiites from Kuanhsi-Chutung area. Acta Geol. Taiwanica 23: 35-62.

Chen, C. H., Chung, S. L. and Lee, C. Y., 1987. Genesis of Neogene continental margin alkali basalts and tholeiites in western Taiwan and the significance of high-pressure megacrysts and lherzite inclusion. Acta Geol. Taiwanica 25: 111-132.

Chen, J. C., 1973. Geochemistry of basalts from Penghu Islands. Proc. Geol. Soc. China 16: 23-36.

Chen, J. C. and Kato, Y., 1989. Geochemistry of volcanic rocks from the Ryukyu islands: Compared with andesitic rocks from northern Taiwan. Acta Oceanogr. Taiwanica 22:

116-128.

Chen, S. J., 1988. Isotope and geochemistry of Neogene basalts in western Taiwan. MS thesis, Geology, NTU.; Taipei, Taiwan (Chinese).

Chi, W. R., 1981. Nannofossils. CPC Exploration and Research Center; Miaoli (Chinese).

Chung, S. H., 1992. Geochemistry and Fission-track dating of Zircon in basaltic rocks from Chingshuikeng area. MS Thesis, NTU.; Taipei, Taiwan (Chinese).

Chung, S. L. and Chen, C. H., 1990. Origin of clinopyroxene and amphibole megacrysts in the alkali basaltic rocks from western Taiwan as constrained by REE geochemistry. Proc. Geol. Soc. China 33: 177-204.

Chung, S. L., Jiang, S. H. and Chen, C. H., 1985. REE distribution and petrogenesis of basaltic rocks from Kuanhsi-chutung area, northern Taiwan: Acta Geol. Taiwanica 23: 63-76.

Chung, S. L., Sun, S. S., Tu, K., Chen, C. H. and Lee, C.Y., 1994. Late Cenozoic basaltic volcanism around Taiwan Strait, SE China: Product of lithosphere-asthenosphere interaction during continental extension. Chem. Geology 112: 1-20.

Coleman, R. B., Lee, D. E., Beatty, L. B. and Brannock, W. W., 1965. Eclogites and eclogites, their differences and similarities. Bull. Geol. Soc. Am. 76: 483-508.

Coombs, D. S., Cas, R., Kawachi, Y., Landis, C. A., McDonough, W. F. and Reay, A., 1986. Cenozoic volcanism in north and east Otags, *In*: Smith, I. E. M. (ed.), Late Cenozoic volcanism in New Zealand. publications of Royal society of America Bulletin 82: 1327-1340.

Cox, K. G., Bll, Y. G. and Pankhurst, R. J., 1979. The interpretation of Igneous Rocks. Allen and Unwin; London.

Davidson, J. P., 1987. Isotopic and trace element constraints on the petrogenesis of subduction related lavas from Martinique, Lesser Antilles. J. Geophy. Res. 91: 5943-5962.

Dostal, J., Dupuy, C. and Liotard, J. M., 1982. Geochemistry and origin of basaltic lavas from Society Islands. French Polynesia (South Central Pacific Ocean). Bull. Volcanol. 45(1): 51-62.

Dupuy, C. and Dostal, J., 1984. Trace element geochemistry of some continental tholeiites: Earth Planet. Sci. Lett. 67: 61-69.

Ellam, R.M. & Cox, K.G., 1991. An interpretation of Karoo picrite basalts in terms of interaction between asthenospheric and mantle lithosphere. Earth Planet. Sci. Lett. 105: 330-342.

Fan, Q. and Hooper, P. R., 1991. The Cenozoic basaltic rocks of eastern China: petrology and chemical composition. J. Petrology 32: 765-810.

Fraser, K. J., Hawkesworth, C. J., Erlank, A. J., Mitchell, R. H. and Scott-Smith, B. H., 1985/1986. Sr, Nd and Pb isotope and minor element geochemistry of lamproites and kimberlites. Earth Planet. Sci. Lett. 76: 57-70.

Frey, F. A. and Green, D. H., 1974. The mineralogy geochemistry and origin of lherzolite inclusions in Victorian basanites. Geochim. Cosmochim. Acta 38: 1023-1059.

Frey, F. A., Green, D. H. and Roy, S. D., 1978. Integrated models of basalt petrogenesis, A study of quartz tholeiites to olivine melilitites from southeastern Australia utilizing geochemical and experimental petrological data. J. Geol. 19: 463-513.

Frey, F. A., Haskin, M. A., Poetz, J. and Haskin, L. A., 1968. Rare earth abundances in some basic rocks. J. Geophys. Res. 73: 6085-6098.

Gast, P. W., 1968. Trace element fractionation and the origin of tholeiitic and alkaliane magma types: Geochim. Cosmochim. Acta 32: 1057-1086.

Green, T. H., 1980. Island arc and continent-building magmatism: a review of petrogenetic models based on experimental petrology and geochemistry. Tectonopysics 63: 367-385.

Hanson, G. N., 1980. Rare earth elements in

petrogenetic studies of igneous systems. Ann. Rev. Earth Planet. Sci. 8: 371-406.

Hart, S. R., 1984. The Dupal anomaly: a large-scale isotopic anomaly in the southern hemisphere. nature 309: 753-756.

Hart, S. R., 1988. Heterogeneous mantle domains, genesis and mixing chronologies. Earth Planet. Sci. Lett. 90: 273-276.

Hart, S. R. and Brooks, C., 1974. Clinopyroxene-matrix partitioning of K, Rb, Cs, Sr and Ba. Geochim. Cosmochim. Acta 38: 1799-1806.

Hawkesworth, C. J., Kempton, P. D., Rogers, N. W., Ellan, R. M. and van Calsteren, P. W., 1990. Continental lithosphere, and shallow level enrichment processes in the Earth's mantle. Earth Planet. Sci. Lett. 96: 256-268.

Henderson, P., 1984. Rare earth element geochemistry. Elsevier; N.Y.

Ho, C. S., 1969a. Geological significance of potassium-argon ages of the Chimei Igneous Complex in eastern Taiwan. Bull. Geol. Survey Taiwan 20: 63-74.

Ho, C. S., 1969b. Stratigraphy of the Kungkuan Tuff in northern Taiwan. Bull. Geol. Surv. Taiwan 20: 5-13 (Chinese), 41-62 (English).

Ho, C. S., 1971. Geological structure and coal fields of the area between Kuanhsi, Hsinchu and Tahu, Miaoli, Taiwan. Bull. Geol. Surv. Taiwan 23: 5-52 (Chinese), 53-56 (English).

Ho, C. S., 1988. An Introduction to the Geology of Taiwan: Explanatory Text of the Geologic Map of Taiwan. Central Geological Survey, MOEA: 192p.

Ho, C. S. and Hsu, T. L., 1951. Geology of the Chialo coal field, Sinchu, Taiwan. Bull. Geol. Surv. Taiwan. 3: 1-22 (Chinese), 1-12 (English).

Ho, C. S. and Lin, T. H., 1965. Volcanism in the Mushan Formation near Keelung, northern Taiwan. Proc. Geol. Soc. China 8: 24-35.

Ho, C. S., Tsan, S. F., Pan, C. W. and Yang, Y. T., 1954. Geology of the Nanchuang coal field, Miaoli, Taiwan. Bull. Geol. Survey Taiwan 6: 1-36.

Hong, E., 1988. Lithology, sedimentary structers and trace fossils analysis of the upper-Miocene-low Pliocene series in northwestern foothills of Taiwan. Ph. D. Thesis, Geology. NTU.; Taipei, Taiwan.

Hooper, P. R., 1990. The timing of crustal extension and the eruption of continental flood basalts. Nature 345: 246-249.

Hsu, L. C., 1961. Basaltic rocks from the Kuanhsi-Chutung district, northern Taiwan. Acta Geol. Taiwanica 9: 47-78.

Huang, C. Y., 1979. Biometric study of *Lepidocyclina* in the Kungkuan Tuff of northern Taiwan. Acta Geol. Taiwanica 20: 41-51.

Humphris. S. E. and Thompson. G., 1983. Geochemistry of rare earth elements in basalts from the Walvis Ridge:implications for its origin and evolution. Earth Planet. Sci. Lett. 66: 223-242.

Hwang, W. T. and Lo, H. J., 1986. Volcanological aspects and the petrogenesis of the Kuanyin-shan volcanic rocks, northern Taiwan. Acta Geol. Taiwanica 24: 123-148.

Ichikawa, Y., 1930. Explanatory text of the geological map of Taiwan-Toen sheet scale (1:50,000). Bureau of Productive Industries (Government-General of Taiwan) 581: 38 (Japanese), p.8 (English).

Ichikawa, Y., 1931. Explanatory text of the geolocical map of Taiwan-Tikuto sheet scale (1:50,000). Bureau of Productive Industries (Government-General of Taiwan) 582: 23 (Japanese), p.8 (English).

Ichikawa, Y., 1932. Basalts from the vicinity of Okei near Taihoku, Formosa. Transactions Natural History Soc. Formosa 22, 122: 359-364 (Japanese).

Irving, A. J., 1974. Megacrysts from the Newer basalts and other basaltic rocks of south-eastern Australia. Bull. Geol. Soc. Am. 85: 1503-1514.

Irving, A. J., 1978. Flow crystallization: a mechanism for fractionation of primary

magmas at mantle pressure. EOS, 59: 1214.

Juan, V. C., Chen, C. H. and Lo, H. J., 1981. Tectonic implication of Neogene volcanism on the continental shelf of western Taiwan. Memoir Geol. Soc. China 4: 195-205.

Juan, V. C., Chen, C. H. and Lo, H. J., 1984. Basaltic rock types in various tectonic setting in Taiwan. Proc. Geol. Soc. China 27: 11-24.

Juan, V. C., Lo, H. J. and Chen, C. H., 1979. Genetic relationship of the Neogene alkali and tholeiitic magmas and the nature of the upper mantle beneath the continental shelf of the western Taiwan. Proc. Geol. Soc. China 22: 24-38.

Juang, W. S., 1981. Analysis of international rock standards by atomic absorption spectroscopy. Proc. Geol. Soc. china 24: 28-39.

Juang, W. S., 1988. Geochronology and chemical variations of late Cenozoic volcanic rocks Taiwan. Ph. D. Thesis, Inst. Oceanogr., NTU.; Taipei, Taiwan (Chinese).

Juang, W. S., 1992. Volcanic activity and Igneous Rock in Taiwan. Natl. Mus. Nat. Sci.; Taichung, Taiwan (Chinese).

Juang, W. S., 1993. Diversity of Quaternary basaltic magma in northern Taiwan. Bull. Natl. Mus. Nat. Sci. 4: 125-166.

Juang, W. S., 1995. Geochemistry of ultramafic xenoliths and granulites in Miocene alkali basalts from Taiwan. 1995 Annual Meeting Program and Extended Abstracts, Geol. Soc. China 324-328.

Juang, W. S. and Bellon, H., 1984. The potassium-argon dating of andesites from Taiwan. Proc. Geol. Soc. China 27: 86-100.

Juang, W. S. and Chen, J. C., 1989. Geochronology and geochemistry of volcanic rocks in northern Taiwan. Bull. Central Geol. Surv. 5: 31-66 (Chinese).

Juang, W. S. and Chen, J. C., 1990. Geochronology and chemical variations of volcanic rocks along the arc-continent collision zone in eastern Taiwan. Bull. Natl. Mus. Nat. Sci. 2: 89-118.

Juang, W. S. and Chen, J. C., 1992. Geochronology and geochemistry of Penghu basalts, Taiwan Strait and their tectonic significance. J. Southeast Asian Earth Sci. 7, No. 2/3: 185-193.

Kay, R. P. and Gast, P. W., 1973. The rare earth content and origin of alkali basalts. J. Geol. 81: 653-682.

Keng, W. P., 1961. Geology of the Kuanhsi coal field, Hsinchu, Taiwan. Bull. Geol. Surv. Taiwan 13: 15-43 (Chinese), 5-9 (English).

Keng, W. P., 1962. Geology of the Shangping coal field, Hsinchu, Taiwan. Bull. Geol. Surv. Taiwan 14: 1-13 (Chinese), 1-6 (English).

Keng, W. P., 1967. Geology of the Chiahsien-Chishan area, southern Taiwan. Bull. Geol. Surv. Taiwan 19: 1-13 (Chinese), 1-8 (English).

Kuno, H., 1950. Petrology of Hakone volcano and the adjacent area, Japan. Bull. Geol. Soc. Am. 61: 957-1020.

Kuno, H., 1959. Origin of Cenozoic petrographic provines of Japan and surrounding areas. Bull. Volcanologique, Ser. II(20): 37-76.

Kuno, H., 1960. High alumina basalt. J. Petrol. 1: 121-145.

Kuno, H., 1966. Lateral variation of basalt magma type across continental margins and island arcs. Bull. Volcano 29: 195-222.

Lan, C. Y., Shen, J. J. S. and Lee Typhoon, 1986. A Rb-Sr isotopic study of andesites from Lutao, Lanhsu, and Hsiao-Lanhsu, eruption ages and isotopic heterogeneity. Bull. Inst. Earth Sci. 6: 211-226.

Le Roex, A. P., 1986. A geochemical correlation between source region signatures of southern African kimberlites and South Atlantic hotspots. Nature (London) 324: 243-245.

Le Roex, A. P., Cliff, R. A. & Adair, B. J. I., 1990. Tristan da Cunha, South Atlantic: Geochemistry and petrogenesis of a basanite-phonolite lava series. Journal of Petrology 31: 779-812.

Le Roex, A. P., Dick, A. J. B. and Fisher, R. L., 1989. Petrology and geochemistry of

MORB from 25°E to 46°E along the southwest Indian Ridge: Evidence for contrasting styles of mantle enrichment. J. Petrol. 30: 947-986.

Lee, C. Y., 1985. Trace element geochemistry of major basaltic rocks from Penghu area. MS. thesis. Geology, NTU.; Taipei, Taiwan (Chinese).

Li, X. H., 1988. Geochemical study on the Wanyangshan-Zhuguangshan granitoids and implications for the crustal evolution in South China, Ph. D. Thesis, Institute, Guangzhou (Chinese).

Liu, C. H. and Pan, Y. S., 1984. Seismic stratigraphic study on the tertiary sequences in the Hsinchu Basin Taiwan. Petrol. Geol. Taiwan 20: 97-112.

Liu, S. K. and Chen, J. C., 1991. Geochemical studies of Cenozoic basalts from northern, western-central and offshore Taiwan. Special Pub. Central Geol. Surv. 5: 39-58.

Machado, N., Ludden, J. N., Brooks, C. and Thompson, G., 1982. Fine scale isotopic heterogeneity in the sub-Atlantic mantl. Nature 295: 226-228.

Mason, B. and Moore, C. B., 1982. Pricipal of geology. 4th edition. Smith and Wyllie .

McDermott, F., Defant, M. J., Hawkesworth, C. J., Maury, R. C. and Joron, J. L., 1993. Isotope and trace element evidence for three component mixing in the genesis of north Luzon arc lava (Philippines). Contrib. Mineral Petrol. 113: 9-23.

McDonald G. A. and Katsura T., 1964. chemical composition of Hawaiian lavas. J. Petrol. 5: 82-133.

McDougall, I., Polach, H. A. and Stipp, J. J., 1969. Excess radiogenic argon in young subaerial basalts from Auckland volcanic field, New Zealand. Geochim. Cosmochim. Acta 33: 1485-1520.

Meschede, M., 1986. A method of discriminating between different types of Mid-Ocean Ridge basalts and continental tholeiites with the Nb-Zr-Y diagram. Chemical Geology 56: 207-218.

Miki G. K., 1991. Chronology and paleomagnetic study of the formation of Ryukyu Arc - history of Ryukyu Arc and Okinawa Trough. Ph. D. Thesis. Inst. Natural Science, Nat. Nagoya Univ., Japan.

Nelson, D. R., McCulloch, M. T. and Sun, S. S., 1986. The origin of ultrapotassic rocks as inferred from Sr, Nd and Pb isotopes. Geochim. Cosmochim. Acta 50: 231-245.

O'Hara, M. J., 1977. Geochemical evolution during fractional crystallization of a periodically refilled magma chamber. Nature 266: 503-507.

Onuma, N., Hirano, M. and Isshiki, N., 1983. Genesis of basalt magmas and their derivatives under the Izu Islands, Japan, inferred from Sr/Ca-Ba/Ca systematics. J. Vol. Geother. Res. 18: 511-529.

Palacz, Z. N. and Saunders, A. D., 1986. Coupled trace element and isotope enrichment in the Cook-Austral-Samoa islands., southwest Pacific. Earth Planet. Sci. Lett. 79: 270-280.

Pearce, J. A., 1976. Statistical analysis of major element patterns in basalts. J. Petrol. 17: 15-43.

Pearce, J. A., 1980. Geochemical evidence for the genesis and eruptive setting of lavas from Tethyan ophiolites. In Panayiotou A. (ed.). Ophiolites, Proceeding Inter-national Ophiolite Symposium, Cyprus. Geol. Surv. Cyprus, Nicosia: 261-272.

Pearce, J. A., 1982. Trace element characteristics of lavas from destructive plate boundaries. *In:* Thorpe, R. S. (ed.). Andesites: orogenic and andesites and related rocks. pp. 525-548. Wiley; Chichester.

Pearce, J. A., 1983. The role of sub-continental lithosphere in magma genesis at destructive plate margins: *In:* Hawkesworth, C. J. and Norry, M. M. (eds.). Continental basalts and Mantle Xenoliths. pp. 230-249 Shiva; Nantwich.

Pearce, J. A. and Cann, J. R., 1973. Tectonic setting of basic volcanic rocks determined

using trace element analysis. Earth Planet. Sci. Lett. 19: 290-300.

Pearce, J. A. and Gale, G. H., 1977. Identification of ore-deposition environment from trace-element geochemistry of associated igneous host rocks, in volcanic processes in ore genesis. pp. 14-24. Institution of Minining and Geological Society of London.

Pearce, J. A. and Norry, M. J., 1979. Petrogenetic implications of Ti, Zr, Y and Nb variations in volcanic rocks: contri. Miner. Petrol. 69: 33-47.

Perfit, M. R., Gust, D. A., Bence A. E., Arculus R. J. and Taylor S. R., 1980. Chemical characteristic of island arc basalts: Implication for mantle source. Chem. Geol. 30: 227-256.

Philpotls, J. A. and Schnetzier, C. C., 1970. Pheocryst-matrix partition coefficients for K, Rb, Sr and Ba with applications to anorthosite and basalt genesis. Geochim. Cosmochim. Acta 34: 307-322.

Ratcliffe, N. M., 1987. High TiO2 metadiabase dikes of the Hudson Highlands, New York and New Jersey: Possible late Protozoic rift rocks in the New York Recess. Am. J. Sci. 287: 817-850.

Richard, M., Bellon, H., Maury, R. C., Barrier, E. and Juang, W. S., 1986. Miocene to Recent calc-alkalic volcanism in eastern Taiwan: K-Ar ages and petrography. Mem. Geol. Soc. Taiwan, 7: 369-382.

Richard, M. A., Duncan, R. A. and Courtillot, V. E., 1989. Flood basalts and hotspot tracks: plume heads and tails. Science 246: 103-107.

Richardson, S. H., Erlank, A. J., Duncan, A. R. and Reid, D. J., 1982. Correlated Nd, Sr and Pb isotope variation in Walvis Ridge basalts and implications for the evolution of their mantle source. Earth Planet. Sci. Lett. 59: 327-342.

Ringwood, A. E., 1975. The petrological evolution of island arc system. J. Geol. Soc. London 130: 183-204.

Ringwood, A. E., 1990. Slab-mantle interactions. 3. Petrogenesis of intraplate magmas and structure of the upper mantle. Chem. Geol. 82: 187-207.

Ru, K. and Pigott, J. D., 1986. Episodic rifting and subsidence in the South China Sea. AAPG 70: 1136-1155.

Rutcliffe, N. M., 1987. High TiO2 metadiabase dikes of Hudson Highlands, New York recess. Am. J. Sci. 287: 817-850.

Saggerson, E. P. and Williams, L. A. V., 1964. Ngurumanite from southern Kenya and its bearing on the origin of the rocks in the northern Tanganyika alkaline district. J. Petrol. 5: 40-81.

Saunders, A. D., 1984. The rare earth element characteristic of igneous from the ocean basin. *In*: Henderson, P. (ed.). Rare earth element geochemistry pp. 205-236. Elsevier.

Schilling, J. G., 1975. Azores mantle blob: rare earth evidence. Earth Planet. Sci. Lett. 25: 103-115.

Shapiro, L. and Brannock, W. W., 1962. Rapid analysis of silicate, carbonate and phosphate rocks. U.S. Geol. Survey Bull. 1144A.

Shaw, D. M., 1970. Trace element fractionation during anatexis. Geochim. Cosmochim. Acta 34: 236-243.

Shaw, D. M., 1972. Development of the early continental crust. Pt. I. Use of trace element distribution coefficient models for the Proto-Archaean crust. Can. Jour. Earth Sci. 9: 1577-1595.

Smet, T., Hertogen, J., Gijbels, R. and Hoste, J., 1978. A group separation scheme for radiochemical neutron activation analysis for 24 trace elements in rocks and minerals. Anal. Chim. Acta 101: 45-62.

Steiger, R.H. and Jäger, E., 1977. Subcommission on geochronology convention on the use of decay constants: In Geo-and-cosmochronology. Earth Planet. Sci. Lett. 36: 359-362.

Strong, D. F., 1972. Petrology of the island of Moheli, western Inland Ocean. Geol. Soc.

Am. Bull. 83: 389-406.

Sun, S. C., 1982. The Tertiary basins of offshore Taiwan. Proc. 2nd ASCOPE Conf. and Exhib., pp. 125-135.

Sun, S. S., 1980. Lead isotopic study of young volcanic rocks from mid-ocean ridge, ocean islands and island arc. Philos. Trans. Roy. Soc. London A297: 409-445.

Sun, S. S. and Hanson, G. N., 1975. Origin of Ross island basanitoids and limitation upon the heterogeneity of mantle source for alkali basalts and nephelinites. Cont. Min. Petrol 52: 77-106.

Sun, S. S. and McDonough, W. F., 1989. Chemical and isotopic systematics of oceanic basalts: implications for mantle composition and processes. *In:* Saunders, A. D. & Norry M. J. (eds.). Magmatism in Ocean Basins. Geological Society, London, Special Publication 42: 313-345.

Sun, S. S., Nesbitt, R. W. and Sharaskin, A. Y., 1979. Geochemical characteristics of mid-ocean ridge basalts. Earth Planet. Sci. Latt. 44: 119-138.

Sun, S. S and Nesbitt, R. W., 1977. Chemical heterogeneity of the Archean mantle, composition of the Earth and mantle evolution. Earth Planet. Sci. Lett. 35: 429-448.

Swanson, D. A., Wright, T. L., Hooper, P. R. and Bentley, R. D., 1979. Revisions in stratigraphic nomenclature of the Columbia River Basalt group. US Geol. Surv. Bull. 1457: 1-59.

Tarney, J., Wood, D. A., Saunders, A. D., Cann, J. R. and Varnet, J., 1980. Nature of mantle heterogeneity the North Atlantic: evidence from deep sea drilling. Philos. Trans. Roy. Soc. London A297: 179-202.

Taylor, B. and Hayes D. E., 1983. Origin and history of the south China Sea Basin: *In:* Hayew D. E. (ed.). the Tectonic and Geologic Evolution of southeast Asian Seas and Islands: part 2. pp. 23-56. Am. Geophys. Union.

Taylor, S. R. & McLennan, S. M., 1985. The continental crust: its composition and evolution. Blackwell Scientific Publications.

Teng, L. S., Chen, C. H., Wang, W. S., Liu, T. K., Juang, W. S. and Chen, J. C., 1992. Plate kinematic model for late Cenozoic arc magmatism in northern Taiwan. J. Geol. Soc. China 35(1): 1-18.

Thompson, R. N., 1977. Primary basalts and magma genesis III: Alban Hills, Roman comagmatic province, Centrl Italy. Contrib. Min. Petrology 50: 91-108.

Tsan, S. F., 1962. Geology of the Chiopanshan area, Taoyuan. Bull. Geol. Surv. Taiwan 14: 15-28 (Chinese), 7-11 (English).

Tsao, S. J., Hong, E. S., Song, S. R., Chu, H. T. and Chung, S. H., 1992. The absolute age of the Boundary between Nanchuang and Kueichulin Formation. Special Publication Cent. Geol. Survey 6: 223-234.

Tu, K., Flower, M. F. J., Carlson, R. W., Xie, G., Chen, C. and Zhang, M., 1992. Magmatism in the South china Basin, 1. Isotopic and trace-element evidence for an endogenous Dupal mantle component. Chem. Geol., 97: 47-63.

Tu, M. K. and Chen, W. C., 1990. Chungli. Explantary Text Geol. Map Taiwan Sheet 7. Central Geol. Surv.

Tu, M. K. and Chen, W. C., 1991. Chutung. Explantary Text Geol. Map Taiwan Sheet 13, Central Geol. Surv.

Turekian, K. K., 1963. The chromium and nickel distribution in basaltic rocks and eclogites. Geochim. Cosmochim. Acta 27: 835-846.

Wang, W. S., 1989. Volcanic geology and fission track dating of the Tatun Volcano Group, northern Taiwan: MS Thesis, Inst. Geology, NTU., Taipei, Taiwan (Chinese).

Wang, Y. and Huang, T., 1953. A stratigraphical study of the Kungkuan Tuff formation, northern Taiwan. Acta Geol. Taiwanica 5: 35-46.

Wass, S. Y. and Rogers, N. W., 1980. Mantle metasomatism-precursor to continental alkaline volcanism. Geochim. Cosmochim. Acta 44: 1811-1823.

Weaver, B. L. 1991. The origin of ocean island basalts end-member compositions: trace element and isotopic constraints. Earth Planetary Science Letters 104: 381-397.

Weaver, B. L., Wood, D. A. Tarney, J. and Joron, J. L., 1986. Role of subducted sediment in the genesis of ocean-island basalts: Geochemical evidence from South Atlantic Ocean islands. Geology 14: 275-278.

Wilson, W., 1989. Igneous petrogenesis. Unwin Hyman; London.

Wood, D. A., Joron, J. L. and Treuil, M., 1979. A re-appraisal of the use of trace elements to classify and discriminate between magma series erupted in different tectonic setting. Earth Planet. Sci. Latt. 45: 326-336.

Yang, H. Y., Wu, H. C. and Chou, T. F., 1981. Igneous rocks in the well in the west-central Taiwan. Explor. Prod. 4: 123-124 (Chinese).

Yang, T. Y., Liu, T. K. and Chen, C. H., 1988. Thermal event records of the Chimei Igneous Complex: constraint on the ages of magma activities and the structural implication based on fission track dating. Acta Geol. Taiwanica 26: 237-246.

Yen, T. P., 1950. Neogene and Quaternary basalts in Taiwan. Quart. Jour. Taiwan Museum 3, No.1: 33-54.

Yen, T. P., 1958. Cenozoic volcanic activity in Taiwan.: Taiwan Mining Industry 10, Nos.1-2:1-39.

Yen, T. P., Chen, J. C. and Chen, C. H., 1981. Spatial variations in the geochemistry of Pleistocene andesites in northern Taiwan. Ti-Chih 3: 95-104 (Chinese).

Yoder, H. S. Jr. and Tilley, C. E., 1962. Origin of basalt magmas: an experimental study of nature and synthetic rock systems. J. Petrol. 3: 342-532.

Yu, H. S., 1988. Tectonic evolution of the Pearl River Mouth Basin of the South China Coast. Acta Oceanogr. Taiwanica 20: 79-94.

Yuan, J. W., 1981. Radiometric ages of the igneous bodies in the wells in the western central Taiwan. Rep. Explor. Prod. 4: 363-366.

Zindler, A. and Hart, S. R., 1986. Chemical geodynamics. Annual Reviews of Earth & Plantary Science 14: 493-571.

Revised manuscript accepted March 20, 1996

臺灣西部麓山帶玄武岩之定年與地球化學研究

莊文星

摘 要

臺灣西部麓山帶在中新世沈積作用進行的時候，火山作用不斷地在沈積盆地中活動。在臺灣北部，幾乎所有的中新世地層，都在不同地區曾發現玄武岩質凝灰岩、凝灰質角礫岩或火山熔岩。以往依照火山岩露頭所處周遭沈積岩作地層對比，在時代上劃分爲公館、尖石和角板山三個火山活動期。其中以公館和角板山期較活躍，而尖石期火山岩地表甚少露出。鉀—氬法定年的結果顯示，西部麓山帶的火山活動大致上可分爲中新世早期（21.2 ± 0.4～ 16.3 ± 0.4 Ma）與中新世中晚期（14.1 ± 0.4 ～ 7.1 ± 0.5 Ma）二大階段，亦即相當於公館期與角板山期的火山活動歷史。公館期火山活動定年之區域包括南港—深坑區、清水坑區（中和—土城區）、山子腳區（樹林—山佳區）。角板期火山岩包括桃園縣復興鄉角板山及石門水庫一帶、新竹縣關西—竹東及其他零星分布之火山岩體（如桃園縣鶯歌尖山、臺北縣三峽土城與高雄縣旗山木柵等）。

中新世西部麓山帶的玄武岩岩性主要可分爲矽質與鹼性玄武岩二大類，兩者雖具有截然不同的主要與微量元素成分，但其不共容親岩漿元素間的比值接近定值，推測可能代表源自相同的來源地函，且來源地函具有輕稀土元素富化現象。

由地體構造環境區別性元素 Ti、Nb、Ta 或 Zr—Ti—Y，Nb—Zr—Y、Th—Hf—Ta 等區別圖與整體不共容元素分布圖特性判斷，中新世西部麓山帶火山岩皆落入板塊內大陸玄武岩的分布範圍，顯示火山活動時，地體構造環境屬大陸斷裂體系。

不論公館其或角板山期矽質或鹼性玄武岩，其共容元素 Co、Cr、Ni 和 Sc 均隨 MgO／ΣFeO 之增大而增高。由此系統性變化，可以看出中新世麓山帶玄武岩都是歷經固液相平衡，結晶分化在岩漿的分化過程中可能曾經發生過。公館期鹼性玄武岩以橄欖石、斜輝石的結晶分化爲主，尙伴隨有鈦鐵氧化物或斜長石等礦物的結晶分化。公館期與角板山期鹼性玄武岩其不共容元素與 MgO／ΣFeO 之變化趨勢相背離，可能意謂著角板山期鹼性玄武岩曾受到閃石類礦物結晶分化作用的影響。

根據同位素與微量元素的研究，目前推測矽質與鹼性玄武岩可能分別代表二個獨立的岩漿型態。鹼性玄武岩是由富化的上部地函物質，經由 10～20% 部分熔融而得，而矽質玄武岩則是由較淺處未受換質之地函兩輝橄欖岩經 5～10% 平衡部分熔融作用而產生。由於原始岩漿來源之地函物質的富化程度、部分熔融與歷經橄欖石、斜輝石或角閃石的結晶分化的差異，乃衍生出中新世西部麓山帶玄武岩岩漿演化的歧異。

西部麓山帶與澎湖玄武岩化學與火山年代相仿，這一連串的火山活動可能是由於中國南海的擴張所引起的第三期熱力與斷裂作用所造成。中新世西部麓山帶與澎湖玄武岩釹、鍶和鉛同位素具有區域性的變化，而西部麓山帶角板山期火山岩杜巴異常顯著。根據不共容元素比值的變化趨勢顯示賦存於中新世地層之玄武岩的富化程度是漸變的。由地殼物質的加入難以闡釋角板山期火山岩的微量元素之變異，可能是由於地函的富化導致具有杜巴異常的地函源特性。

關鍵詞: 玄武岩, 臺灣西部, 地球化學, 鉀-氬法定年, 岩石成因